VERTICAL MOTION OF RIGID FOOTINGS

by

John Lysmer

A dissertation submitted in partial fulfillment
of the requirements for the degree of
Doctor of Philosophy in the
University of Michigan
1965

Doctoral Committee:

Professor Frank E. Richart, Jr., Chairman
Professor Glen V. Berg
Professor Samuel K. Clark
Associate Professor Wadi S. Rumman

To my wife

ACKNOWLEDGEMENTS

The research described in the present dissertation constitutes part of the work carried out under contract No. DA-22-079-ENG-340 with the U. S. Army Engineer Waterways Experiment Station, Vicksburg, Mississippi. And the Author wishes to thank this organization for their financial support and flexible cooperation through the past four years.

The research was done under the supervision of Dr. Frank E. Richart, Jr., Professor and Chairman of the Department of Civil Engineering at The University of Michigan. The importance of Professor Richart's connection with the present work cannot be overemphasized. Not only did he provide an apparently inexhaustible source of information and able guidance in connection with the project but his, and Mrs. Richart's, interest and encouragement were major factors in the Author's decision to undertake a doctoral study in the first place and their support was a constant encouragement during the execution of the research. Needless to say that the Author is deeply thankful to Professor and Mrs. Richart.

The Author also wants to thank the researchers who have been working on the experimental part of the above project. First of all, Dr. John R. Hall, Jr., Assistant Professor of Civil Engineering at The University of Michigan, for many fruitfull discussions and for supervising the experimental part of the project. Secondly, Dr. Yong S. Chae, Assistant

Civil Engineering at Rutgers University, New
ew Jersey and Mr. Vince P. Drnevich, M.S.,
dent and Research Assistant at the Department
ineering, University of Michigan, for providing
ntal data presented in the present dissertation.
, but not least, the Author wishes to thank
teed for typing both the draft and the original.

TABLE OF CONTENTS

LIST OF ILLUSTRATIONS

LIST OF SYMBOLS

A	Amplitude of displacement, Eq. 33
A_o	Initial amplitude of displacement, Eq. 134
A_{res}	Maximum displacement (at resonance) for constant force excitation, Eq. 94
B	Mass ratio for footing-soil system, Eq. 74
$\overline{B}$	Mass ratio for simple damped oscillator, Eq. 24
C	Frequency dependent coefficient of viscous damping, Fig. 2
D	Magnification factor for some given pulse shape, Eq. 153
D_{max}	Displacement spectrum for some given pulse shape, Eq. 154
E_p	Constrained elastic modulus (no side contraction) of elastic half space, Eq. 30
F	Complex displacement function for system S, Eq. 2. In particular a "massless" soil-footing system, Eq. 53
F_1	Real part of F
F_2	Imaginary part of F
$\overline{F}$	Complex displacement function for System S + m, Eq. 8
$\overline{F}_1$	Real part of $\overline{F}$
$\overline{F}_2$	Imaginary part of $\overline{F}$
G	Shear modulus for elastic half-space, Fig. 8
I_1	Integral, Eq. 202
I_2	Integral, Eq. 203

LIST OF SYMBOLS (Continued)

J_o	Zero order Bessel function of the first kind
J_1	First order Bessel function of the first kind
J_n	The n^{th} term of a series of integrals, Eq. 207
K	Frequency-dependent spring constant, Fig. 2
K	Cut-off value for x, Eq. 179
K_1	Particular cut-off value, Eq. 206
K_2	Particular cut-off value, Eq. 216
M	Magnification factor for constant force system, p. 8
M_r	Magnification factor for rotating mass system, Eq. 105
N	Number of highest order term in Fourier Series, Eq. 121
N	Large integer, Eq. 236
N_1	Large integer, Eq. 206
N_2	Large integer, Eq. 216
O	Name of reference point, Fig. 1
P(t)	Vertical force acting on system S, positive when downwards, Fig. 1
P(x)	Auxiliary polynomial, Eq. 168
P_o	Amplitude of harmonic force acting on system S, Eq. 1. In particular the reaction between m and S
Q(t)	Vertical force acting on system S + m, positive when downwards, Fig. 3
Q_o	Amplitude of force acting on system S +m, Eq. 7
Q_o	The peak value of the pulse shown in Fig. 25
Q_1	Amplitude of exciting force for unit frequency ratio, Eq. 103 and Eq. 112
R	Residual after cutting off the integral at x = K, Eq. 180

$R(t)$	Soil reaction in the interface between footing and soil including the effect of gravity, p. 82
S	Name of a general elastic system, Fig. 1
$S + m$	Name of the elastic system formed by adding a mass m to system S, Fig. 3
T	Period of free motion for elastic system, Eq. 132
V_P	Velocity of P-waves in the elastic half space, Eq. 32
V_R	Velocity of Rayleigh surface waves in the elastic half space, p. 70
V_s	Velocity of S-waves in the elastic half space, Eq. 41
W	Weight of Footing, Eq. 88
W_{total}	The sum of the static and the rotating masses of a rotating-mass system, Eq. 110
a	Distance ratio, Eq. 51
a_o	Frequency ratio for footing-soil system, Eq. 42
$\bar{a}_o$	Frequency ratio for simple damped oscillator, Eq. 21
a_1	The smallest of the values a, a_o, $\lvert a_o - a \rvert$, Eq. 225
a_m	Distance or frequency ratio corresponding to the radius r_m, Eq. 63
a_n	Frequency ratio for the n^{th} term of the Fourier series for displacements, Eq. 127
b	Mass ratio used by other authors, Eq. 74
b_n	Magnification factor for the n^{th} term of the Fourier series for displacements, Eq. 126
$bes(x)$	Auxiliary function, Eq. 162
c	Coefficient of viscous damping for simple damped oscillator, Fig. 4. In particular the simplified analog for the footing-soil system, Eq. 85

c_1	Dimensionless damping coefficient, Eq. 46
c_1	Coefficient, Eq. 194
c_2	Coefficient, Eq. 195
c_3	Coefficient, Eq. 196
c_4	Coefficient, Eq. 198
c_5	Coefficient, Eq. 199
c_n	Amplitude of n^{th} term in the Fourier series for the pulse train, Eq. 121
c_∞	Constant defined by Eq. 56
$c_{j,m}$	Influence coefficient expressing the displacement of a point j due to a uniform loading on the m^{th} ring, Eq. 65
d	Duration of pulse, Fig. 25
den'(x)	Derivative of the denominator of w(x), Eq. 171
e	= 2.7183 = Base of natural logarithms, Eq. 1
f	Complex displacement function used by Bycroft (2) a.o., Eq. 52
f_1	Real part of f
f_2	Imaginary part of f
f(x)	Rayleigh's function, Eq. 58
f*(x)	Auxiliary function, Eq. 160
f**(x)	Auxiliary polynomial, Eq. 161
g	Acceleration of gravity = 386.4 in/sec^2, Eq. 245
g	Complex surface displacement function, Eq. 50
g_1	Real part of g, Eq. 176
g_2	Imaginary part of g, Eq. 176
$g_{j,m}$	Specific value of Reissner's surface displacement function expressing the displacement of point j caused by a uniform harmonic loading over a circular area of radius r_m, Eq. 62

$h(x)$	Auxiliary function, Eq. 169
i	Imaginary unit, Eq. 1
i	Summation index, Eq. 130
j	Index referring to a surface point of the elastic half space, Fig. 15
j	Integer controlling the time interval between the pulses of the pulse train shown in Fig. 25
k	Spring constant, Eq. 2
k_1	Dimensionless spring constant, Eq. 46
ℓ	Eccentricity of rotating mass, Fig. 22
m	Mass, Fig. 3. In particular mass of footing, Fig. 10
m	Index denoting a particular member of the ring system or a point on surface of the half space, Fig. 15
m	Number of intervals in piecewise linear pulse, Fig. 26b
m	Exponent, Eq. 202
m_1	Rotating mass, Fig. 22
n	Total number of rings in the ring system, Fig. 15
n	General summation index, Eq. 204
$\mathrm{num}'(x)$	Derivative of the numerator of $w(x)$, Eq. 171
$o(x^{-n})$	A quantity which vanishes faster than x^{-n} as x goes to infinity.
p	Vertical surface loading on elastic half-space, positive when downwards, Fig. 8
p_o	Amplitude of uniform harmonic surface loading on elastic half space, Fig. 8
q_m	Complex, dimensionless pressure coefficient, Eq.13
q_1	Real part of q_m treated like a continuous function of a, Eq. 72

q_2	Imaginary equivalent of q_1, Eq. 72
r	Horizontal distance from center of footing, Fig.10
r_o	Radius of footing, Fig. 10
r_m	Largest radius of m^{th} ring, Fig. 15
r_n	Largest radius of ring system, equivalent to r_o, Fig. 15
$r(x)$	Auxiliary function, Eq. 163
s	Ratio between the velocities of S-waves and P-waves in the elastic half space, Eq. 31
t	Time, Eq. 1
t_1	Time required to reduce the amplitude of vibration to a fraction ε_1 of it's initial value, Eq. 134
$t(x)$	Auxiliary function, Eq. 164
u	Dummy variable in integration, Eq. 124
$u(x)$	Auxiliary function, Eq. 165
$v(x)$	Auxiliary function, Eq. 166
$w(x)$	Auxiliary function, Eq. 167
x	Vertical displacement of an interior point of the elastic half space, positive when downwards, Fig.8
x	Independent variable in integrations etc., Eq. 57 and Appendix I
x_o	Ratio between the velocity of shear waves and the velocity of Rayleigh waves, Eq. 58
x_n	Maximum displacement during the n^{th} free oscillation of a damped system, Eq. 99
x_n	n^{th} approximation to x_o in a Newton iteration process, Eq. 182
y_n	Ordinate of piecewise linear pulse, Fig. 26b
z	Depth below surface of elastic half space, Fig. 8

α	Coefficient, Eq. 202
α_n	Fourier coefficient, Eq. 124
β	Coefficient, Eq. 202
β_n	Fourier coefficient, Eq. 124
γ	Unit weight of soil (elastic half-space), Eq.88
δ	Vertical displacement, positive when downwards, Fig. 1
$\dot{\delta}$	$= d\delta/dt$ = Velocity, Eq. 3
$\ddot{\delta}$	$= d^2\delta/dt^2$ = Acceleration, Eq. 9
δ_j	Total vertical displacement of point j, Eq. 64
δ_{jm}	Vertical displacement of point j due to the loading on the m^{th} ring, Eq. 61
δ_{max}	Largest absolute displacement
δ_{ln}	Logarithmic decrement, Eq. 99
δ_{static}	Static displacement under the load Q_o
ε_1	Small constant used to control the error made by using a pulse train instead of a single pulse. Controls the distance between the individual pulses, Eq. 135
ε_2	Small constant used to control the error made by cutting off the Fourier series at the n^{th} term, Eq. 140
λ_s	Wave length of S-waves in the elastic half-space, Eq. 42
μ	Poisson's ratio for elastic half-space, Fig. 8
ξ	Dimensionless duration of pulse, Eq. 152
π	3.1416
ρ	Mass density of elastic half-space
σ	Tensile stress on a horizontal plane of the elastic half-space, Eq. 34

LIST OF SYMBOLS (Continued)

τ	Dimensionless time, Eq. 151
φ	Phase shift between displacement and exciting force, Eq. 16
φ_n	Phase shift between the n^{th} term of the Fourier series for displacement and the corresponding term in the series for exciting force, Eq. 128
ψ_n	Phase of the n^{th} term of the Fourier series for the pulse train, Eq. 121
ω	Angular frequency of steady state motion, Eq. 1
ω_d	Natural damped frequency for a simple oscillator, Eq. 97
ω_{res}	Resonance frequency for constant force excitation, Eq. 93
Δ	Allowable error, Eq. 234
Δ_n	Upper limits for error, Eqs. 213, 215, 218, 223, 225, 229 and 231
Φ	Pulse shape function, Fig. 26

I. INTRODUCTION

It is the objective of this work to describe the dynamic behavior of footings and to develop practical methods for dynamic analysis. The investigations are limited to the simple case of a rigid circular footing resting on a plane soil surface and excited by a vertical time-dependent force in the axis of symmetry.

In order to arrive at a model which can be analysed mathematically it is assumed that the subsoil can be considered as a perfectly elastic, isotropic and homogeneous half-space and that only normal stresses are transferred at the interface between footing and soil.

Half-space models have been used by several investigators, notably Reissner (1) who, in 1936, developed a method for finding the steady-state surface displacements of an elastic half space for any given surface pressure distribution with axial symmetry. Through the work of other investigators, such as Sung (2), Bycroft (3) and Hsieh (4), the art has since been developed to the point where it is possible to calculate the steady state response of a rigid footing-soil system in the low frequency range. Fortunately, this range includes the operating frequencies of most machinery and the

above solutions are therefore useful for many practical purposes. This was clearly shown in a paper by Richart (5), who also considered the rocking and sliding modes of vibration.

In the present work it is shown how the frequency range can be extended to include all frequencies of steady-state motion and also how this complete steady state solution can be used to calculate the transient response caused by an arbitrary pulse loading. The analytical solutions compare well with test results by Fry (6), Chae (7), and Drnevich, Hall and Richart (8).

The above system differs from most classical dynamic systems in that it is of infinite dimensions. This geometrical peculiarity causes an apparent loss of energy by wave propagation into the half space. It will be shown in this work that the effect of the energy loss is comparable to that of the dashpot in a simple damped oscillator. This observation has led the author to the adoption of a simplified spring-dashpot analog for practical calculations. The new analog differs from previously suggested analogs in that its components (mass, dashpot, spring) are independent of the frequency of the exciting force. The analog can therefore be used to predict the response to dynamic pulses of arbitrary shape by means of the classical methods for a damped oscillator (phase-plane methods, numerical integrations, etc.).

II. STEADY-STATE MOTION

General Theory

Before focusing the attention on the elastic half-space model it is appropriate to study a larger class of dynamic systems.

Consider a linear dynamic system S which is excited by a periodic vertical force P(t) of frequency ω and amplitude P_o. That is:

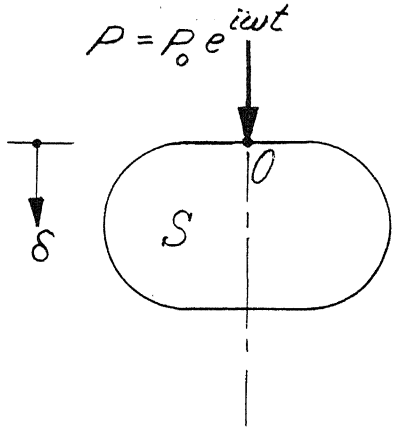

Fig. 1
System S

$$P = P_o e^{i\omega t} \qquad (1)$$

Furthermore, let it be assumed that P attacks at a point O which is such that the displacement δ of point O is vertical at all times. The class of dynamic systems thus defined clearly includes all systems which are axially symmetric about a vertical axis through O, and the systems which will be considered in the following are of this type.

The system S may or may not exhibit viscous damping and

it may be of finite or infinite dimensions.

In the case of steady-state motion it is known that all forces and displacements are harmonic with the circular frequency ω and proportional to the amplitude P_o of the exciting force. The displacement δ can therefore be written in the form:

$$\delta = \frac{P_o}{k} F e^{i\omega t} \qquad (2)$$

where k is a quantity having the dimension force/length and F is a dimensionless function.

The quantity k will be called the spring constant and can usually be put equal to the static spring constant of the system S. There are however members of the above class of systems for which this is not possible (i.e., if S consists of just a dashpot) and in this case a different choice must be made.

The time-independent, complex function $F = F_1 + iF_2$ is in general a function of the frequency ω and the properties of the system S. It will, in the following, be referred to as the displacement function*for the system S.

It should be noted that if k is the static spring constant then we must have $F = F_1 = 1$ for $\omega = 0$.

---

* The displacement function is proportional to the quantity compliance used by authors favoring electro-mechanical analogies.

It is of interest to investigate if there exists a simple damped oscillator which as far as the displacement δ is concerned, can be used as an analog for the system S. In particular we are interested in a massless system of the type shown in Fig. 2. This system has the equation of motion:

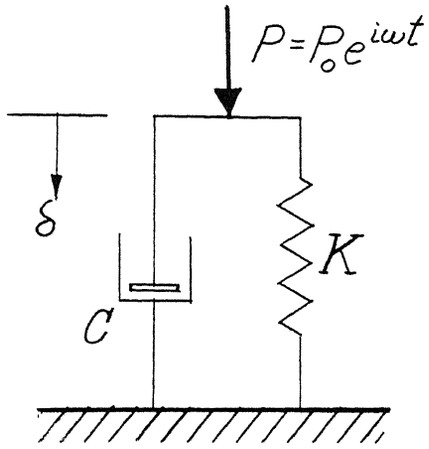

Fig. 2
Analog for
System S

$$C\dot{\delta} + K\delta = P_o e^{i\omega t} \qquad (3)$$

where the system parameters C and K are real.

By substitution of Eq. 2 into Eq. 3 we find:

$$i\omega CF + KF = K \qquad (4)$$

and separation of the real and imaginary parts gives the following linear equations:

$$\left.\begin{aligned} -\omega F_2 C + F_1 K &= K \\ \omega F_1 C + F_2 K &= 0 \end{aligned}\right\} \qquad (5)$$

which have the solution:

$$\left.\begin{aligned} K &= \frac{F_1}{F_1^2 + F_2^2}\, K \\ C &= \frac{-F_2/\omega}{F_1^2 + F_2^2}\, K \end{aligned}\right\} \qquad (6)$$

These expressions show that it is indeed possible to determine suitable parameters C and K if one allows them to be functions of the frequency ω of the exciting force.

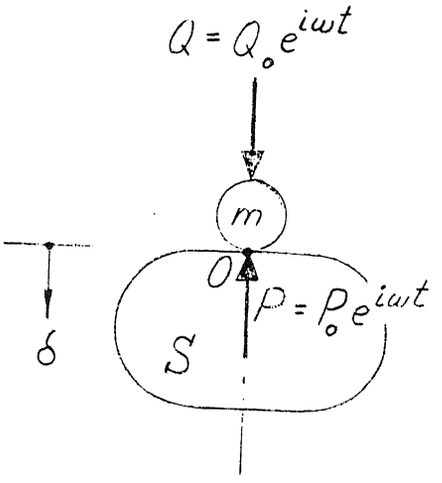

Fig. 3
System S + m

Next consider the dynamic system S + m, which is formed by supplementing the system S by a rigid mass m at point O. Suppose this new system is excited by a vertical harmonic force:

$$Q = Q_o e^{i\omega t} \qquad (7)$$

acting on the added mass m. Then this new system will belong to the class defined above and there will therefore exist a displacement function $\bar{F} = \bar{F}_1 + i\bar{F}_2$ such that the displacement δ of the mass m (and hence of the point O) can be written in the form:

$$\delta = \frac{Q_o}{k} \bar{F} e^{i\omega t} \qquad (8)$$

A connection between F and $\bar{F}$ can be found by introducing the reaction P acting on m (and the system S) at point O. This force is related to the displacement δ through Eq. 2, and it must also satisfy the equation of motion for the mass m. Using the sign rule indicated in Fig. 3, this equation of motion is:

$$m\ddot{\delta} = Q_0 e^{i\omega t} - P_0 e^{i\omega t} \tag{9}$$

Differentiation of Eq. 2 and Eq. 8 gives:

$$m\ddot{\delta} = -\frac{m\omega^2}{k} F P_0 e^{i\omega t} \tag{10}$$

$$m\ddot{\delta} = -\frac{m\omega^2}{k} \bar{F} Q_0 e^{i\omega t} \tag{11}$$

which in connection with Eq. 9 yields:

$$P_0 = \frac{Q_0}{1 - \frac{m\omega^2}{k} F} \tag{12}$$

and

$$\bar{F} = \frac{F}{1 - \frac{m\omega^2}{k} F} \tag{13}$$

The displacement of point O in system S + m is consequently by Eq. 8:

$$\delta = \frac{Q_0}{k} \cdot \frac{F e^{i\omega t}}{1 - \frac{m\omega^2}{k} F} \tag{14}$$

This important formula expresses the steady-state solution to the system S + m in terms of the solution to the simpler system S. Its physical importance is best seen if the real part is separated. This will yield the solution to the case when the exciting force is:

$$Q = Q_0 \cos \omega t \tag{15}$$

Performing the process of separation we find the real displacement:

$$\delta = \frac{Q_0}{k} \sqrt{\frac{F_1^2 + F_2^2}{\left[1 - \frac{m\omega^2}{k} F_1\right]^2 + \left[\frac{m\omega^2}{k} F_2\right]^2}} \cos(\omega t + \alpha) \tag{16}$$

where the phase shift is:

$$\varphi = \tan^{-1} \frac{F_2}{F_1 - \frac{m\omega^2}{k}\left(F_1^2 + F_2^2\right)} \tag{17}$$

The square root appearing in Eq. 16 will be called the magnification factor and will be denoted hereafter by the symbol M. It is equal to the absolute value of $\bar{F}$.

Simple Damped Oscillator

The use of the theory developed above is clearly illustrated by the following simple example. Consider the massless damped system S shown in Fig. 4. This system clearly belongs to the class of dynamic systems covered by the theory, and it will therefore have a steady-state solution of

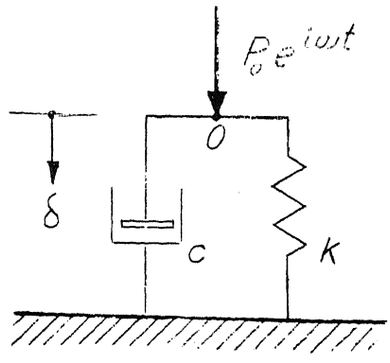

Fig. 4
System S

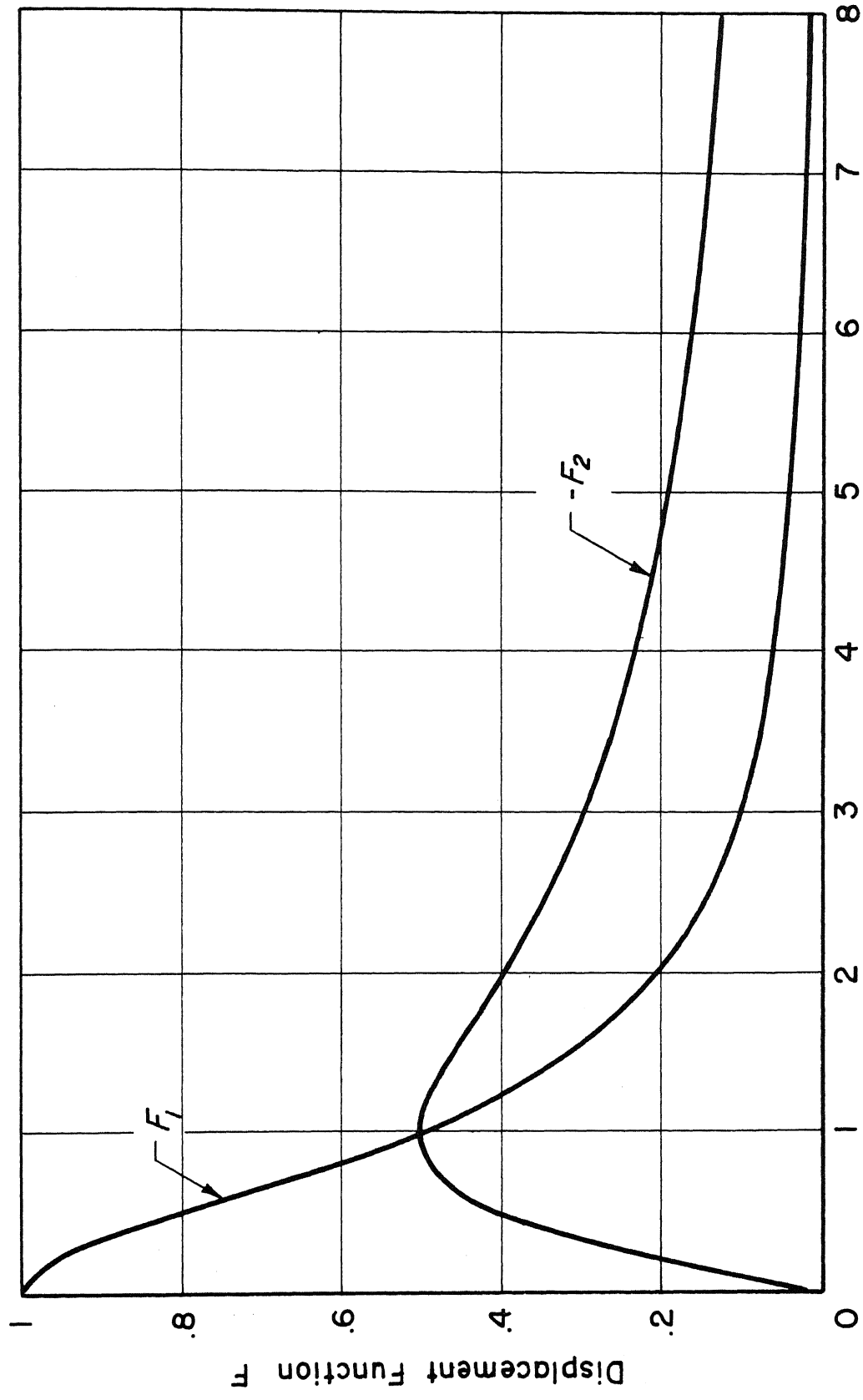

Fig. 5 Displacement Function for Simple Damped Oscillator

the form:

$$\delta = \frac{P_o}{k} F e^{i\omega t} \tag{18}$$

The equation of motion for point O is:

$$c\dot{\delta} + k\delta = P_o e^{i\omega t} \tag{19}$$

which after substitution of Eq. 18 yields the following displacement function:

$$F = \frac{1}{1 + i\frac{c}{k}\omega} = \frac{1}{1 + i\bar{a}_o} \tag{20}$$

where

$$\bar{a}_o = \frac{c}{k}\omega \tag{21}$$

is a dimensionless number which will be called the frequency ratio for the damped oscillator.

Separation of the real and imaginary parts of Eq. 20 gives:

$$\left.\begin{aligned} F_1 &= \frac{1}{1 + \bar{a}_o^2} \\ F_2 &= \frac{-\bar{a}_o}{1 + \bar{a}_o^2} \end{aligned}\right\} \tag{22}$$

These two functions are shown in Fig. 5 and play an important role in the subsequent sections. Note that substitution of Eq. 22 into Eq. 6 gives the expected result: C = c = constant and K = k = constant, and that the displacement function F has the asymptote:

$$\left.\begin{aligned} F_1 &\to 1/\bar{a}_o^2 \\ F_2 &\to -1/\bar{a}_o \end{aligned}\right\} \quad \text{for} \quad \bar{a}_o \to \infty \qquad (23)$$

Having determined the displacement function for the system S it is now a simple matter to determine the displacement of the more general oscillator shown in Fig. 6.

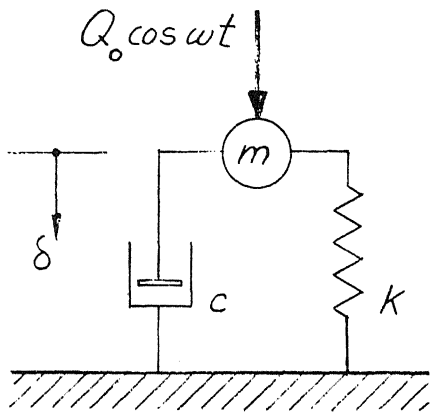

Fig. 6
System S + m

Before writing down the solution, it is convenient to introduce the so called mass ratio $\bar{B}$ defined by:

$$\bar{B} = \frac{km}{c^2} \qquad (24)$$

This parameter is a dimensionless number which can be thought of as a scaled measure for the mass m.

Noting that $\bar{B}\bar{a}_o^2 = m\omega^2/k$ we obtain from Eqs. 16, 17 and 22 the following displacement for the general damped oscillator:

$$\delta = \frac{Q_o}{k} M \cos(\omega t + \varphi) \qquad (25)$$

where

$$\tan \varphi = \frac{-\bar{a}_o}{1 - \bar{B}\bar{a}_o^2} \tag{26}$$

and

$$M = \sqrt{\frac{1}{\left(1 - \bar{B}\bar{a}_o^2\right)^2 + \bar{a}_o^2}} \tag{27}$$

The magnification factor M is of special interest. Its variation with $\bar{a}_o$ for different values of $\bar{B}$ is shown in Fig. 7.

It is easily shown analytically that whenever $\bar{B} > \frac{1}{2}$ the response spectra shown in Fig. 7 will exhibit resonance peaks of the heights:

$$\max M = \frac{\bar{B}}{\sqrt{\bar{B} - 1/4}} \tag{28}$$

at the frequency ratios:

$$\bar{a}_o = \frac{\sqrt{\bar{B} - 1/2}}{\bar{B}} \tag{29}$$

For $\bar{B} \leq \frac{1}{2}$ no peaks exist and the largest displacement occurs for the case of static loading.

The above form of the solution for the simple damped oscillator is of course equivalent to the more usual form found in standard textbooks, which use the dimensionless parameters $\omega\sqrt{m/k}$ and $c/2\sqrt{km}$.

The advantage of using $\bar{a}_o = \omega\, c/k$ and $\bar{B} = km/c^2$ is that

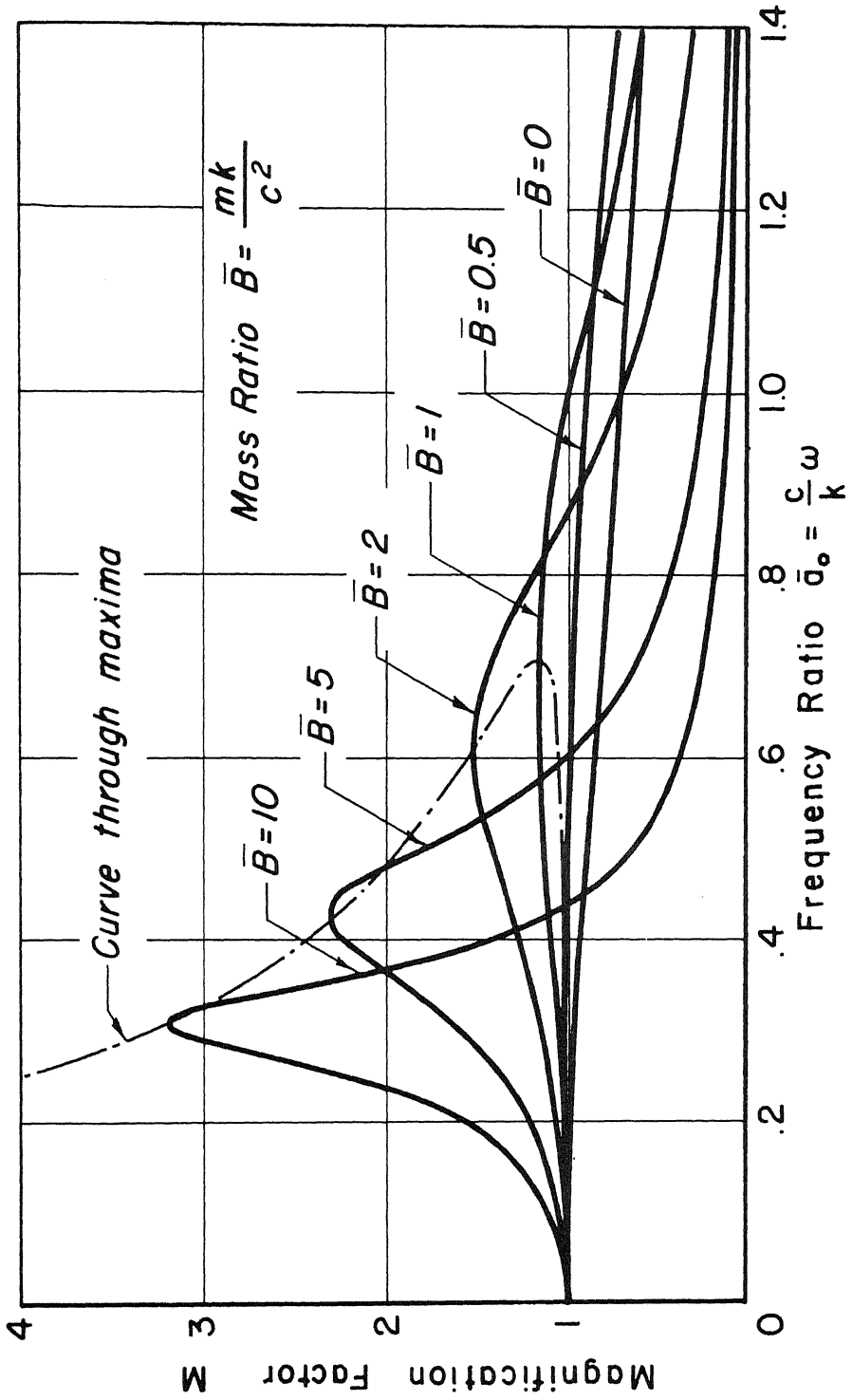

Fig. 7 Steady-State Spectra for Simple Damped Oscillator

the effect of frequency and mass can be studied separately, and for the systems which will be considered below this advantage greatly outweighs the disadvantage that this method fails for the undamped case (c = 0).

Elastic Half Space With Uniform Loading

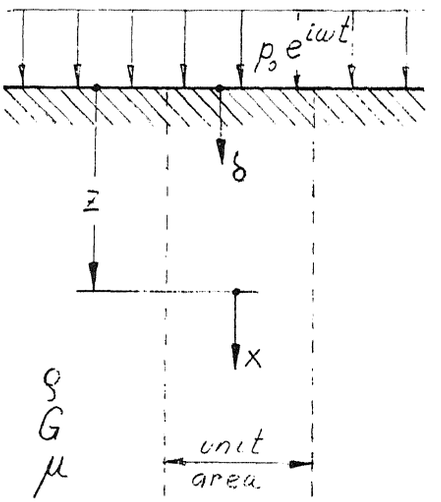

Fig. 8
Uniformly Loaded
Elastic Half Space

In a subsequent section we will need the steady-state solution for the system shown in Fig. 8. It consists of a perfectly elastic half space (soil) with the mass density ρ and the elastic constants G and μ. The half space is excited by a vertical, uniform surface loading $p = p_o e^{i\omega t}$ per unit area, and we are interested in the displacement δ of the free surface.

It is clear that it is sufficient to look at a column of unit area. Since no horizontal displacements occur, this column will behave like a rod with zero lateral displacement and its elastic modulus (constrained modulus) is therefore:

$$E_p = G/s^2 \qquad (30)$$

where

$$s^2 = \frac{1-2\mu}{2(1-\mu)} \tag{31}$$

The velocity of the P-waves propagated along the rod is:

$$V_p = \sqrt{\frac{E_p}{\rho}} = \frac{1}{s}\sqrt{\frac{G}{\rho}} = \frac{V_s}{s} \tag{32}$$

where V_s is the velocity of shear waves (S - waves). No reflected wave will occur since the rod is infinitely long and the displacements of the rod must therefore be of the form:

$$x = A\, e^{i\omega(t - z/V_p)} \tag{33}$$

which is the general expression for a sinusoidal wave with amplitude A propagated downwards with the constant velocity V_P.

The tensile stress on a horizontal plane is:

$$\sigma(z) = E_p \frac{\partial x}{\partial z} = -iAE_p \frac{\omega}{V_p} e^{i\omega\left(t - z/V_p\right)} \tag{34}$$

and the stress boundary condition at the surface (z = 0) gives consequently:

$$\sigma(0) = -p_o e^{i\omega t} = -iAE_p \frac{\omega}{V_p} e^{i\omega t} \tag{35}$$

or

$$A = \frac{-ip_o}{\omega\sqrt{\rho E_p}} = \frac{-isp_o}{\omega\sqrt{\rho G}} \tag{36}$$

Hence, by Eq. 33, the displacement δ at the surface is:

$$\delta = -\frac{isp_o e^{i\omega t}}{\omega\sqrt{\rho G}} \tag{37}$$

This is exactly the steady-state solution of the differential equation:

$$\frac{\sqrt{\rho G}}{s}\dot{\delta} = p_o e^{i\omega t} \tag{38}$$

which is also the equation of motion for the simple damped oscillator shown in Fig. 9.

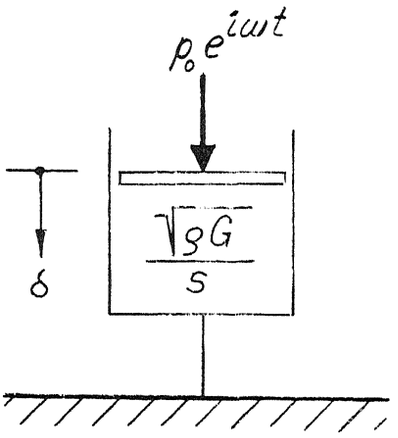

Fig. 9
Analog for
Half Space

This oscillator, which consists of just a dashpot with the damping coefficient:

$$c = \frac{\sqrt{\rho G}}{s} \tag{39}$$

can therefore be used as an analog for the uniformly loaded half space as long as we are only interested in the displacement of the surface.

This analogy between energy dissipation due to wave

propagation and that due to viscous damping is of great interest, since it allows us to study the behavior of an infinite system by considering a simple finite system. It is one of the aims of this paper to show that it is possible to extend this idea to more complicated systems. In particular, we will study a system consisting of a rigid circular footing resting on the surface of an elastic half space.

The material elements of an elastic half space possess no damping properties. The observed energy dissipation is therefore entirely due to the infinite geometry of the system, and it will in the following be referred to as geometrical damping, as opposed to viscous damping, which is usually related to a material property, such as the viscosity of a fluid.

Rigid Circular Footing

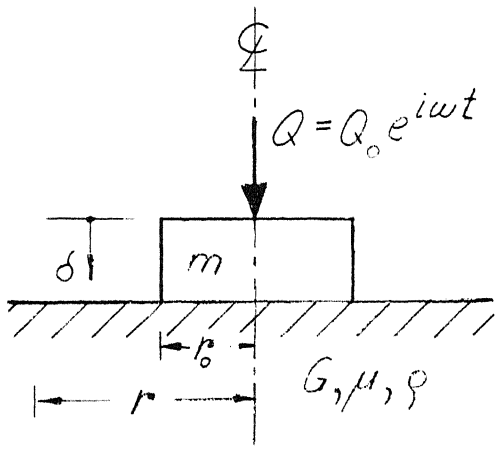

Fig. 10
Footing-Soil System

We now turn to the key matter of the present work, the idealized half-space model for the footing-soil system. This system, which is shown in Fig.10, consists of a circular rigid footing of mass m which rests upon a homogeneous, isotropic and perfectly elastic half space with the physical constants G, μ and ρ .

It was shown on page 7 that one can find the steady-state

solution for this system by first finding the displacement function for the case m = 0. The solution for m ≠ 0 will then follow from Eq. 14.

If Poisson's ratio is given, then F can at the most depend on the parameters ω, r_o, G and ρ. The only dimensionless ratio which can be formed by these is the frequency ratio:

$$\alpha_o = \omega r_o \sqrt{\rho/G} \tag{40}$$

and since F is dimensionless we therefore conclude that it is a function of μ and a_o only.

The physical importance of a_o becomes clear if one notes that the velocity of shear waves (S - waves) in an elastic solid is:

$$V_S = \sqrt{G/\rho} \tag{41}$$

Hence the frequency ratio can also be written in the forms:

$$\alpha_o = \omega \frac{r_o}{V_S} = 2\pi \frac{r_o}{\lambda_S} \tag{42}$$

where λ_S is the wave length of S-waves in the half space.

These relations show that one can look at a_o either as a frequency, based on the time r_o/V_S which it takes a shear wave to travel from the center to the edge of the footing, or as a measure for the radius of the footing in relation

to the length of the waves propagated in the elastic half space.

The static spring constant for a rigid footing is known to be:

$$k = \frac{4 G r_o}{1 - \mu} \tag{43}$$

and the expression for the displacement is by Eq. 2:

$$\delta = \frac{P_o}{k} F(a_o, \mu)\, e^{i\omega t} \tag{44}$$

The parameters of the corresponding spring-dashpot analog are then by Eq. 6 and Eq. 42:

$$\left.\begin{aligned} K &= \frac{F_1}{F_1^2 + F_2^2}\, k = k_1 k \\ C &= \frac{-F_2/a_o}{F_1^2 + F_2^2}\, \frac{k r_o}{V_s} = c_1 \frac{k r_o}{V_s} \end{aligned}\right\} \tag{45}$$

where the coefficients c_1 and k_1 defined by:

and

$$\left.\begin{aligned} k_1 &= \frac{F_1}{F_1^2 + F_2^2} \\ c_1 &= \frac{-F_2/a_o}{F_1^2 + F_2^2} \end{aligned}\right\} \tag{46}$$

are dimensionless functions of a_o and μ .

By substitution of Eqs. 45 into Eq. 3 we obtain the following equation of motion for a massless footing-soil

system:

$$c_1 \frac{k\varepsilon}{V_s} \dot{\delta} + k_1 K \delta = P_o e^{i\omega t} \qquad (47)$$

Before considering this equation in more detail we must study the behavior of c_1 and k_1. This requires knowledge of the displacement function F. The analytical determination of this function involves the solution of the wave equation for an elastic solid with a mixed boundary condition, namely, a zero stress condition on the free surface of the half space and a uniform displacement condition under the footing. This difficult mathematical problem has not yet been solved exactly and it is therefore necessary to rely on certain analytical and numerical approximations which will be discussed later.

Low Frequencies

Sung (2) and later Bycroft (3) made the plausible assumption that if the footing is small compared to the wavelength of the vibrations set up in the half space, that is if a_o is small, then the pressure distribution under the footing is close to the pressure distribution for the static case ($\omega = a_o = 0$). This distribution is known from the theory of elasticity and can be expressed by:

$$p(r) = \frac{P_o}{2\pi r_o \sqrt{r_o^2 - r^2}} \qquad (48)$$

Sung (2) and Bycroft (3) therefore replaced the mixed boundary condition with the pure stress condition:

$$p(r,t) = \begin{cases} \dfrac{P_o e^{i\omega t}}{2\pi r_o \sqrt{r_o^2 - r^2}} & , \; r < r_o \\ 0 & , \; r > r_o \end{cases} \tag{49}$$

and were then able to obtain approximate solutions for the surface displacements of the half space for the low frequency range, $a_o < 1.5$.

The vertical displacement of a surface point at the distance r from the axis of symmetry can be written in the form:

$$\delta(r,t) = \frac{P_o}{G r_o} g(a, a_o, \mu) e^{i\omega t} \tag{50}$$

where the distance ratio a is defined by:

$$a = \frac{r}{V_s} \omega = 2\pi \frac{r}{\lambda_s} \tag{51}$$

which is simply a generalization of the definition of the frequency ratio a_o, see Eqs. 40 and 42.

The surface displacement function $g = g_1 + ig_2$ is dimensionless and time-independent, and is characteristic for the chosen boundary condition. In the case of Sung's and Bycroft's solutions this condition is the static pressure distribution defined by Eq. 49.

Sung (2) determined only the displacement at the center

of the footing (a = 0), while Bycroft (3) went a step further and calculated the displacement of the footing as a weighted average of the displacements* over the loaded area. Hence, Bycroft's solution is to be preferred over Sung's.

Bycroft calculated the displacement of the footing positive when upwards and wrote his final solution in the form:

$$\delta = \frac{P_c}{G r_o} f(a_o, \mu) e^{i\omega t} \qquad (52)$$

The real and imaginary parts of his displacement function $f = f_1 + if_2$ are shown in Fig. 11.

Comparison between Eq. 44 and Eq. 52 shows that Bycroft's displacement function is connected to the normalized displacement function F used in the present work through the simple expression:

$$F = \frac{-4}{1-\mu} f \qquad (53)$$

and this formula has been used to prepare Fig. 12 which shows that for any practical purpose we can consider F to be independent of Poisson's ratio. This is, of course, the main reason for introducing the normalized displacement function.

From Fig. 12 and Eq. 46, we can directly calculate the corresponding values of the functions c_1 and k_1. The result is shown in Fig. 13.

* These displacements are not uniform since the assumed pressure distribution is not the actual one.

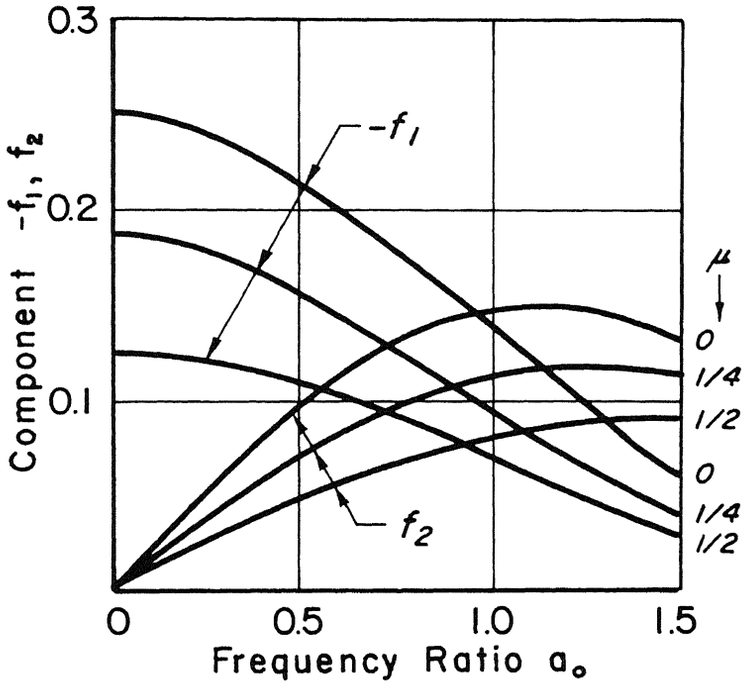

Fig. 11 Bycroft's Displacement Function

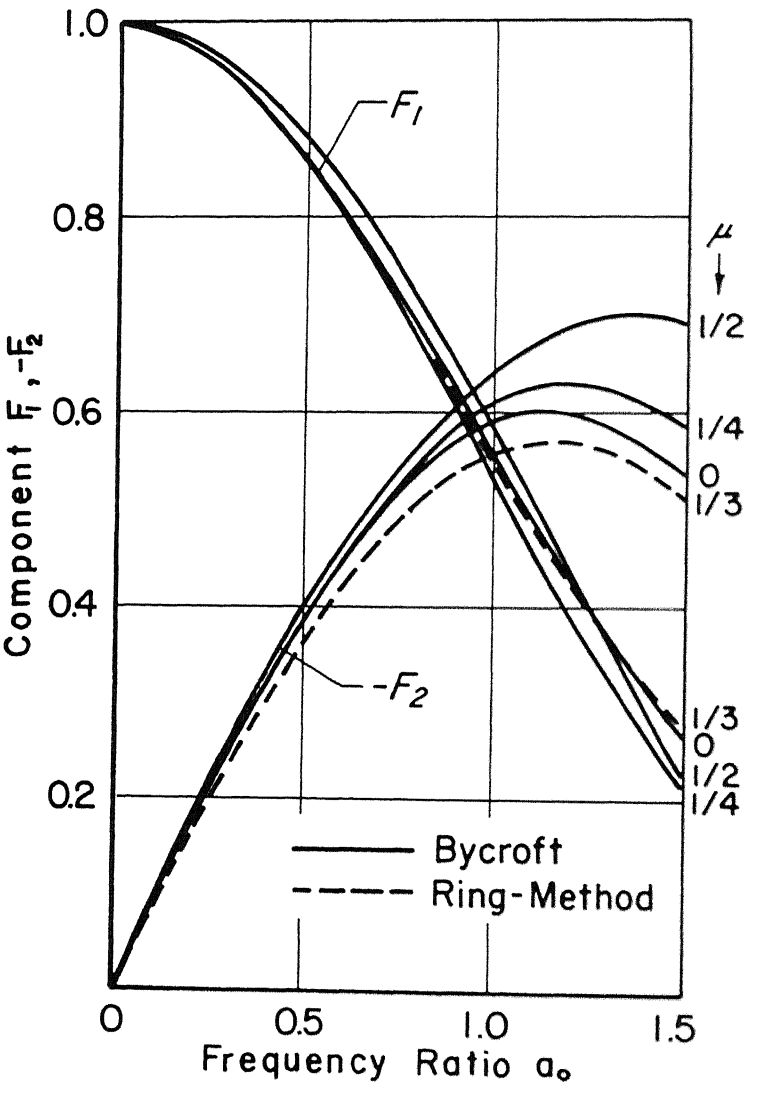

Fig. 12 The Displacement Function F

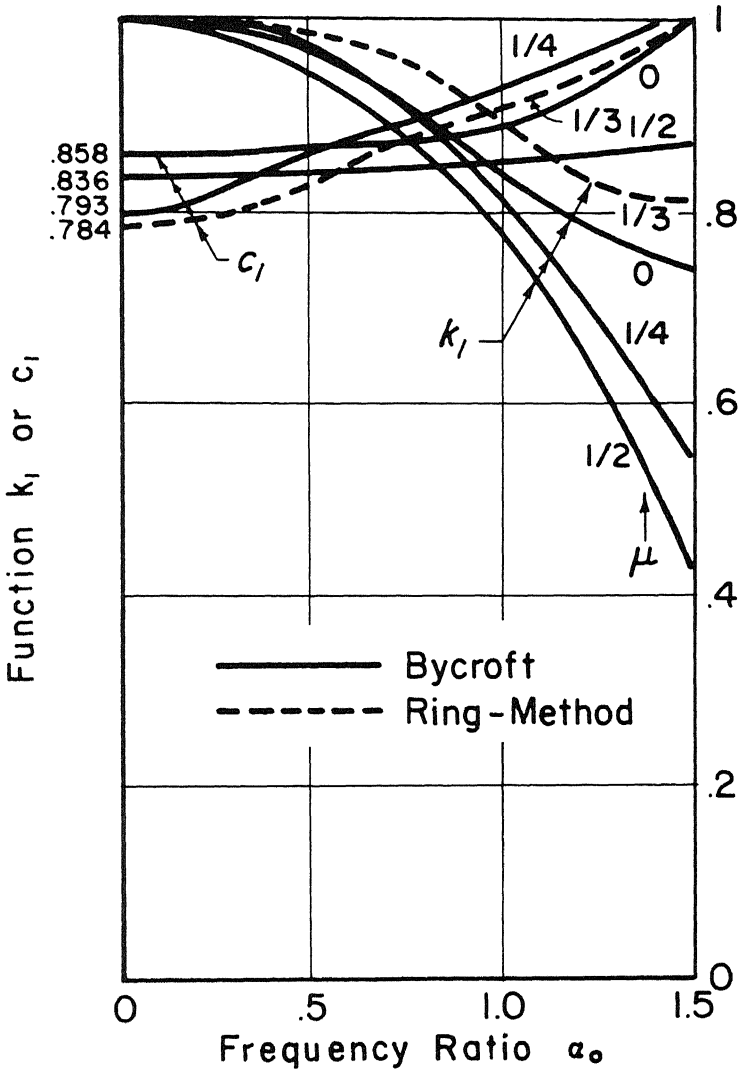

Fig. 13 The Functions k_1 and c_1

High Frequencies

When the radius of the footing is much larger than the wave length of the waves in the half space, that is when a_o is much greater than unity, we expect the displacement to approach the solution for uniformly loaded half space. This problem was solved on page 14, where we found the displacement given by Eq. 37, which can also be written in the form:

$$\delta = \frac{P_o}{k}\left[\frac{-2\sqrt{2}\,i(1-2\mu)^{1/2}}{\pi a_c (1-\mu)^{3/2}}\right] e^{i\omega t} \qquad (54)$$

where $k = 4Gr_o/(1-\mu)$ = pseudo spring constant

r_o = an arbitrary, but large radius

$P_o = \pi r_o^2 p_o$ = total force on area with radius r_o

$a_o = \omega r_o/V_s$ = frequency ratio

Eq. 54 is in the standard form (Eq. 2) and we conclude that the asymptote for the displacement function F is:

$$F \approx \frac{-i}{a_o c_\infty}, \text{ for } \quad a_o \to \infty \qquad (55)$$

where

$$\frac{1}{c_\infty} = \frac{2\sqrt{2}}{\pi}\,\frac{(1-2\mu)^{1/2}}{(1-\mu)^{3/2}} \qquad (56)$$

This asymptote is similar to the one found for the simple damped oscillator, see Eq. 23.

The variation of the coefficient $1/c_\infty$ with Poisson's ratio is shown in Fig. 14. It will be seen that in the range $0 < \mu < 0.4$ the error made by setting $1/c_\infty = 0.92$ for all μ is smaller than 6% which is quite insignificant for most practical problems. That $1/c_\infty = 0$ for $\mu = \frac{1}{2}$ is not surprising since this case corresponds to a situation where the half space is incompressible.

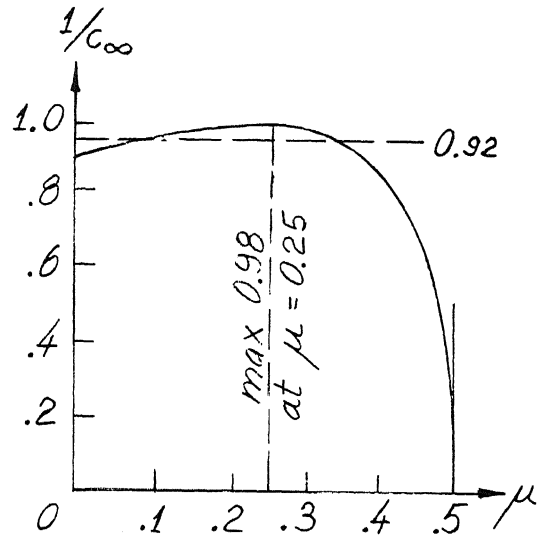

Fig. 14
Varation of $1/c_\infty$
with Poisson's Ratio

Intermediate Frequencies

At very low and very high frequencies we could estimate the distribution of the pressure under the footing. This method fails completely in the approximate range $1.5 < a_o < 8$, where the wavelengths of the waves propagated through the elastic half space and the dimension of the footing are of the same order of magnitude. A special method will therefore be developed for solving the problem in this range. The method is based on Reissner's (1) original solution for a uniform pressure distribution, and it will, for reasons which become apparent later, be called the ring method.

Reissner showed that the surface displacement function*

* For definition see Eq. 50 on page 21.

for the case of a uniform pressure distribution over a circular area of radius r_o is:

$$g(a,a_o) = \frac{1}{\pi}\int_0^{\infty} \frac{\sqrt{x^2-s^2}}{f(x)} J_1(a_o x) J_0(ax)\,dx + i\frac{\sqrt{x_o^2-s^2}}{f'(x_o)} J_1(a_o x_o) J_0(a x_o) \quad (57)$$

where

$$f(x) = (2x^2 - 1)^2 - 4x^2\sqrt{x^2-s^2}\sqrt{x^2-1} \quad (58)$$

x_o = The positive root of $f(x)$

J_o & J_1 = Bessel functions of the first kind

Equation 57 is valid for all values of a and a_o, but the integral has never been evaluated except for a = 0 and $a = a_o$, for which cases it is possible to establish a solution by series. As will be understood from the following, it is desirable to evaluate $g(a, a_o)$ for a larger range of a and a_o, and such an evaluation has been carried out in Appendix I, for the special case of Poisson's ratio equal to 1/3.

The actual pressure distribution under a rigid footing is not uniform, but varies in both phase and magnitude with the distance r from the center of the footing. However, in view of the rotational symmetry it can be assumed that the pressure is uniform over the area of any narrow ring which is concentric with the footing. The footing can therefore be replaced by the ring system shown in Fig. 15.

This system consists of n rings of equal width and the radii are consequently related through:

$$r_m = \frac{m}{n} r_n \quad (59)$$

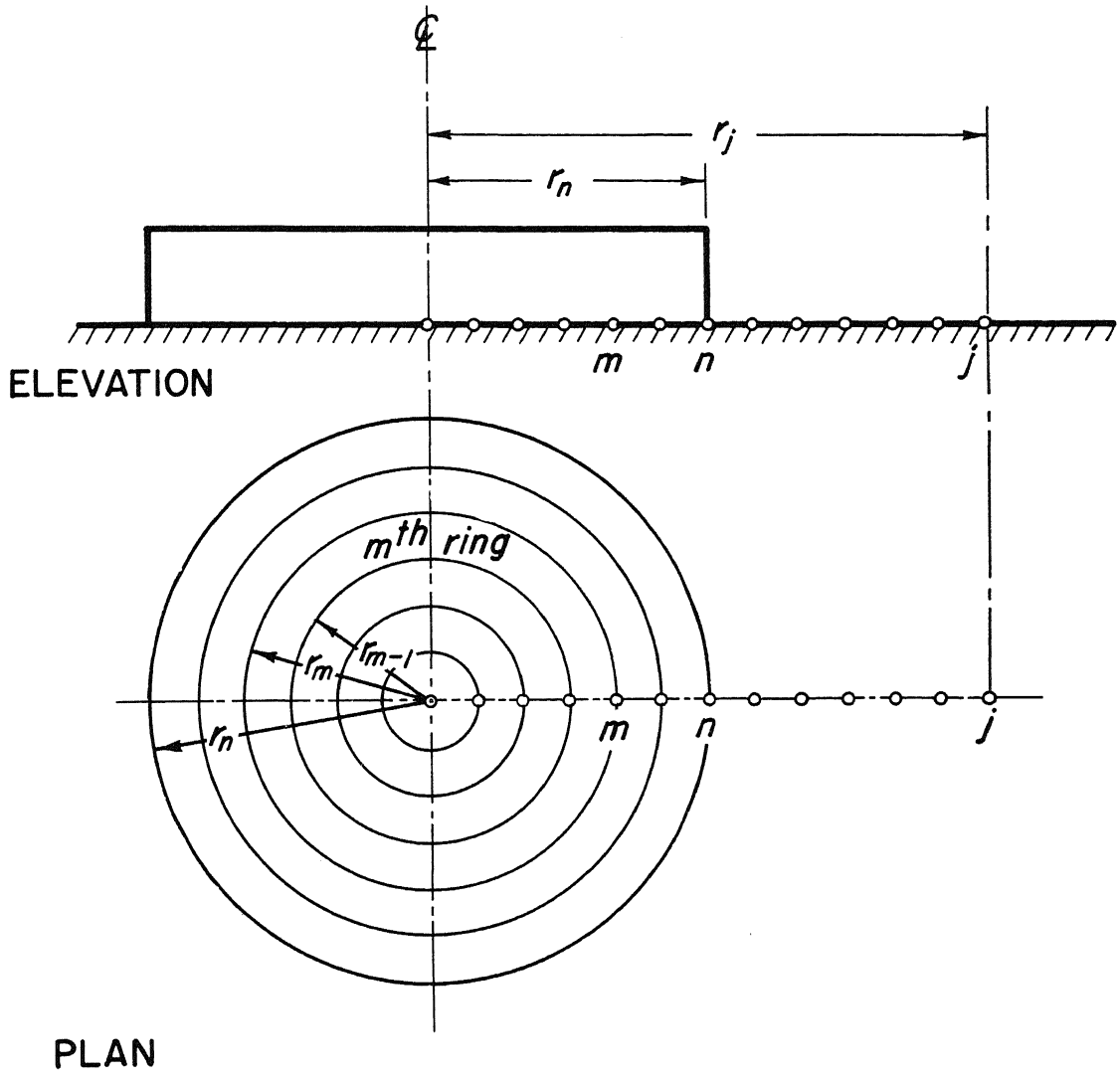

Fig. 15 Ring System

where r_n is identical to the parameter r_o used above.

The pressure over the m^{th} ring is uniform and harmonic and can be written as:

$$p_m = \frac{P_o}{\pi r_n^2} q_m e^{i\omega t} = \left(\frac{m}{n}\right)^2 \frac{P_o}{\pi r_m^2} q_m e^{i\omega t} \qquad (60)$$

where the pressure coefficient q_m is the ratio between the pressure over the m^{th} ring and the average pressure over the footing.

For small amplitudes of vibration the principle of superposition will be valid, and the vertical displacement of point j, due to the loading on the m^{th} ring, can therefore be calculated by Eq. 50. After a series of elementary calculations one arrives at the expression:

$$\delta_{jm} = \frac{P_o q_m}{G r_n n}\left[m g_{jm} - (m-1) g_{j,m-1}\right] e^{i\omega t} \qquad (61)$$

where

$$g_{jm} = g(a_j, a_m) \qquad (62)$$

$$a_m = \frac{m}{n} a_n = \frac{m}{n} \frac{r_n}{V_s} \omega \qquad (63)$$

The total displacement of point j can be found by summation over all the rings, and is most conveniently written in the form:

$$\delta_j = \frac{P_o e^{i\omega t}}{G r_n n} \sum_{m=1}^{n} q_m c_{jm} \qquad (64)$$

where

$$c_{jm} = m g_{jm} - (m-1) g_{j,m-1} \tag{65}$$

is a known influence coefficient.

If the above ring system is to be compatible with a rigid footing, it must be required that all the points j=1, 2...,n have the same displacement. The following must therefore be satisfied:

$$\delta_j = \delta_{j+1} \quad , \; j = 1, 2, \cdots, (n-1) \tag{66}$$

Substitution of Eq. 64 into this shows that the pressure coefficients q_m must satisfy the n-1 equations:

$$\sum_{m=1}^{n} q_m (c_{jm} - c_{j+1,m}) = 0 \quad , \; j = 1, 2, \cdots (n-1) \tag{67}$$

It must also be required that the total force over the n rings is equal to the exciting force $P_o e^{i\omega t}$. This condition yields the linear equation:

$$\sum_{m=1}^{n} a_m (2m-1) = n^2 \tag{68}$$

which is easily obtained from Eq. 60.

The relationships Eq. 67 and Eq. 68 form a complete set of n linear equations from which the pressure coefficients q_m can be determined. Both the coefficients and the

unknowns in these equations are complex variables, but this causes little extra difficulty as the complex equations can be transformed into a set of 2n linear equations between real quantities by simple separation of the real and imaginary parts.

Once the pressure coefficients are determined the vertical displacement of the footing can be calculated from Eq. 64 with j = n, i.e.:

$$\delta = \frac{P_o e^{i\omega t}}{G r_n n} \sum_{m=1}^{n} q_m c_{nm} \qquad (69)$$

This equation is of the same form as Eq. 52, and it is readily seen that the displacement function f is:

$$f(a_n, \mu) = \frac{1}{n} \sum_{m=1}^{n} q_m c_{nm} \qquad (70)$$

The displacement function F follows then from Eq. 53:

$$F(a_n, \mu) = \frac{-4}{n(1-\mu)} \sum_{m=1}^{n} q_m c_{nm} \qquad (71)$$

The ring method described above has been programmed for the IBM 7090 computer, and several runs have been made using systems of up to 20 rings and a value of 1/3 for Poisson's ratio.

The most significant result is the displacement function F shown with a dashed line in Fig. 16 and Fig. 12 and in tabular form on page 111 of Appendix II. It agrees well with

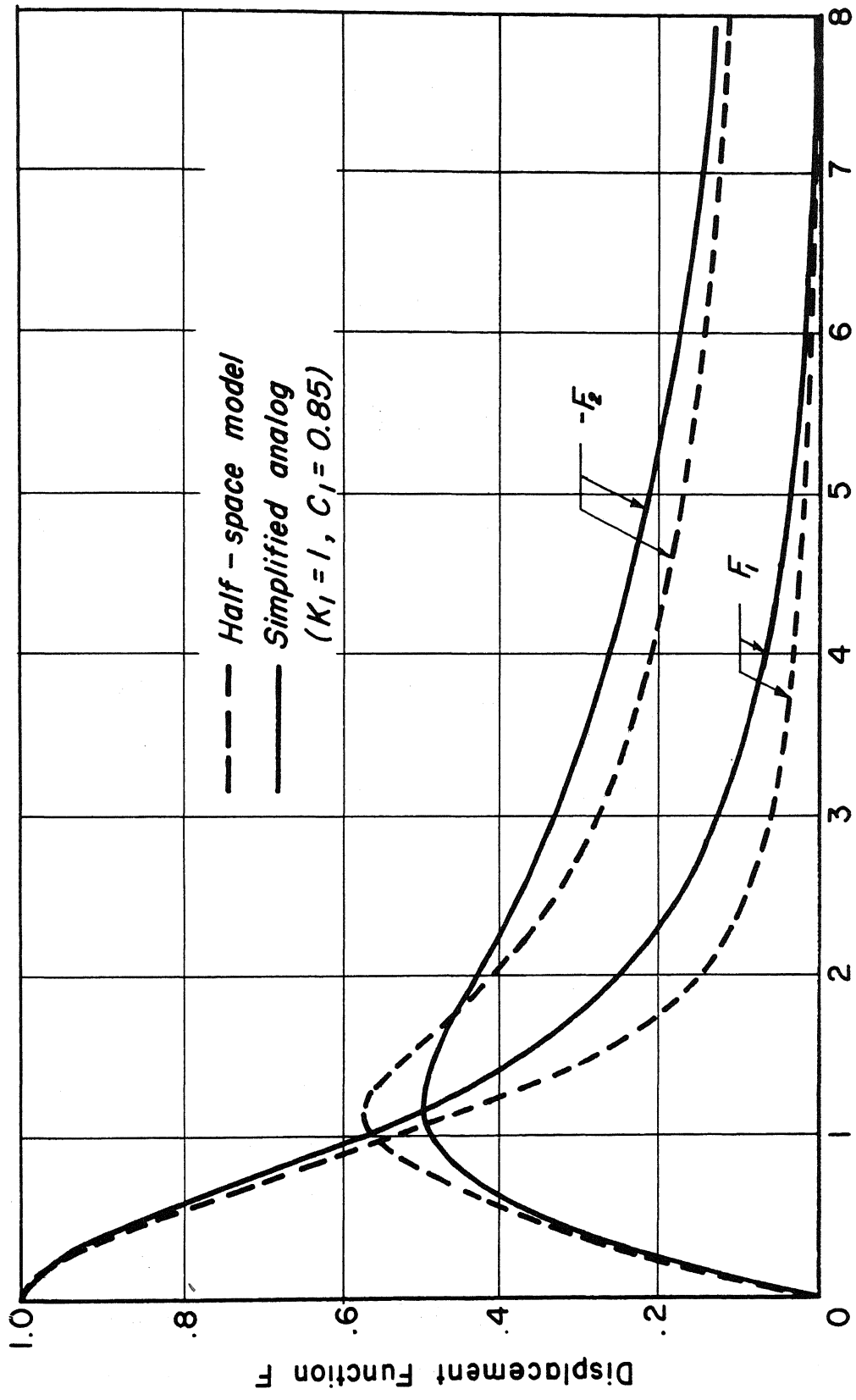

Fig. 16 Displacement Function for Footing-Soil System

Bycroft's solution in the low frequency range and approaches the asymptote given by Eq. 55.

It should be noted that the displacement function for the rigid footing-soil system is very similar to the displacement function for a spring-dashpot system, see Fig. 5.

It was shown previously that F is virtually independent of Poisson's ratio for both low and very high values of a_o. It is therefore realistic to assume that the variation of F is approximately as shown in Fig. 16 for all values of Poisson's ratio.

Knowing F we can again calculate c_1 and k_1. The results of these calculations are shown in Fig. 17 and also, for the low frequency range, in Fig. 13 (dotted curve).

It can be shown that $\lim_{a_o \to \infty} c_1 = c_\infty$, which was defined by Eq. 56. Also, it can be shown that $\lim_{a_o \to \infty} k_1$ exists, but the actual value is not known. This, however, is of little importance since the term $k_1 k \delta$ in Eq. 47 becomes insignificant at high frequencies.

Pressure Distribution

It is not the intention here to describe in detail the variation of the dynamic pressure distribution under a rigid footing, but, since it is generated as a by-product of the ring method, a single example is shown in Fig. 18. The steps shown are the real and imaginary parts of the pressure coefficients q_m, defined by Eq. 60, while the curves marked q_1 and q_2 are the supposed envelopes for the limiting case

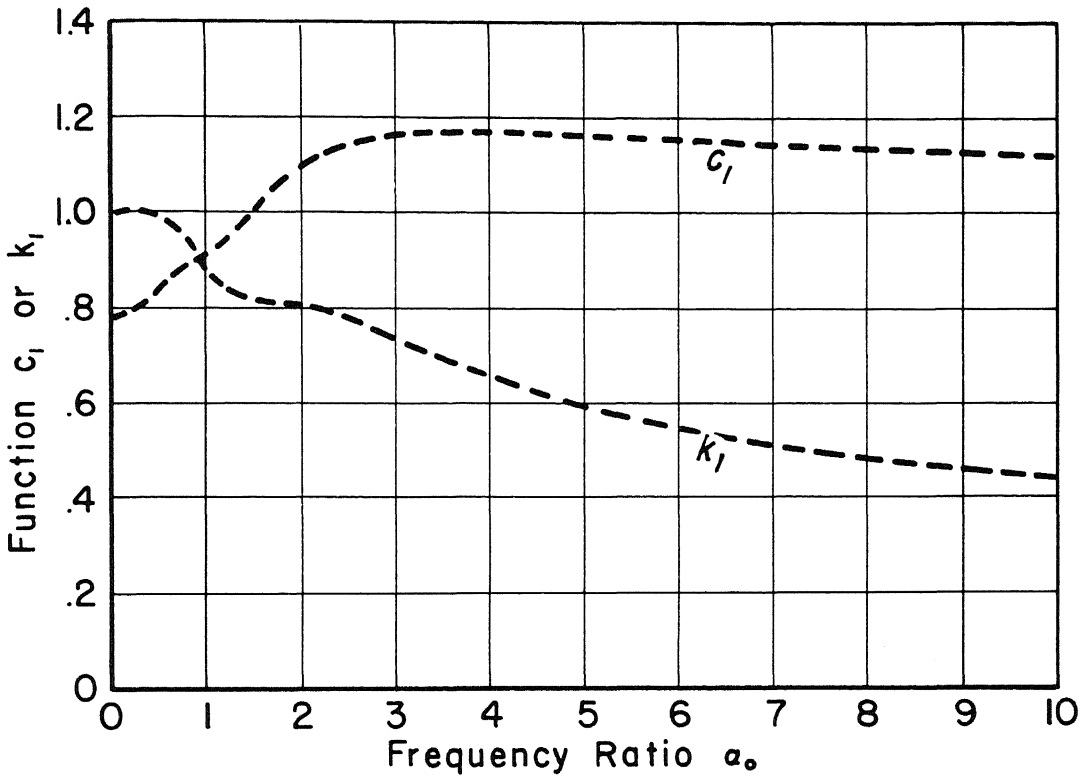

Fig. 17 The Functions k_1 and c_1
for Poisson's Ratio = 1/3

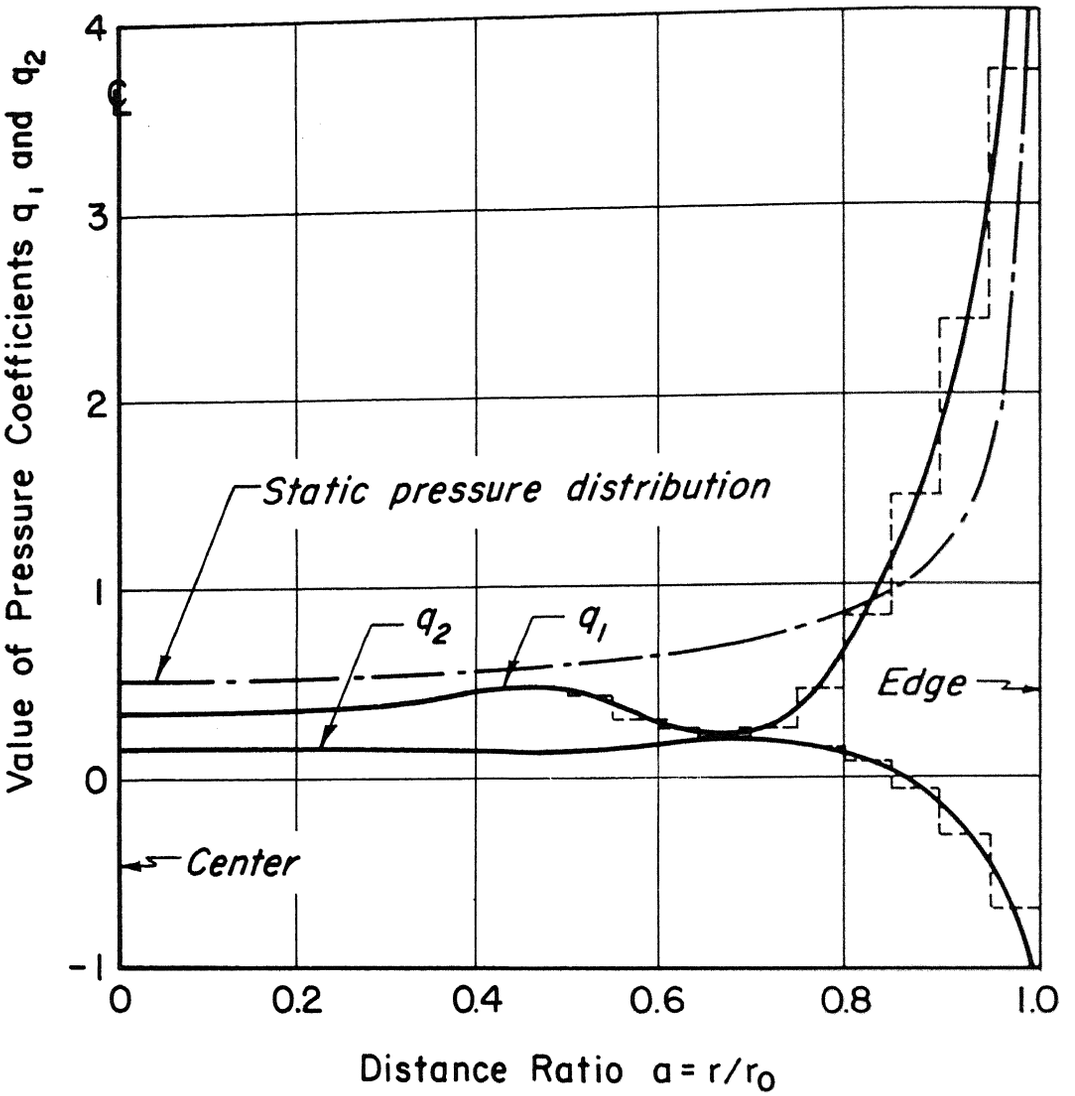

The real part of the pressure is

$$p(t) = \frac{P_0}{\pi r_0^2} (q_1 \cos \omega t - q_2 \sin \omega t)$$

Fig. 18 Pressure Distribution for the Case: $a_0 = 1$

of infinitely many rings. The pressure distribution is at any given time:

$$p(r,t) = \frac{P_o}{\pi r_o^2}(q_1 + iq_2)e^{i\omega t} \tag{72}$$

It will be seen that even at the relatively low frequency ratio $a_o = 1$ the distribution deviates significantly from the static distribution, which according to Eq. 49 is:

$$\left.\begin{aligned} q_1 &= \frac{1}{2\sqrt{1-(r/r_o)^2}} \\ q_2 &= 0 \end{aligned}\right\} \tag{73}$$

At higher frequencies the distribution becomes more complicated. The central part of the distribution remains relatively uniform while the part near the edge starts to oscillate violently forming a diverging wave.

Displacements of the Free Surface

Another by-product of the ring method is information about the vertical displacements of the free surface in the vicinity of an oscillating rigid footing. This displacement will vary in both phase and magnitude with the distance from the footing forming the vertical component of the Rayleigh wave (R-wave) created by the disturbance.

The displacement is readily calculated from Eq. 64 which is also valid for j greater than n. This equation can, therefore, be used to calculate not only F but also the complete surface displacement function defined by Eq. 50. Fig.

19 shows the real and imaginary parts of g for the special case, $a_o = 1$, and Poisson's ratio equal to 1/3.

The displacement has the form of a divergent wave. The wave length, in terms of the dimensionless distance a, is slightly shorter than 2π. By the definition of a, Eq. 51, this indicates that the actual wave length is slightly shorter than the wave length of the shear waves in the half space. This is in agreement with the current theories for the propagation of R-waves. See Rayleigh (9) or for a more recent presentation Ewing, Jardetsky and Press (10).

Response Spectra

Having determined the displacement function F we can now turn to the case where the footing has a certain mass m. It is here convenient to introduce the mass ratio:

$$B = \frac{m}{k}\left(\frac{V_s}{r_o}\right)^2 = \frac{1-\mu}{4}\frac{m}{\rho r_o^3} \qquad (74)$$

which is such that:

$$B a_o^2 = m\omega^2/k \qquad (75)$$

The above mass ratio is proportional to the mass ratio $b = m/\rho r_o^3$ used by other authors: Richart (5), Sung (2), etc.

The equation of motion can be obtained from Eq. 47 simply by adding an inertia term:

$$m\ddot{\delta} + c_1 \frac{k r_o}{V_s}\dot{\delta} + k_1 k \delta = Q_o e^{i\omega t} \qquad (76)$$

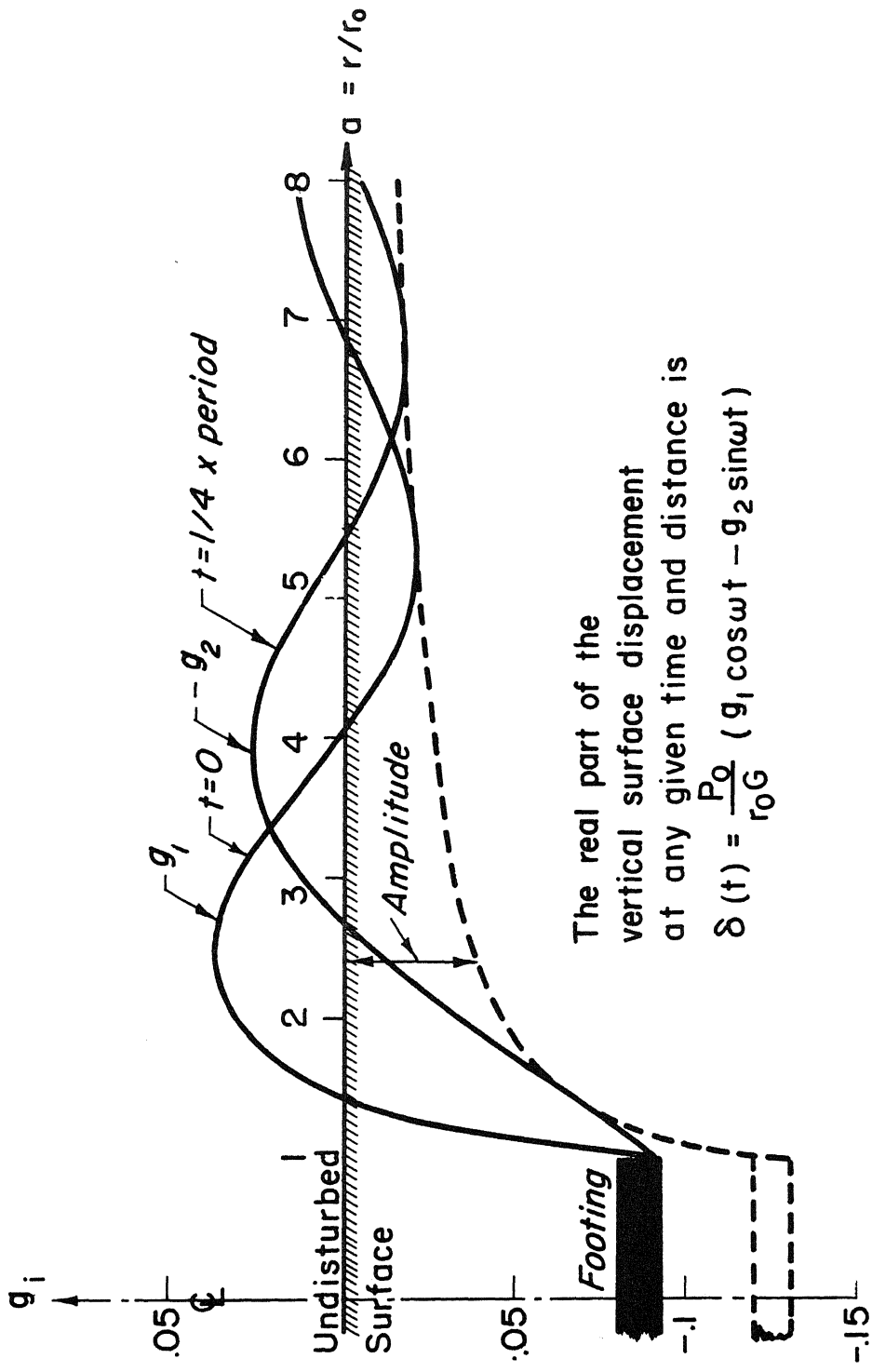

Fig. 19 Surface Displacements for the Case: $a_o = 1$, $\mu = 1/3$

which has a solution of the form:

$$\delta = \frac{Q_o}{K} \bar{F} e^{i\omega t} \tag{77}$$

This gives upon substitution into Eq. 76 the displacement function:

$$\bar{F} = \frac{1}{(k_1 - Ba_o^2) + ic_1 a_o} \tag{78}$$

The magnification factor, defined on page 8, is therefore:

$$M = \left|\bar{F}\right| = \frac{1}{\sqrt{(k_1 - Ba_o^2)^2 + (c_1 a_o)^2}} \tag{79}$$

from which the response spectra shown by solid lines in Fig. 20 have been calculated using the functions c_1 and k_1 shown in Fig. 16.

It was mentioned on page 34 that F is practically independent of Poisson's ratio and the same is therefore to be expected for $\bar{F}$. In fact, it is easily shown that the relative variation of $\bar{F}$ with μ is smaller than that of F. Hence, the spectra shown in Fig. 20 can be used for all values of Poisson's ratio.

The phase shift is:

$$\varphi = \tan^{-1} \frac{-c_1 a_o}{k_1 - Ba_o^2} \tag{80}$$

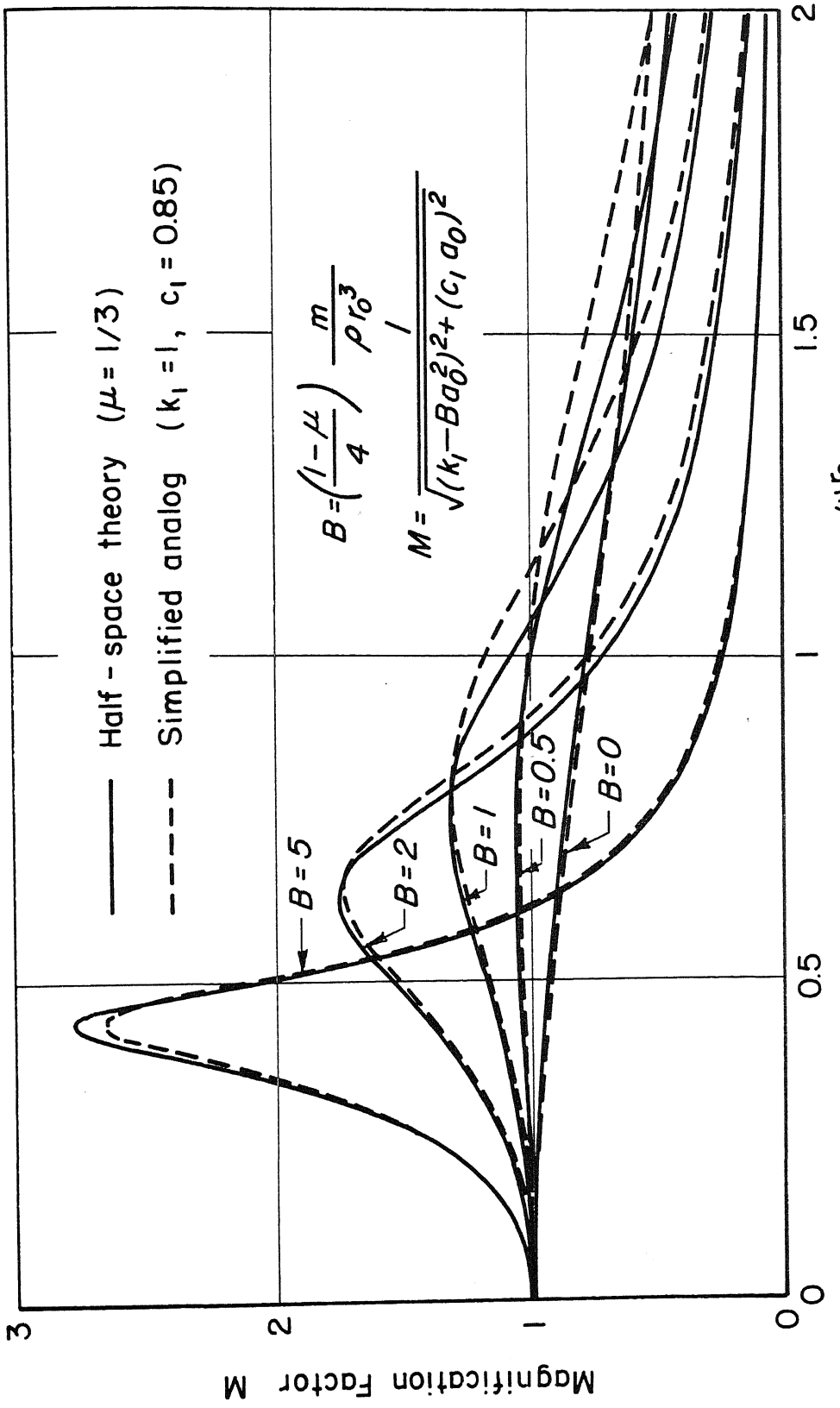

Fig. 20 Steady-State Spectra for Footing-Soil System

and the displacement caused by the exciting force $Q_o \cos \omega t$ is finally:

$$\delta = \frac{Q_o}{K} M \cos(\omega t + \varphi) \qquad (81)$$

Simplified Analog

The practical application of the above theory has shown that only limited agreement can be achieved between observed and calculated amplitudes. This is mainly due to discrepancies between the theoretical half-space model and an actual footing-soil system, the soil phase of which is generally nonlinear, inhomogeneous and imperfectly described. The mathematical difficulties involved in the strict use of the half-space model are therefore hardly justified, and even crude approximations can be introduced in practical calculations, without reducing the reliability of the calculated response. In particular, we can attempt to replace the half-space system with a simple damped oscillator with similar dynamic properties. One way of doing this would be to assign appropriate constant values to the functions c_1 and k_1 appearing in Eq. 76. This can be done as follows:

Since it has been established that c_1 and k_1 are bounded, see page 34, we conclude from Eq. 78 that for $B \neq 0$, which is generally the case, we have:

$$\overline{F} \approx \begin{cases} 1/k_1 \approx 1 & ; \quad a_o \ll 1 \\ -1/Ba_o^2 & , \quad a_o \gg 1 \end{cases} \qquad (82)$$

The last of these, with Eqs.75 and 77,gives the displacement:

$$\delta = -\frac{Q_o}{k}\frac{1}{Ba_o^2}e^{i\omega t} = \frac{-Q_o}{m\omega^2}e^{i\omega t} \qquad (83)$$

which shows that for $B \neq 0$ and $a_o \gg 1$ the response of the footing-soil system is completely independent of the properties of the elastic half space, hence we can choose c_1 and k_1 very freely in the high frequency range. This could also have been deduced from Eq. 76 by observing that the inertia term dominates the left side at high frequencies.

Equation 82 shows that in order to have agreement for the static case we must choose $k_1 = 1$. It also shows that at very low frequencies we can assign any value to c_1.

The influence of c_1 is strongest at the resonance peaks, that is in the range $0.3 < a_o < 0.8$, and it is therefore reasonable to choose c_1 as an average value over this range. Fig. 13 shows that 0.85 is appropriate. Thus,let:

$$c_1 = 0.85 \text{ and } k_1 = 1.00 \qquad (84)$$

This is equivalent to replacing the footing-soil system by a <u>simplified analog</u> consisting of a simple damped oscillator with the physical parameters:

$$\begin{aligned} m &= \text{mass of footing} \\ c &= 0.85\frac{k r_o}{V_s} = \frac{3.4}{1-\mu} r_o^2 \sqrt{G\rho} \\ k &= \frac{4Gr_o}{1-\mu} = \text{static spring constant} \end{aligned} \qquad (85)$$

The error made by this apparently bold approximation is surprisingly small as can be seen in Fig. 20 where the response spectra for the simplified analog are shown with dotted lines.

The relative error can be calculated from:

$$\frac{\Delta M}{M} = 1 - \sqrt{\frac{(k_1 - Ba_o^2)^2 + (c_1 a_o)^2}{(1 - Ba_o^2)^2 + (0.85\, a_o)^2}} \qquad (86)$$

and Fig. 21 shows how this error varies with a_o and B. It will be seen that the error is small in the important range $a_o < 0.8$ where both amplitudes and resonance frequencies can be calculated from the analog with an error which does not exceed 8%.

For larger values of a_o and small values of B the relative error might be as great as 35%. However, B-values below $\frac{1}{2}$, which correspond to very large and very light footings, are not usually encountered in practice and an error of 35% would therefore be most unusual. Furthermore, the absolute value of an error of this type will be small since it occurs on the tail of the response spectrum (see Fig. 20).

Another way of comparing the solution for the half-space model with that of the simplified analog is to compare the displacement functions for the two systems. This has been done in Fig. 16, which corresponds to the most unfavorable case B = 0.

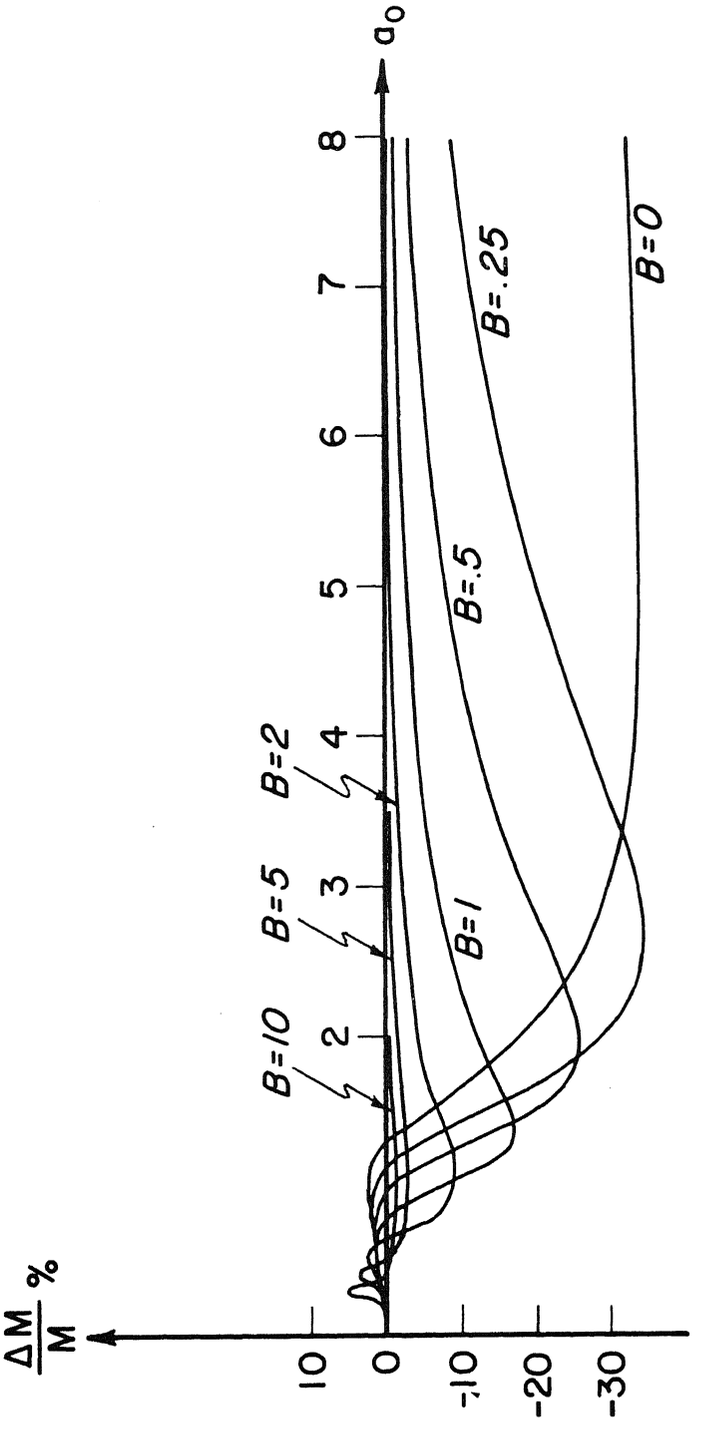

Fig. 21 The Relative Difference between the Spectra of the Half-Space Model and the Simplified Analog

Practical Formulas

Assuming the acceptance of the above simplified analog we can now set up the following set of formulas for the steady-state motion of the footing-soil system in Fig. 10:

Spring constant $$K = \frac{4 G r_o}{1-\mu} \tag{87}$$

Mass ratio $$B = \frac{1-\mu}{4} \frac{m}{\rho r_o^3} = \frac{1-\mu}{4} \frac{W}{\gamma r_o^3} \tag{88}$$

Frequency ratio $$a_o = \omega r_o \sqrt{\rho/G} = \omega r_o / V_s \tag{89}$$

Displacement amplitude $$A = \frac{Q_o/K}{\sqrt{(1-Ba_o^2)^2 + (0.85 a_o)^2}} \tag{90}$$

Phase shift $$\varphi = \tan^{-1} \frac{-0.85 a_o}{1 - B a_o^2} \tag{91}$$

Displacement $$\delta = A \cos(\omega t + \varphi) \tag{92}$$

Resonance occurs only when $B \gtrsim 0.36$ and one can establish the following approximate formulas for the resonance condition:

Resonance frequency $$\omega_{res} = \frac{V_s}{r_o} \frac{\sqrt{B - 0.36}}{B} \tag{93}$$

Resonance amplitude $$A_{res} = \frac{Q_o}{K} \frac{B}{0.85\sqrt{B - 0.18}} \tag{94}$$

Equations 3 and 4 were arrived from Eqs. 28 and 29 by observing that the mass and frequency ratios for the analog are:

$$\bar{B} = B\, k_1 / c_1^2 \approx B / 0.85^2 \qquad (95)$$

$$\bar{a}_o = a_o\, c_1 / k_1 \approx 0.85\, a_o \qquad (96)$$

Free Vibrations

Since the steady-state response spectra for the footing-soil system and its simplified analog show good agreement for all frequencies we can conclude that the two systems will behave similarly not only for steady-state excitation, but also for other types of dynamic loading. In particular, their free motions will be similar.

The natural damped frequency for a simple linear oscillator is:

$$\omega_d = \frac{k}{c} \frac{\sqrt{\bar{B} - 0.25}}{\bar{B}} \qquad (97)$$

Hence, by Eqs. 85 and 95, we obtain the following expression for the natural damped frequency of a footing-soil system:

$$\omega_d = \frac{V_s}{r_o} \frac{\sqrt{B - 0.18}}{B} \qquad (98)$$

which is good for B $\gtrsim$ 1/4. For B-values smaller than this the motion is either non-oscillatory or very strongly damped. Such small B-values are rarely encountered in technical applications.

The logarithmic decrement for a damped oscillator can

be shown to be:

$$\delta_{ln} = \ln (x_n / x_{n+1}) = \pi / \sqrt{B - 0.25} \qquad (99)$$

where x_n and x_{n+1} are consecutive displacement amplitudes to the same side. By substitution of Eq. 95 into this we obtain the following approximation to the logarithmic decrement for a footing-soil system:

$$\delta_{ln} = 2.67 / \sqrt{B - 0.18} \qquad (100)$$

Mass ratios higher than B = 5 are rarely encountered in practice and since the logarithmic decrement for this case is as high as 1.22, corresponding to $x_n / x_{n+1} = 3.4$, we conclude that <u>all normal footing-soil systems are strongly damped</u> by geometrical dispersion of wave energy.

<u>Rotating-Mass Systems</u>

Many important dynamic systems, such as mechanical oscillators and machine foundations, are excited by one or more eccentric rotating masses. A typical member of this class of systems is shown in Fig.22. The system is identical to the system S + m in Fig. 3 except for the mass m_1 which rotates relative to the mass m with eccentricity ℓ and angular frequency ω . The spring

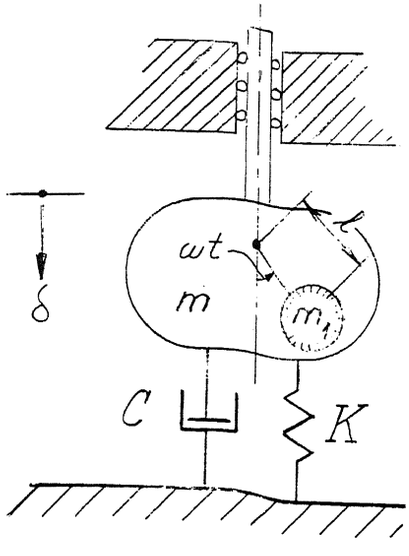

Fig. 22
Rotating-Mass System

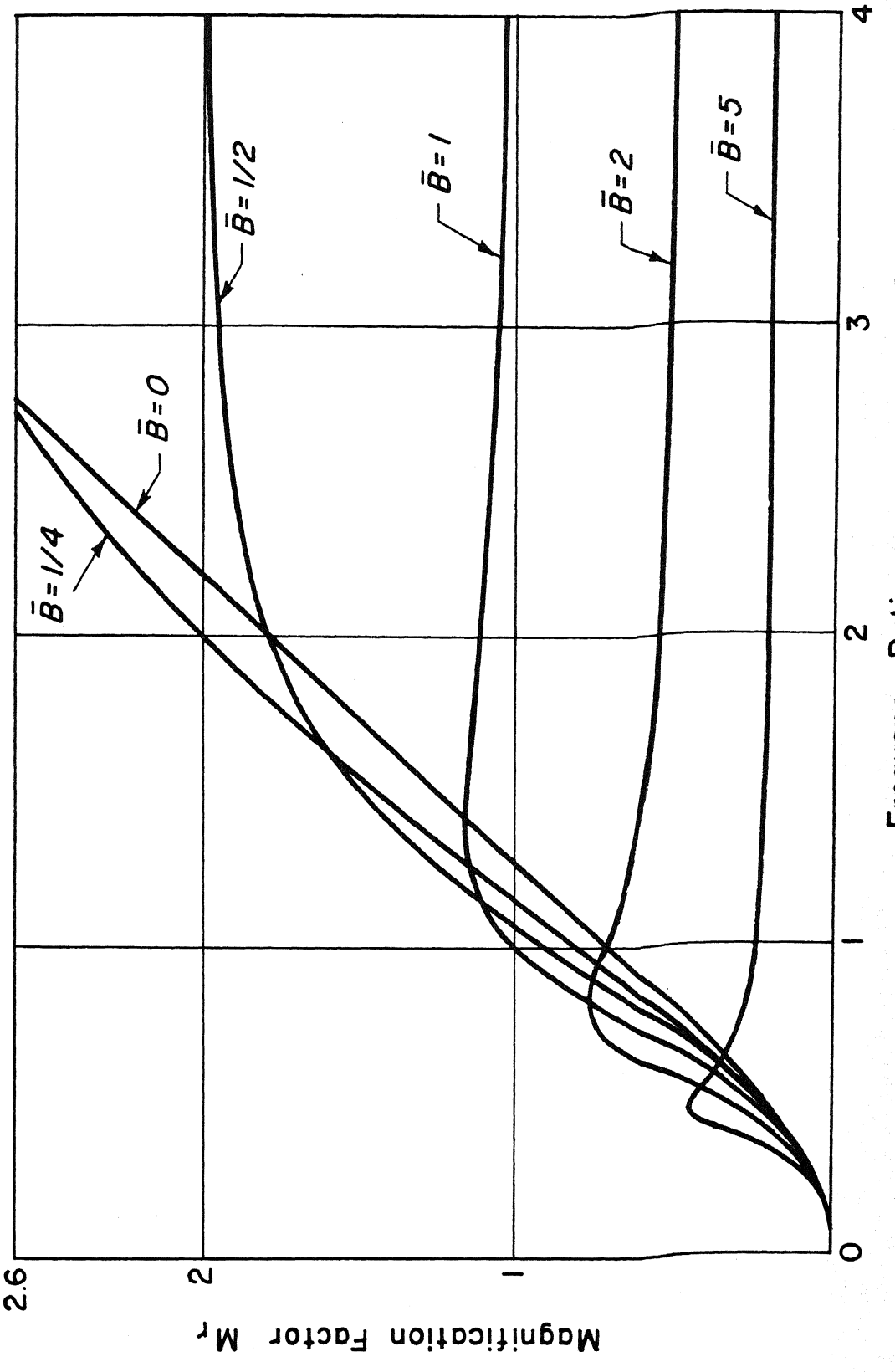

35)

36)

ing-

will

constant K and the damping constant C are frequency dependent and are defined by Eq. 6.

The equation of motion for the mass m is:

$$(m+m_1)\ddot{\delta} + C\dot{\delta} + K\delta = \omega^2 \ell m_1 \cos\omega t \qquad (101)$$

which shows that the system behaves like a system with the mass $m + m_1$ excited by the harmonic force $\omega^2 m_1 \ell \cos \omega t$.

For the special case of the simple damped oscillator, see Fig. 6, we can write this force as:

$$Q = \bar{a}_o^2 Q_1 \cos\omega t \qquad (102)$$

where

$$Q_1 = \left(\frac{k}{c}\right)^2 m_1 \ell \qquad (103)$$

Substitution of Eq. 102 into Eq. 25 gives directly the displacement:

$$\delta = \frac{Q_1}{k} \bar{a}_o^2 M \cos(\omega t + \phi) \qquad (104)$$

where M and ϕ are given by Eqs. 26 and 27 respectively.

The variation of the magnification factor:

$$M_r = \bar{a}_o^2 M = \bar{a}_o^2 \Big/ \sqrt{(1-\bar{B}\bar{a}_o^2) + \bar{a}_o^2} \qquad (105)$$

where

$$\bar{B} = k(m+m_1)/c^2 \qquad (106)$$

is shown in Fig. 23. For $\bar{B} > \frac{1}{2}$ it exhibits a resonance peak at:

$$\bar{a}_o = 1/\sqrt{\bar{B} - 1/2} \qquad (107)$$

with

$$\max M_r = 1/\sqrt{\bar{B} - 1/4} \tag{108}$$

and for all values of $\bar{B}$ it approaches the limit $1/\bar{B}$ as the frequency goes to infinity. This implies that the amplitude of displacement has the limit:

$$\lim_{\omega \to \infty} |\delta| = \frac{\ell m_1}{m + m_1} \tag{109}$$

This last formula is true for all rotating-mass systems of the general type shown in Fig. 22.

For the case of the half-space model it is practical to introduce the mass ratio:

$$B = \frac{m + m_1}{k} \left(\frac{V_s}{r_o}\right)^2 = \frac{1 - \mu}{4} \frac{W_{total}}{\gamma r_o^3} \tag{110}$$

With this variable the equivalents of Eqs.102 to 105 become:

$$Q = a_o^2 Q_1 \cos \omega t \tag{111}$$

$$Q_1 = \ell m_1 \left(\frac{V_s}{r_o}\right)^2 \tag{112}$$

$$\delta = \frac{Q_1}{k} M_r \cos(\omega t + \varphi) \tag{113}$$

$$M_r = a_o^2 M = \frac{a_o^2}{\sqrt{(k_1 - B a_o^2)^2 + (c_1 a_o)^2}} \tag{114}$$

The phase shift φ is, as for the constant force oscillator, given by Eq. 80.

The variation of M_r is shown in Fig. 24. The full lines correspond to the solution for the half-space model (c_1 and k_1 from Fig. 17) and the dotted lines correspond to a new simplified analog obtained by setting:

$$k_1 = c_1 = 0.90 \tag{115}$$

for all frequencies. This choice of k_1 and c_1 gives a somewhat smaller error in the practical region of resonance, see below, than the simplified analog defined by Eq. 84.

The new simplified analog is a simple damped oscillator for which:

$$\bar{a}_o = a_o c_1 / k_1 = a_o \tag{116}$$

$$\bar{B} = B k_1 / c_1^2 = B / 0.9 \tag{117}$$

These relations, in connection with Eqs. 107 and 108 give directly the following approximate formulas for the determination of the resonance peaks:

$$a_o = \sqrt{\frac{0.9}{B - 0.45}} \tag{118}$$

$$\max M_r = \sqrt{\frac{0.9}{B - 0.225}} \tag{119}$$

No peaks exist when $B \lesssim 0.45$ and the maxima for $B < .9$ are hardly significant enough to be classified as resonance peaks. Even for the heaviest footings we rarely encounter mass ratios greater than 5, and the practical range of resonance frequencies is therefore approximately $0.7 < a_o < 1.4$.

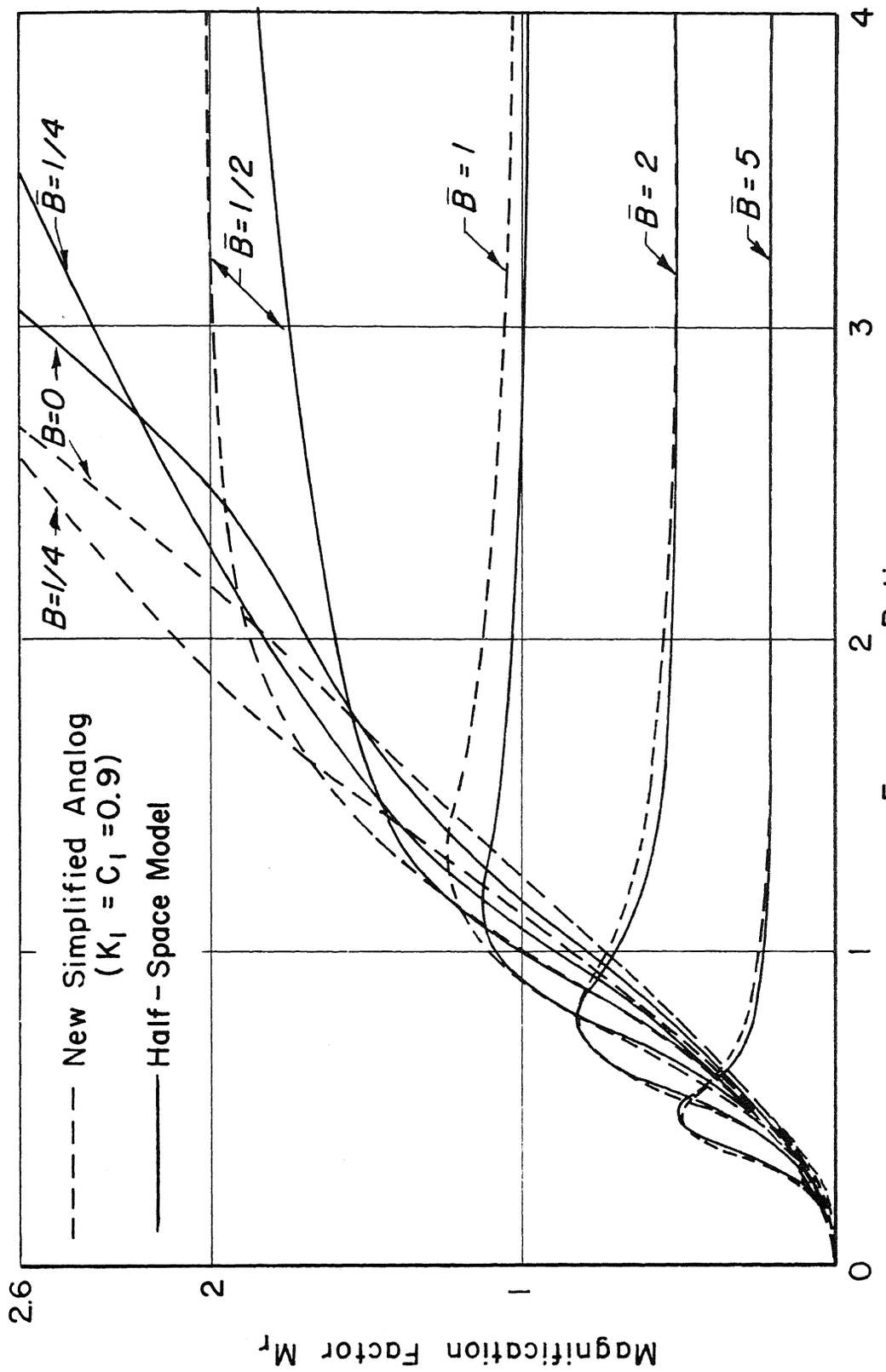

Fig. 24 Rotating-Mass Spectra for Footing-Soil System

III TRANSIENT MOTION

Numerical Method

The transient motion of a strongly damped linear system excited by a pulse of arbitrary shape and duration can be determined by a simple Fourier analysis if the steady-state solution for the system is known at all frequencies. In order to show this we first consider the motion of a footing-soil system excited by the vertical dynamic loading shown in Fig. 25. This loading consists of a train of identical pulses of alternating sign and duration d. The pulses are equally spaced with the time interval jd (j = integer), and the loading is therefore periodic with the period 2jd. The individual pulses can be expressed in the form:

$$Q(t) = Q_o \Phi\left(t/d\right) \tag{120}$$

where Q_o is the maximum value of the force, and Φ is a dimensionless pulse-shape function, see Fig. 26a.

The pulse train shown in Fig. 25 can be developed into a Fourier series of the form:

$$Q(t) = Q_o \sum_{n=0}^{N} c_n \cos\left(\frac{(2n+1)\pi t}{jd} + \psi_n\right) \tag{121}$$

where N is a large integer and

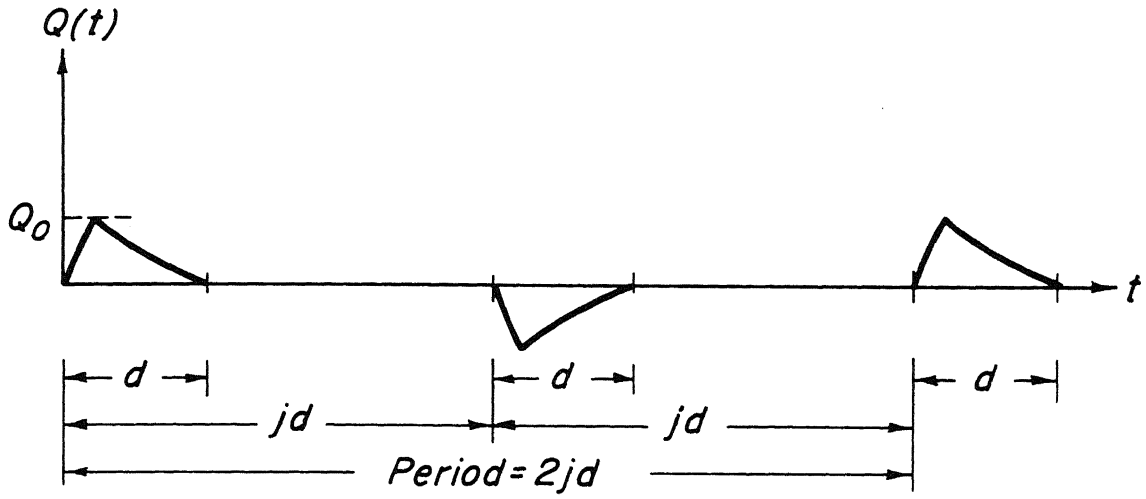

Fig. 25 Typical Pulse Train

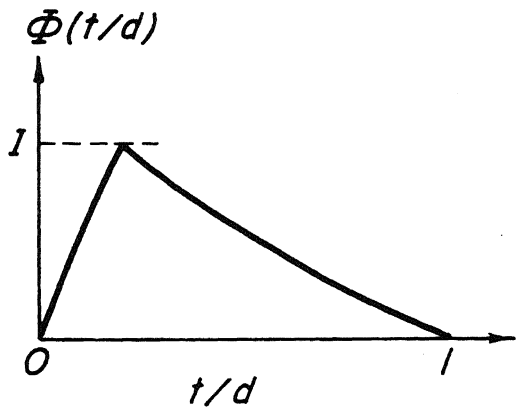

Fig. 26a

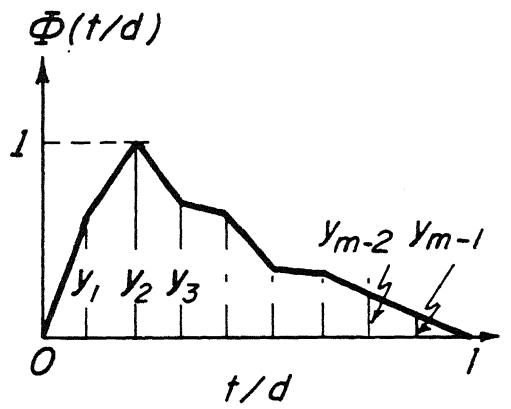

Fig. 26b

Typical Pulse-Shape Functions

$$c_n = \sqrt{\alpha_n^2 + \beta_n^2} \tag{122}$$

$$\psi_n = \tan^{-1} \frac{-\beta_n}{\alpha_n} \tag{123}$$

$$\left.\begin{aligned} \alpha_n &= \frac{2}{j} \int_0^1 \Phi(u) \cos\left(\frac{(2n+1)\pi}{j} u\right) du \\ \beta_n &= \frac{2}{j} \int_0^1 \Phi(u) \sin\left(\frac{(2n+1)\pi}{j} u\right) du \end{aligned}\right\} \tag{124}$$

For small amplitudes the principle of superposition is valid and a Fourier series for the displacement can therefore be obtained by applying Eq. 81 to each of the terms of Eq. 121. This gives:

$$\delta(t) = \frac{Q_o}{k} \sum_{n=o}^{N} b_n \cos\left(\frac{2n+1}{jd}\pi t + \varphi_n + \psi_n\right) \tag{125}$$

where

$$b_n = \frac{c_n}{\sqrt{(k_1 - B a_n^2)^2 + (c_1 a_n)^2}} \tag{126}$$

$$a_n = \frac{2n+1}{jd} \pi \frac{r_o}{V_s} \tag{127}$$

$$\varphi_n = \tan^{-1} \frac{-c_1 a_n}{k_1 - B a_n^2} \tag{128}$$

The variables k_1 and c_1 are functions of a_n and can be obtained from Fig. 17 or calculated from Eq. 46. Or, if it is desired to base the calculations on the simplified analog they can be set at the constant values 1.00 and 0.85 respectively.

Equation 126 shows that:

$$b_n \longrightarrow \frac{c_n}{Ba_n^2} \longrightarrow \frac{c_n}{n^2} \times const., \text{ for } n \longrightarrow \infty \qquad (129)$$

hence the series defined by Eq. 125 converges faster than the series given by Eq. 121. This means that a good approximation to the response of the footing can be obtained with a reasonably small number N of harmonics of the pulse train. This corresponds to the well-known phenomena for multi-degree of freedom systems, that most of the response occurs in the lower modes of vibration. A method for choosing the number N will be given below, see Eq. 143.

Now consider the behavior of the system under the influence of a pulse train with large spacing between the pulses (j large). During the period while a pulse is acting, energy is fed into the system and the amplitude of vibration will therefore increase. During the subsequent period, when no force is acting, the system will perform free vibrations which, since the system is strongly damped, will die out after a few oscillations. Hence, when the consecutive pulse arrives, the system will behave as if the previous pulse had never existed.

Consequently, if the above analysis is performed with a sufficiently large choice of j, the result will be a periodic displacement which, within each half period corresponds to the displacement due to a single pulse.

The above calculations are easily performed on an electronic computer and a FORTRAN II program for pulse shapes of

the piecewise linear type shown in Fig. 26b is presented in Appendix II. The program calculates not only the displacements but also the velocities and the accelerations which are easily obtained by differentiation of Eq. 125.

The piecewise linear pulse used in the program is particularly convenient because it makes it possible to replace the integral expressions of Eq. 124 by the following finite sums which are easy to handle in the computer:

$$\left.\begin{aligned} \alpha_n &= \frac{2jm}{(2n+1)^2\pi^2}\sum_{i=0}^{m}(2y_i - y_{i-1} - y_{i+1})\cos\frac{2n+1}{jm}i\pi \\ \beta_n &= \frac{2jm}{(2n+1)^2\pi^2}\sum_{i=0}^{m}(2y_i - y_{i-1} - y_{i+1})\sin\frac{2n+1}{jm}i\pi \end{aligned}\right\} \quad (130)$$

where

$$y_{-1} = y_o = y_m = y_{m+1} = 0 \quad (131)$$

The pulse type also has the advantage that the exciting force can be defined simply by specifying the ordinates y_1, $y_2 \cdots$, y_{m-1}, the duration d and the force level Q_o.

The Integers N and j

A few remarks should be given as to the choice of the integers j and N.

If the footing-soil system is of the oscillatory type, B large, it has, according to Eqs. 98 and 100, the approximate natural period:

$$T = \frac{2\pi}{\omega_d} \approx 2\pi\frac{r_o}{V_s}\sqrt{B} \quad (132)$$

and the logarithmic decrement:

$$\delta_{ln} = 2.7/\sqrt{B} \tag{133}$$

Hence, the amplitude of free vibration will vary as:

$$A = A_0 e^{-\left(\frac{2.7\,t}{\sqrt{B}\,T}\right)} \tag{134}$$

and the time t_1 necessary to reduce the amplitude to a fraction ε_1 of the initial amplitude is:

$$t_1 = -\frac{\ln \varepsilon_1}{2.7} T\sqrt{B} \approx -6B\frac{r_o}{V_s}\log_{10}\varepsilon_1 \tag{135}$$

For footing-soil systems of the non-oscillatory type, B small, it can be shown by considering the simplified analog that the amplitude varies according to the law:

$$A = A_0 e^{-\left(\frac{t\,V_s}{0.85\,r_o}\right)} \tag{136}$$

hence, we have for this case:

$$t_1 = -0.85\frac{r_o}{V_s}\ln\varepsilon_1 \approx -2\frac{r_o}{V_s}\log_{10}\varepsilon_1 \tag{137}$$

The estimates, Eq. 135 and Eq. 137, can be combined into the upper bound:

$$t_1 \approx -(2+6B)\frac{r_o}{V_s}\log_{10}\varepsilon_1 \tag{138}$$

which for all values of B can be used as an appropriate time interval between the individual pulses of the pulse train. This gives the following criterion for the integer j:

$$j > 1 - (2+6B)\frac{r_o}{V_s d}\log_{10}\varepsilon_1 \tag{139}$$

An appropriate choice of the integer N can be obtained by the condition that the magnification factor corresponding to the highest frequency ratio a_N appearing in the series Eq. 125 should be smaller than a certain value, say ε_2 . This gives by Eqs. 79 and 84 the following restriction on a_N:

$$\frac{1}{(1 - B a_N^2)^2 + (0.85 a_N)^2} < \varepsilon_2^2 \tag{140}$$

which since we generally have $Ba_N^2 \gg 1$ reduces to:

$$B a_N^2 > 1/\varepsilon_2 \tag{141}$$

But a_N is by Eq. 127:

$$a_N = \frac{(2N+1)\,\pi}{j\,d}\,\frac{r_0}{V_S} \tag{142}$$

which with Eq. 141 gives the following bound for N:

$$N > \frac{V_S\, j\, d}{2\pi\, r_0 \sqrt{B\varepsilon_2}} \tag{143}$$

The integer N can often be chosen considerably smaller than indicated by this inequality but such a reduction requires special consideration in each case.

It is usually rational to choose the ε's appearing in Eqs. 139 and 143 to be identical, say 0.05 or 0.01. Smaller values are hardly justified for practical calculations.

Trapezoidal Pulse

Consider the footing-soil system defined by:

$$\left.\begin{aligned} r_o &= 5\ ft\ ,\ G = 2500\ psi \\ W &= 483\ kips\ ,\ \gamma = 128.68\ pcf \\ \mu &= 1/3 \end{aligned}\right\} \quad (144)$$

The velocity of shear waves in the half space is by Eq. 41:

$$V_s = \sqrt{\frac{2500 \times 144}{128.68/32.17}} = 300\ ft/sec \quad (145)$$

and the mass ratio is by Eq. 74:

$$B = \frac{(1 - 1/3) \times 483{,}000}{4 \times 128.68 \times 5^3} = 5 \quad (146)$$

The latter shows that the system is of the oscillatory type. The damped natural frequency is by Eq. 98:

$$\omega_d = \frac{300}{5}\ \frac{\sqrt{5 - 0.18}}{5} = 26.3\ sec^{-1} \quad (147)$$

and the corresponding period is:

$$T = \frac{2\pi}{\omega_d} = 0.24\ sec \quad (148)$$

The logarithmic decrement is by Eq. 100:

$$\delta_{ln} = \frac{2.67}{\sqrt{5 - 0.18}} = 1.22 \quad (149)$$

and the ratio between consecutive amplitude maxima in free vibration is therefore 3.4 indicating a strongly damped system.

Now let this system be excited by the pulse shown in

Fig. 27. This pulse has the property of being constant, equal to 250,000 lb., for a period of 0.9 sec., which is considerably longer than the natural period of the system.

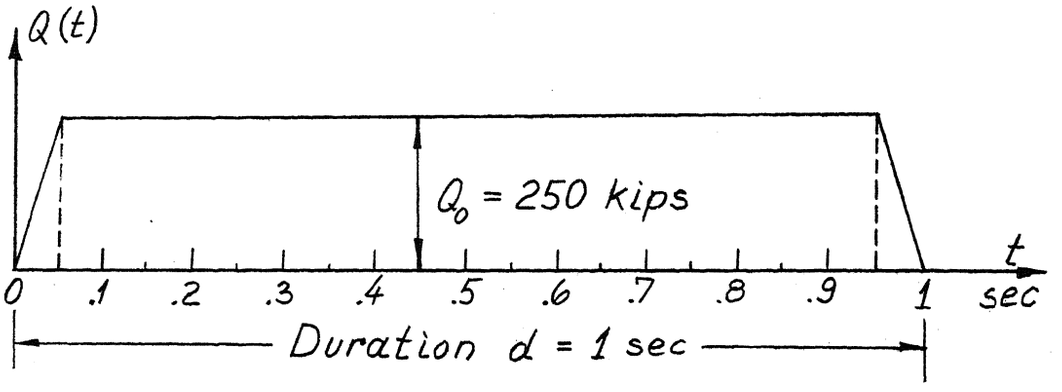

Fig. 27 Trapezoidal Pulse

Drawing from our knowledge of linear damped oscillations we therefore expect the footing to perform damped oscillations about the static displacement:

$$\delta_{static} = \frac{Q_0}{k} = \frac{250{,}000 \times (1-\frac{1}{3}) \times 12}{4 \times 2500 \times 144 \times 5} = 0.278'' \qquad (150)$$

As a check on this expectation the response was calculated by the method outlined above. The ε's were chosen to be 0.05 which gave: j = 2 and N = 40. The actual computer output is shown on page 116, and the displacements are shown graphically in Fig. 28 (full curve marked B = 5, G = 2500). It will be seen that the natural frequency, the amount of damping, and the static displacement agree with the figures calculated above.

The curves marked with the mass ratios B = 2, 1 and $\frac{1}{2}$

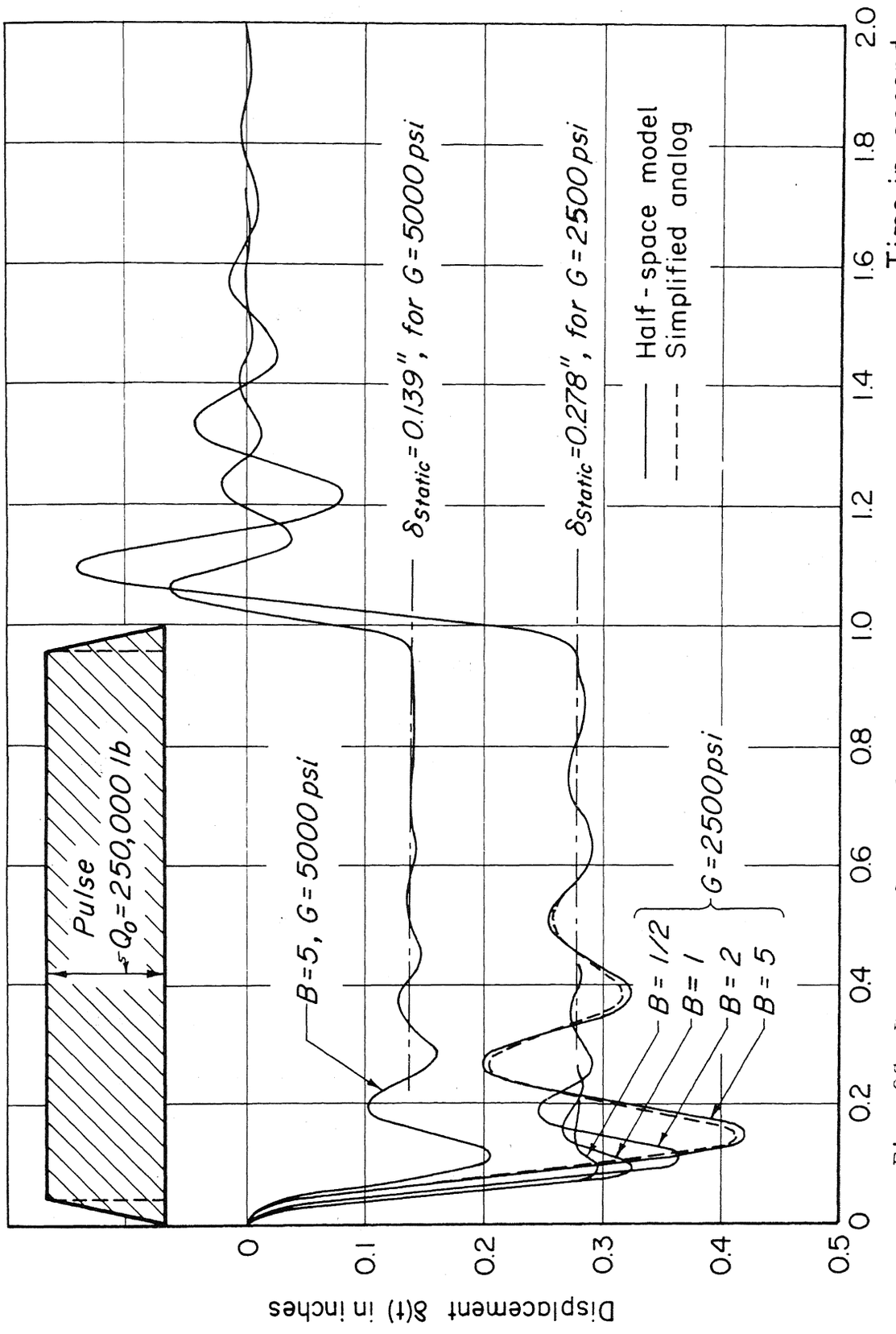

Fig. 28 Response Curves for Trapezoidal Pulse

show the effect of changing the weight of the footing while all other variables are being kept constant. The free motion of a light footing is, as expected, more strongly damped than that of a heavy footing.

An increase of the modulus G of the soil to say G = 5000 psi affects the magnitude of the vibrations of the system, but not its relative damping. This is illustrated by the curve marked B = 5, G = 5000.

All the above curves were obtained by applying the above Fourier method to the half-space model; i.e., using the functions c_1 and k_1 shown in Fig. 17 in the formulas Eqs. 126 and 128.

Exactly the same method can be used for the simplified analog defined by Eqs. 85. This is achieved simply by setting $c_1 = 0.85$ and $k_1 = 1$ and the result for the case B = 5, G = 2500 psi is shown with a dotted line in Fig. 28. The close agreement between the response of the simplified analog and that of the footing-soil system shows, as expected, that the analog can be used, not only for the case of steady-state motion, but also for transient motion.

This observation is of importance for practical calculations since the analog is a classical system, which can be treated by a variety of well known methods, such as numerical integration or phase-plane techniques, which do not require the availability of an electronic computer.

Triangular Pulse

As a second example, we will consider the behavior of a footing-soil system excited by the simple triangular pulse shown in Fig. 29. The displacement is given by Eq. 125, which after introduction of the dimensionless time:

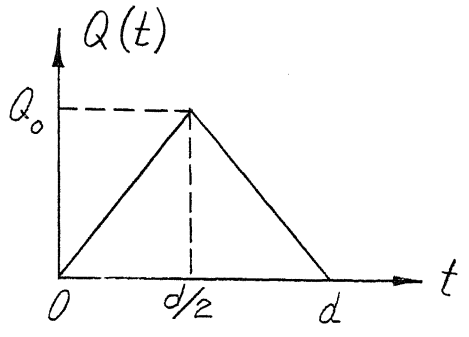

Fig. 29
Triangular Pulse

$$\tau = \frac{V_s}{r_o\sqrt{B}}\, t \qquad (151)$$

and the corresponding dimensionless duration:

$$\xi = \frac{V_s}{r_o\sqrt{B}}\, d \qquad (152)$$

can be written in the form:

$$\delta(\tau) = \frac{Q_o}{k}\, D(\tau, \xi, B) \qquad (153)$$

This expression shows that the maximum displacement can be expressed by:

$$\delta_{max} = \frac{Q_o}{k}\, D_{max}(\xi, B) \qquad (154)$$

where $D_{max}(\xi, B)$ is a dimensionless function which will be called the displacement spectrum. Its variation with ξ and B is shown in Fig. 30, which was determined by application of the above Fourier method to a series of selected footing-soil systems excited by triangular pulses of different duration. The dotted curves in the figure show corresponding

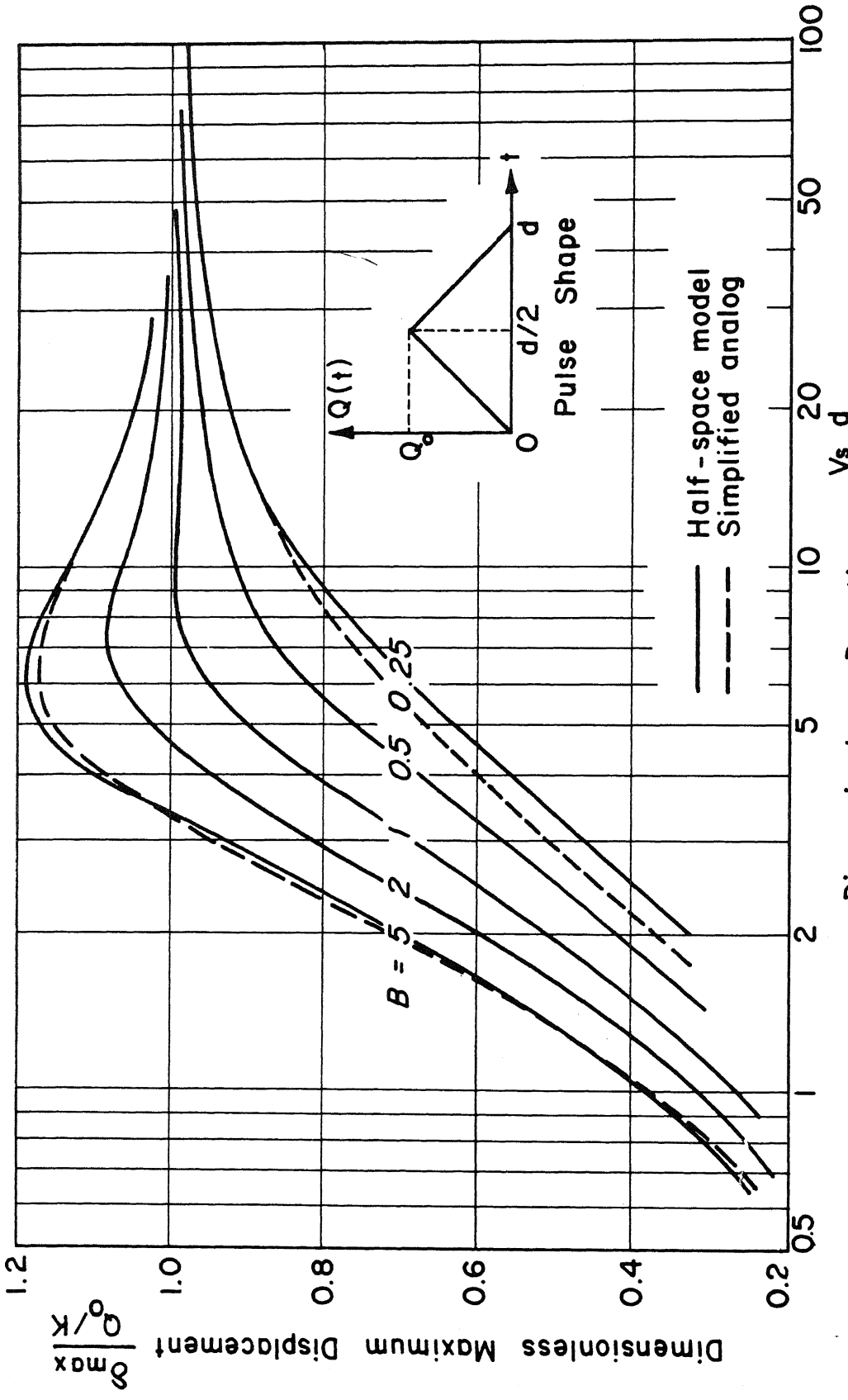

Fig. 30 Displacement Spectrum for Triangular Pulse

values calculated from the simplified analog. The close agreement between the two set of curves confirms again the feasibility of the suggested analog.

Displacement spectra of the type shown in Fig. 30 can be prepared for any pulse shape, not only for maximum displacements but also for maximum velocities and accelerations. They are of great practical interest since they constitute a simple and fast tool for the calculation of the maximum response of a given footing-soil system.

IV COMPARISON WITH TEST RESULTS

Several researchers have presented data which substantiate the elastic half-space theory presented above, at least for small displacements. Most of the data was obtained from steady-state tests in the low frequency range, $a_o < 1.5$, and special attention was given to the resonance condition. Lately this data has been supplemented by results from impact-loading tests.

Determination of Soil Properties

In studying the test results one must bear in mind that only limited agreement with the theory can be expected since soil is not a perfect elastic material. And, even under laboratory conditions it is not homogeneous nor isotropic. The determination of appropriate elastic constants to be used in the theory is therefore a difficult problem. An extensive survey of the available methods has been given by Whitman (11) and only two of the more promising methods will be described here. Both methods are dynamic, which is natural since the dynamic shear modulus of soil can vary widely from the static value, and both methods involve the determination of wave velocities.

The first method is triaxial dynamic testing. This technique has been developed by Shannon et al. (12), Hardin, Richart (13) and Hall (14). It involves the determination of the torsional and longitudinal resonance frequencies of cylindrical triaxial specimens. From these frequencies one can calculate the wave velocities V_s and V_p and the elastic constants of the half space follow then from:

$$\mu = \frac{1/2 - (V_s/V_p)^2}{1 - (V_s/V_p)^2} \tag{155}$$

and

$$G = \rho V_s^2 \tag{156}$$

Equation 155 can be derived from Eqs. 31 and 32 and Eq. 156 follows directly from Eq. 41.

The tests must be carried out at a confining pressure corresponding to the average pressure under the footing. This can be estimated by the theory of elasticity. For clean sand one can obtain a first estimate of G from the test results published by Hardin and Richart (13).

The second method to be discussed here will be called in-situ testing. It consists of two parts. First, the velocity of P-waves is measured by a simple seismic test. In this test a shock is induced at the soil surface by a drop weight or hammer and the arrival time of the first disturbance is recorded by a pick-up placed on the soil surface at a known distance from the source. Since the P-waves travel considerably faster than any other type of waves this gives a direct measurement of V_p. By comparing the arrival times

at different distances it is furthermore possible to determine the variation of V_p with the depth below the surface. For further details see Fry (17).

The second part of the in-situ method is a determination of the velocity V_R of Rayleigh surface waves by a method suggested by Jones (15) and further developed by Ballard (16) and Fry (17). In this method a small vertical oscillator is placed on the soil surface and the nodes of the resulting surface waves, R-waves, are located by means of a portable pick-up. From the distance between the nodes and the known frequency one can then calculate the velocity of the R-waves. This velocity is only slightly smaller than the velocity of S-waves. For soils one can assume that $V_S = 1.05\ V_R$. The actual ratio varies with Poisson's ratio and is equivalent to the variable x_o defined on page 28. Knowing V_S we can again calculate Poisson's ratio μ from Eq. 155 and the shear modulus G from Eq. 156. Without going into details it should be mentioned that the method can be refined to detect variations in V_S with the depth below the surface. This is done by performing the test at different frequencies. The idea being that low frequency R-waves penetrate deeper than waves of high frequency.

Steady-State Tests

Steady-state tests on footings were carried out long before the appearance of the first elastic half-space theories. Notable are the tests carried out at the Deutsche Forschungsgesellschaft für Bodenmekanik (DEGEBO). These

tests were analysed by Hertwig, Fruh and Lorenz (18) who, like the author, compared the vibrations of the footing-soil systems with that of a simple oscillator. However, while the author's model has the same mass as the footing, the above researchers were trying to set up a set of rules for determining the so called in-phase mass, which is the mass which has to be added to the mass of the footing in order to obtain agreement between the observed and the theoretical response. The search was only partly successful since it turned out that the in-phase mass depended on frequency and several other factors. In spite of this, the concept of the in-phase mass has since achieved great popularity among engineers and Hsieh (4) has shown how a frequency-dependent in-phase mass can, in fact, be calculated from the half-space theory.

The U. S. Army Engineer Waterways Experiment Station at Vicksburg, Mississippi, has carried out a very extensive program of steady-state field tests on circular concrete footings having diameters varying from 5 to 16 feet and excited by an oscillator of the rotating-mass type. Data were obtained for 63 tests on a silty clay (loess) and 39 tests on a uniform fine sand. The results were reported by Fry (6) and later analysed by Chae (7) and Whitman (11), who both found good agreement between the observed resonance amplitudes and the corresponding amplitudes calculated by the elastic half-space theory. The standard deviation from the predicted amplitudes was about 30% which must be characterized as satisfactory under field conditions. As could be

expected the agreement with the elastic theory was best for the cohesive soil.

A series of steady-state tests of special interest to the author was carried out at the University of Michigan by Chae (7) who, simultaneously with the author's theoretical work, determined the displacement functions f_1 and f_2 experimentally and studied the dynamic pressure distribution under a rigid footing on dry sand. For this purpose, a special footing was constructed, see Fig. 31. It consisted of a set of concentric steel rings, each of which was connected to a common rigid steel plate through four load cells. The latter were simply short pieces of aluminum tubing instrumented with SR-4 strain gages. These, in connection with additional electronic equipment, made it possible to determine the pressure distribution under the lower plate due to a static or dynamic loading on the upper plate.

The soil used in the tests was highly compacted Ottawa sand contained in a 4'-9" square sand bin with 4' high concrete block walls. The system was driven by an oscillator which could be placed on the upper plate of the footing by means of a special loading frame. The mass ratio B of the system could be varied from approximately 1 to 5 by means of special weights.

A summary of Chae's test results for the displacement function F is shown in Figs. 32 and 33. He actually found a small variation with the mass ratio of the footing, but this has been neglected for the purpose of the present presentation.

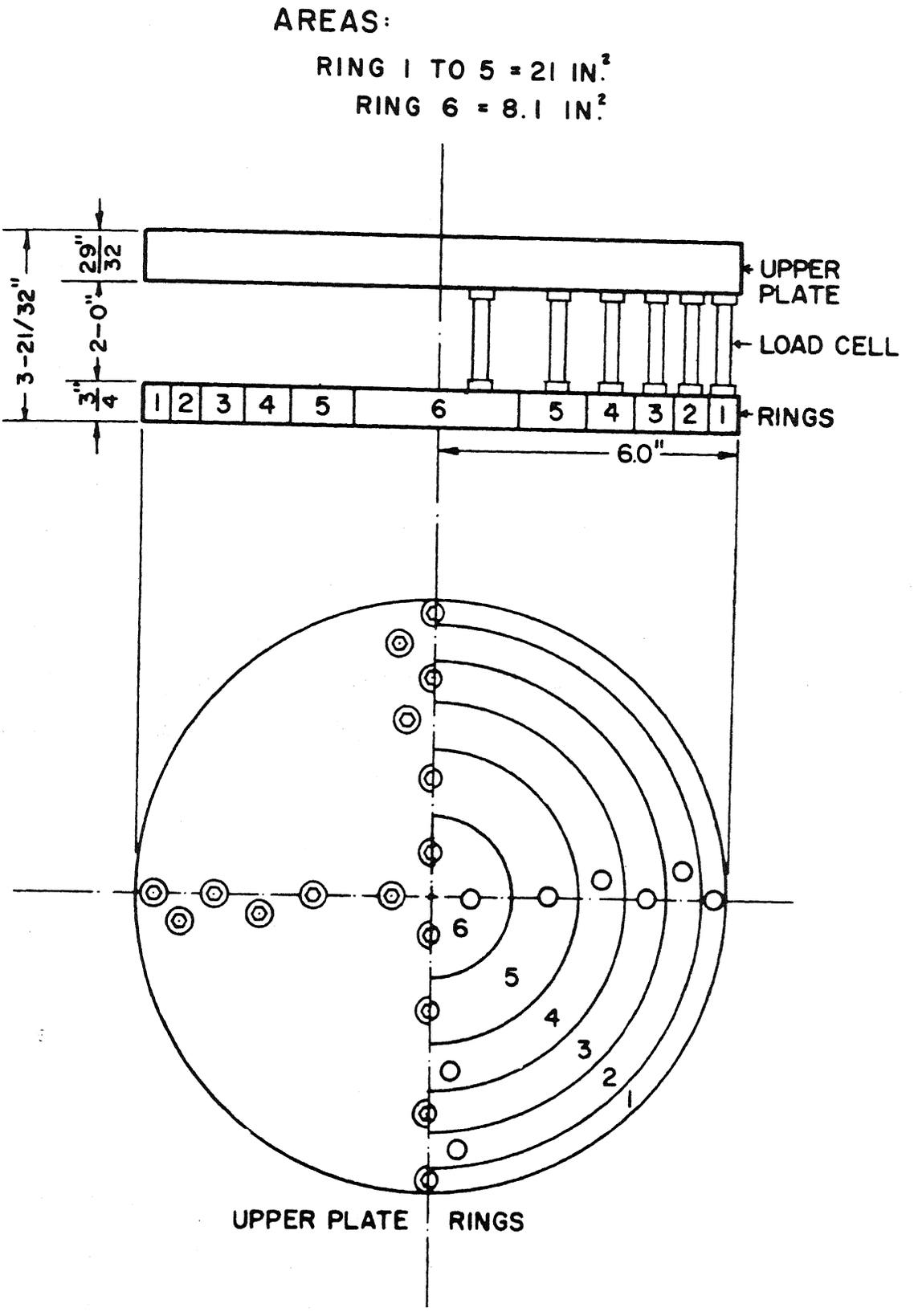

Fig. 31 Special Footing, from Chae (7)

The agreement with the author's theory is good except for F_1 at very low frequencies. This is not surprising since it is well known that the static pressure distribution under a footing on sand deviates drastically from the theoretical distribution given by Eq. 49. The actual pressure has a maximum under the center of the footing and vanishes at the edge. The effect of this change on the elastic half-space theory was studied by Sung (2) who assumed that the pressure distribution was parabolic and obtained the solution for F_1 shown in Fig. 32. It should be noted that Sung's solution is for the center of the loaded area ($r = 0$). The average displacement is therefore somewhat smaller than indicated by the curve. The large deviations on F_2 found at high frequencies can be explained by experimental errors, in particular difficulties in determining the phase shift and the fact that at high frequencies the inertia force from the mass of the footing over shadows the forces from the soil. These latter are therefore difficult to determine accurately and this is again reflected in the large scatter of the experimental values for F_1 and F_2. The inertia effect is, of course, the same as the one from which we profited on page 43 when we established the simplified analog.

Impact Tests

Data on impact tests is scarce in the literature but a series of tests which support the author's theory has been carried out at the University of Michigan and the results will be published shortly by Drnevich, Hall and Richart (8).

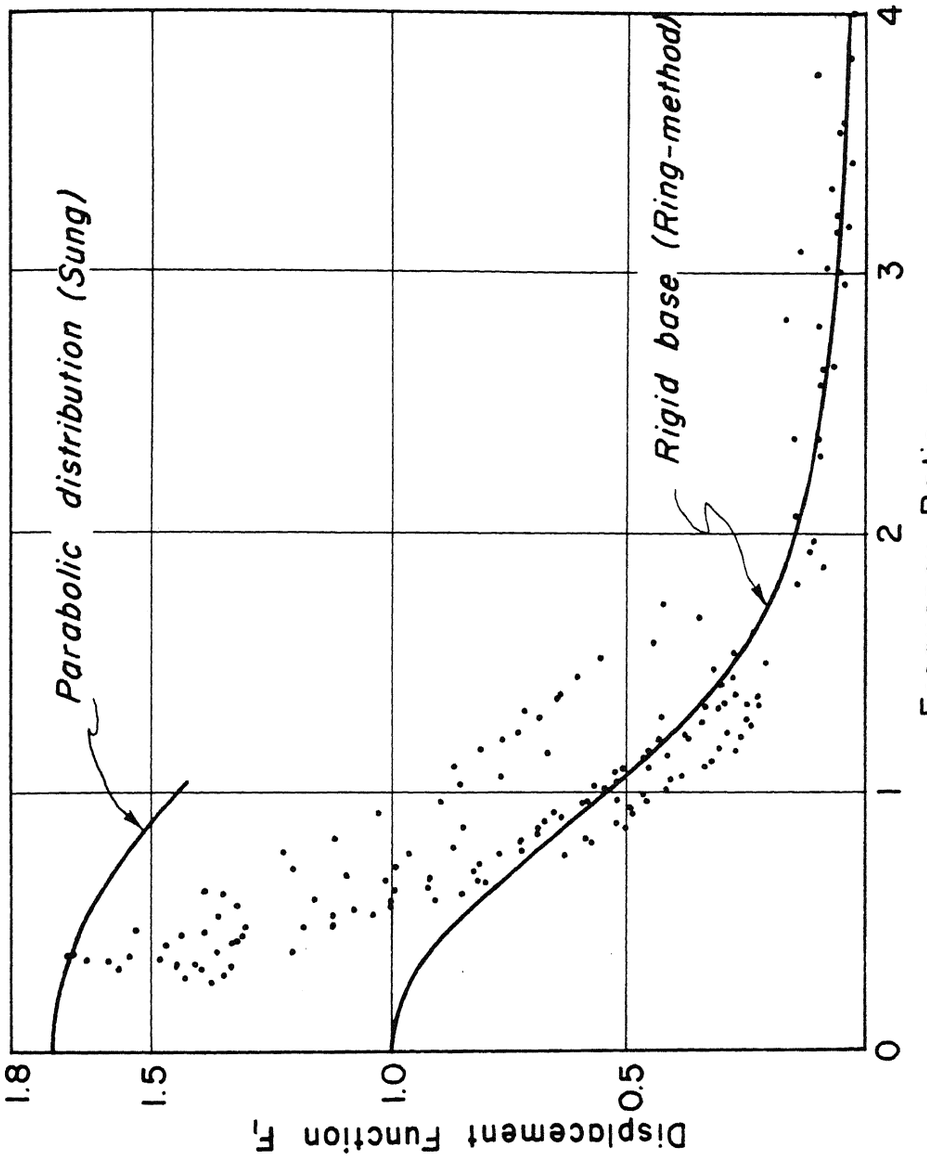

Fig. 32 Experimental Values for F_1 , by Chae (7)

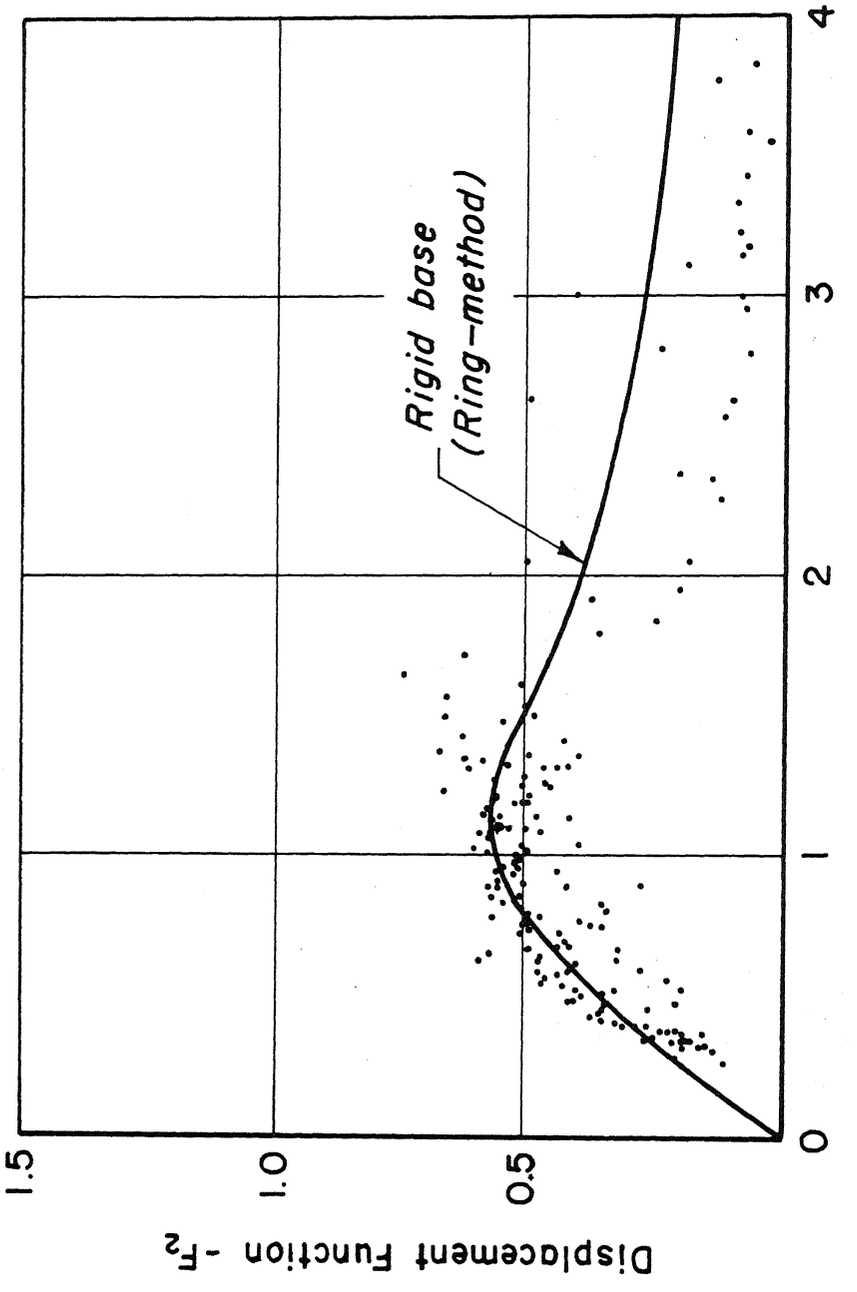

Fig. 33 Experimental Values for F_2 , by Chae (7)

The footing and the soil were exactly the same as that used by Chae (7) but the oscillator was replaced by a mechanism with which a small sand bag could be dropped on the top of a load cell placed on the upper plate of the footing. This simple arrangement made it possible to record the actual impact load on the footing and experience showed that both the shape and the duration of the pulse could be controlled by changing the height of fall and by placing different foam rubber pads on top of the load cell. The displacements were recorded in terms of accelerations which were obtained by means of an accelerometer mounted on the footing. The results of two tests are shown in Figs. 34 and 35 where they are compared with the theoretical response calculated by the method described in Chapter III. The actual computer output for one of the curves in Fig. 35 ($\mu = 1/4$) is shown on page 123 of Appendix II.

The agreement between the theoretical and the experimental curves is excellent up to a certain time, approximately 37 ms for test M-1, and then the curves suddenly lose their similarity. This can be explained as follows: The principal effect of the impact is the propagation of an S-wave from the footing towards the side walls of the sand bin and a P-wave towards the bottom of the bin. Both of these waves will be reflected by the walls. The half-space theory is therefore valid only up to the time when any one of these reflected waves arrive back at the footing. This return time is easily estimated. For test M-1 the shear

wave velocity is $V_s \approx 325$ ft/sec and assuming Poisson's ratio equal to 1/4 we find, by Eq. 32, $V_p = 560$ ft/sec. The S-wave has to travel approximately 4.75 ft; thus it returns back in 15 ms. The P-wave has to travel 8 ft and it returns to the footing in 14 ms. Since the peak of the pulse occurs at approximately 18 ms we can therefore expect serious deviation from the theory after 33 ms. This number agrees well with the 37 ms actually observed. For test T-3 the waves travel faster, therefore the disagreement occurs somewhat earlier.

Finally, it should be noted that it makes little difference which value of Poisson's ratio is used in the calculations. Therefore, it is hardly worthwhile to carry out special tests to establish a correct value for this ratio. An intelligent guess should be sufficient for most practical calculations. A value of 0.33 for dry soil and 0.50 for saturated soil will usually be accurate enough.

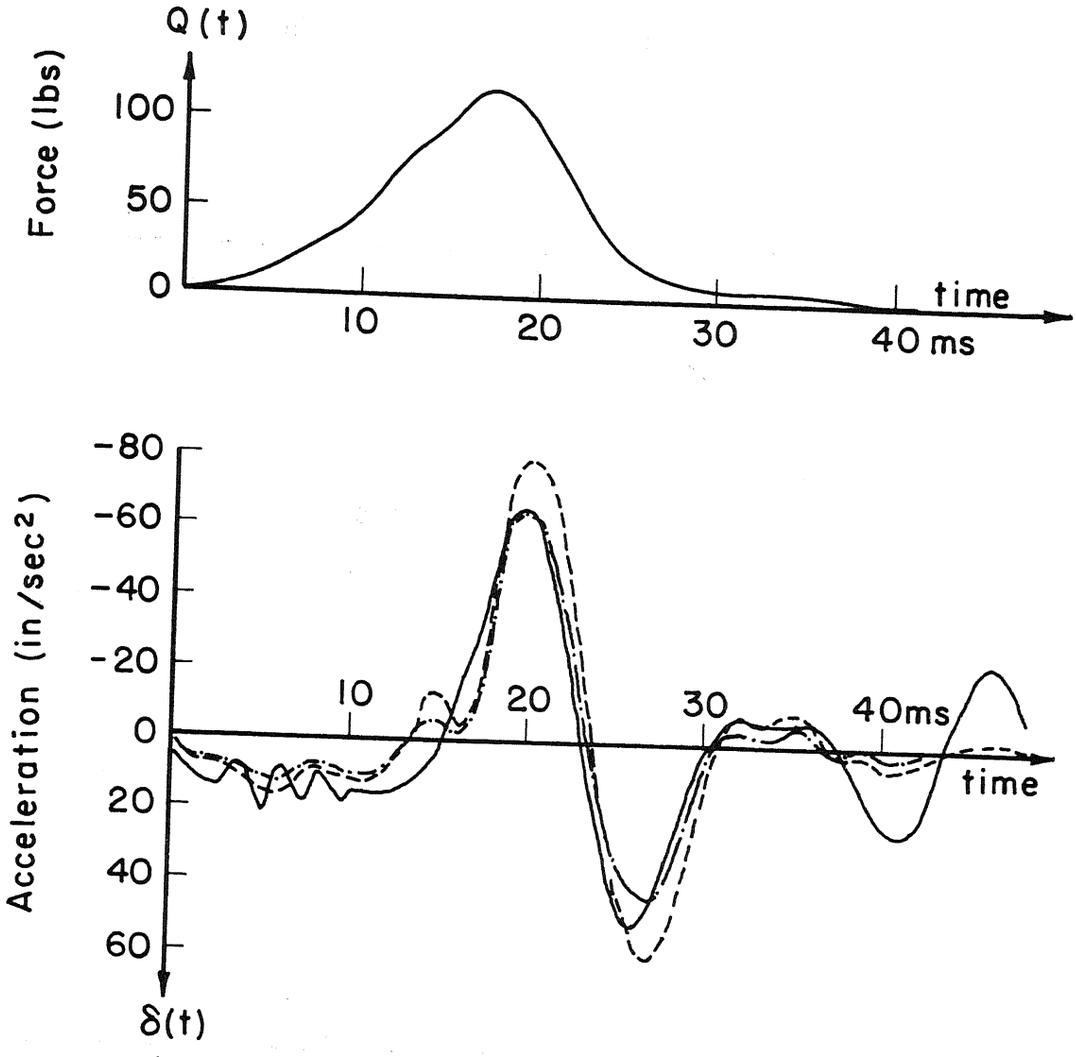

Fig. 34 Test M-1, by Drnevich, Hall and Richart (8)

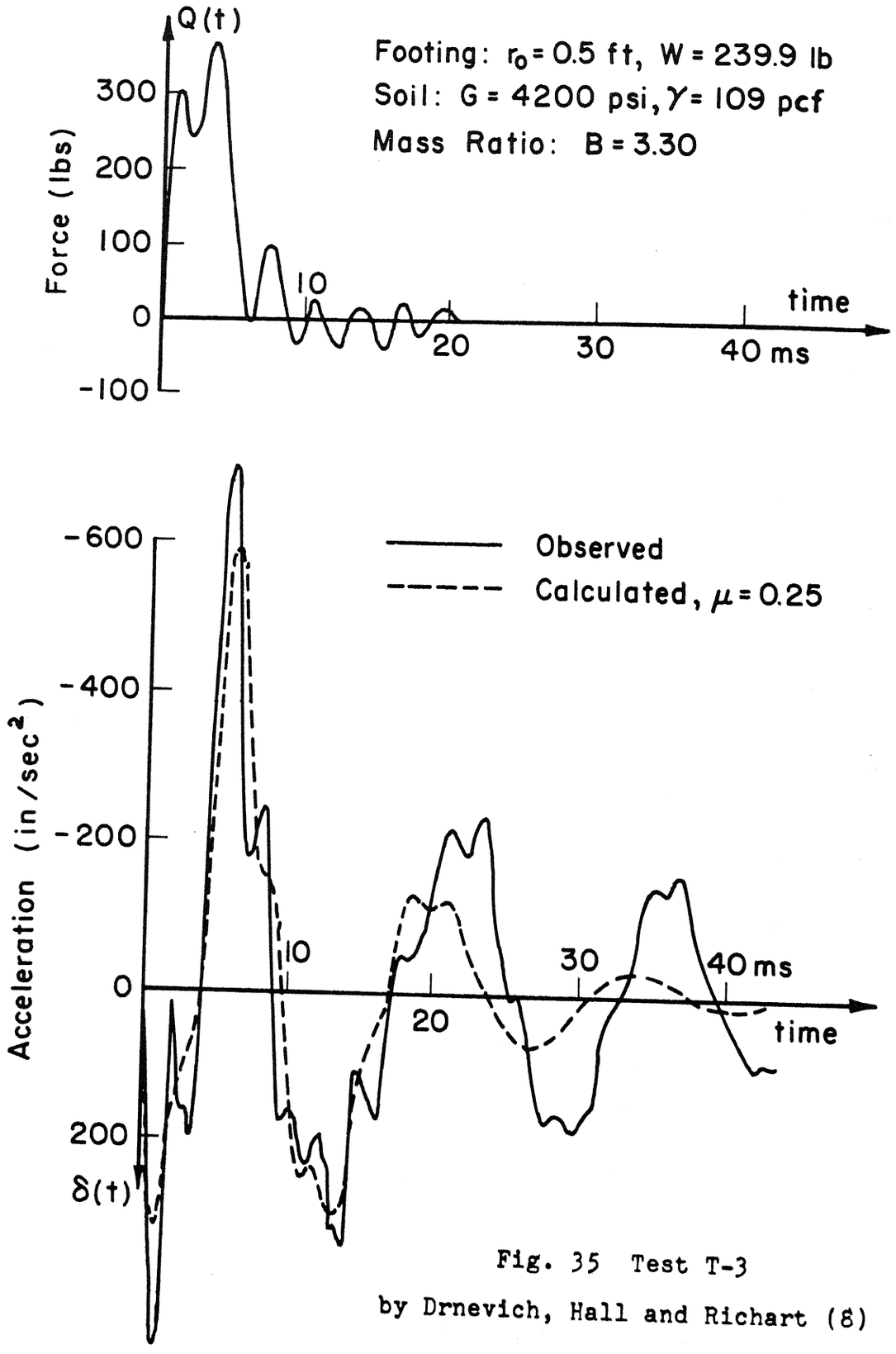

Fig. 35 Test T-3
by Drnevich, Hall and Richart (8)

V CONCLUSION

The half-space model considered in the preceding chapters is a compromise between mathematical convenience and accurate representation of an actual footing-soil system. However, the usefulness of the model has been clearly demonstrated by the fact that the discrepancies between calculated and observed displacements fall well within the range which one can expect for a soil-footing system, which by nature is rather poorly defined.

On the other hand, the observed discrepancies are significantly larger than the differences found between displacements calculated from the half-space model and corresponding displacements calculated from the simplified analog. The conclusion to be drawn from this must be that the simplified analog is to be preferred for its mathematical ease over the -only apparently- more accurate half-space model. Thus, the problem of determining the vertical motion of a footing-soil system has been reduced to the problem of determining the motion of a simple damped oscillator defined by the following equation of motion:

$$m\ddot{\delta} + \frac{3.4}{1-\mu} r_o^2 \sqrt{\rho G}\, \dot{\delta} + \frac{4 G r_o}{1-\mu} \delta = Q(t) \qquad (157)$$

This analog, which is the most important result of the present work, can be solved by several well known methods such as direct or numerical integration, phase plane, etc.

The study shows that all footing-soil systems are strongly damped due to wave propagation into the subsoil. This geometrical damping will generally be much more significant than the material damping of the soil and the latter can therefore be neglected in practical calculations. The damping ratio decreases with increasing mass ratio of the system and the motion of a large and light footing will therefore be more strongly damped than that of a small and heavy footing.

The theory developed in the preceding chapters is a linear theory. It therefore applies only as long as the displacements can be considered small as compared to the size of the footing. Also, it is assumed that the footing and the soil are in physical contact at all times. This means that the soil reaction $R(t) = P(t) + W$ must not become negative in which case the footing will jump free of the ground. This latter limitation is of little consequence for practical design, since footings are usually dimensioned with a certain safety factor against jumping. However, several steady-state test results have been published which indicate that jumping occured during the tests and in some of these tests the deviations from the half-space theory were considerable.

Only the vertical mode of vibration has been considered. However, the nature of the energy dissipation for the other

modes (rocking, sliding, torsion) is basically the same as that of the vertical mode, and it is therefore reasonable to expect that simple spring-dashpot analogs can be developed also for these modes. Once these analogs have been developed it will be a relatively simple matter to include the dynamic characteristics of the foundation in the analysis of a superstructure with several degrees of freedom.

APPENDIX I

REISSNER'S DISPLACEMENT FUNCTION

Reissner's surface displacement function was defined on page 28 but will be repeated here for convenience:

$$g(a,a_o) = \frac{1}{\pi}\int_0^\infty \frac{\sqrt{x^2-s^2}}{f(x)} J_1(a_o x) J_0(ax)\,dx + i\frac{\sqrt{x_o^2-s^2}}{f'(x_o)} J_1(a_o x_o) J_0(a x_o) \quad (158)$$

where

$$s^2 = (1-2\mu)/2(1-\mu)$$

μ = Poisson's ratio

$$f(x) = (2x^2-1)^2 - 4x^2\sqrt{x^2-s^2}\,\sqrt{x^2-1}$$

x_o = The positive real root of $f(x)$

J_o and J_1 = Bessel functions of the first kind

The function $f(x)$ is called the Rayleigh function. It can be shown that this function has only one real positive root x_o, and that this root is slightly greater than unity. Without going into details it should be mentioned that x_o is the ratio between the velocity V_s of shear waves and the velocity V_R of the Rayleigh surface waves for the elastic half space.

The independent variables a and a_o are, according to their definition, always positive and real, and so is the integration parameter x.

The integral appearing in Eq. 158 is not directly suited for numerical integration for the following reasons:

1) The integrand is not defined in the point $x = x_o$ where $f(x)$ has a root
2) The interval of integration is infinite.
3) The integrand is in general complex.
4) At the point $a_o = a = 0$ the integral can attain infinitely many values, depending on the manner in which a and a_o approach the origin.

Function Definitions

Fortunately all the above difficulties can be overcome. In order to show this it is convenient first to consider the behavior of the following functions, which are all related to the Rayleigh function:

$$f(x) = (2x^2-1)^2 - 4x^2\sqrt{x^2-s^2}\sqrt{x^2-1}\ , \begin{cases} 0 \le x \le s \\ 1 \le x < \infty \end{cases} \quad (159)$$

$$f^*(x) = (2x^2-1)^2 + 4x^2\sqrt{x^2-s^2}\sqrt{x^2-1}\ , \begin{cases} 0 \le x \le s \\ 1 \le x < \infty \end{cases} \quad (160)$$

$$f^{**}(x) = f(x)f^*(x) = 16(s^2-1)x^6 - 8(2s^2-3)x^4 - 8x^2 + 1 \quad (161)$$

$$bes(x) = J_o(ax)J_1(a_o x) \quad (162)$$

The intervals shown with Eqs. 159 and 160 are the intervals in which the functions attain real values.

Also consider the following functions:

$$r(x) = \left[\sqrt{s^2-x^2}/f(x)\right] bes(x) \quad , \quad 0 \leq x \leq s \qquad (163)$$

$$t(x) = \left[4x^2(x^2-s^2)\sqrt{1-x^2}/f^{**}(x)\right] bes(x) \quad , 0 \leq x \leq 1 \qquad (164)$$

$$u(x) = \left[(2x^2-1)^2\sqrt{x^2-s^2}/f^{**}(x)\right] bes(x) \quad , s \leq x < \infty \qquad (165)$$

$$v(x) = \left[\sqrt{x^2-s^2}/f(x)\right] bes(x) \quad , 1 \leq x < \infty \qquad (166)$$

$$w(x) = v(x) + v(2x_o - x) \quad , 1 \leq x < \infty \qquad (167)$$

$$P(x) = f^{**}(x)/(x^2-x_o^2) \quad , 0 \leq x < \infty \qquad (168)$$

$$h(x) = \sqrt{x^2-s^2}\, f^{*}(x)\, bes(x)/P(x) = v(x)(x^2-x_o^2) \qquad (169)$$

The intervals shown with the definitions are the intervals in which the functions attain real values. The question as to whether the functions are actually defined in all points of the given intervals will be left to the subsequent sections.

It is clear that the function f*(x) has no root greater than s. Hence, the function f**(x) has only one root $x = x_o$

in the interval $x > s$. Eq. 168 shows that, since f**(x) is a polynomial in x^2 and has the root $x^2 = x_o^2$, also P(x) is a polynomial in x^2. Furthermore, since P(x) has no roots for x greater than s the function h(x) is finite for all values of x greater than unity.

By substitution of Eq. 169 into Eq. 167 we obtain:

$$w(x) = \frac{h(x)}{x^2-x_o^2} + \frac{h(2x_o-x)}{(2x_o-x)^2-x_o^2} \qquad (170)$$

or

$$w(x) = \frac{(x-3x_o)h(x) + (x+x_o)h(2x_o-x)}{(x-x_o)(x+x_o)(x-3x_o)} \qquad (171)$$

This function is not defined in the point $x = x_o$ where both the numerator and the denominator have a root, but its limit for $x \to x_o$ exists and can be found by L'Hospital's theorem. In order to show this we differentiate the numerator and the denominator of Eq. 171 in the point $x = x_o$:

$$num'(x_o) = 2h(x_o) - 4x_o h'(x_o) \qquad (172)$$

$$den'(x_o) = -4x_o \qquad (173)$$

and L'Hospital's theorem gives directly:

$$\lim_{x \to x_o} w(x) = h'(x_o) - \frac{h(x_o)}{2x_o} \qquad (174)$$

Since h(x) is finite and has a finite derivative in the point $x = x_o$ it is obvious that the limit exists. Hence, the singularity of w(x) in the point $x = x_o$ is removable and w(x) is continuous for all values of x greater than unity. The

actual value of the limit can be determined, but it is of no interest as the calculations can be planned in such a way that it is not necessary to know this quantity.

For the special case $s^2 = \frac{1}{2}$ both f*(x) and f**(x) have the root $x^2 = \frac{1}{2}$, and the functions r(x), t(x), and u(x) are therefore not defined in this point. However, also these singularities can be removed, which is easily shown by L'Hospital's theorem.

From what has been said up to this point it is a simple matter to establish that the following functions are real, finite and continuous in the intervals stated below:

$$\left.\begin{array}{lll} r(x) & , & 0 \leq x \leq s \\ t(x) & , & 0 \leq x \leq 1 \\ u(x) & , & s \leq x \leq 1 \\ v(x) & , & 2x_0 - 1 \leq x < \infty \\ w(x) & , & 1 \leq x \leq x_0 \end{array}\right\} \qquad (175)$$

Separation of the Real and Imaginary Parts

Reissner's displacement function can be written as:

$$g(a, a_0) = g_1 + i g_2 \qquad (176)$$

where g_1 and g_2 are the real and imaginary parts respectively. By simple complex algebra, which will not be repeated here, it can be shown that:

$$g_1 = \frac{1}{\pi}\int_s^1 u(x)\,dx + \frac{1}{\pi}\int_1^\infty v(x)\,dx \qquad (177)$$

and

$$g_2 = \frac{1}{\pi}\int_c^s r(x)\,dx + \frac{1}{\pi}\int_s^1 t(x)\,dx - \frac{\sqrt{x_o^2 - s^2}}{f'(x_o)}\,bes(x_o) \quad (178)$$

where, according to Eq. 175, all the integrals are real.

The integrand v(x) is not defined in the point $x = x_o$, but this difficulty can be overcome by writing:

$$\left.\begin{aligned}\int_1^\infty v(x)\,dx &= \int_1^{x_o} v(x)\,dx + \int_{x_o}^{2x_o-1} v(x)\,dx + \int_{2x_o-1}^\infty v(x)\,dx \\ &= \int_1^{x_o}\left[v(x) - v(2x_o - x)\right]dx + \int_{2x_o-1}^\infty v(x)\,dx \\ &= \int_1^{x_o} w(x)\,dx + \int_{2x_o-1}^{K} v(x)\,dx + \pi R\end{aligned}\right\} \quad (179)$$

where

$$R = \frac{1}{\pi}\int_K^\infty v(x)\,dx \quad (180)$$

is the remainder after cutting off the integration at some large value K of the parameter x.

Substitution of Eq. 179 into Eq. 177 gives:

$$g_1 = \frac{1}{\pi}\int_s^1 u(x)\,dx + \frac{1}{\pi}\int_1^{x_o} w(x)\,dx + \frac{1}{\pi}\int_{2x_o-1}^{K} v(x)\,dx + R \quad (181)$$

In this formula, and in Eq. 178, all the integrands are real and continuous in closed intervals of integration and the integrals can therefore be evaluated by numerical integration if x_o and K are given.

Calculation of x_o and $f'(x_o)$

The root x_o is most conveniently determined from f**(x) by Newton's iterative method:

$$x_{n+1}^2 = x_n^2 - f^{**}(x_n) \Big/ \frac{d}{d(x^2)} f^{**}(x_n) \tag{182}$$

where

$$\frac{d}{d(x^2)} f^{**}(x) = 48(s^2-1)x^4 - 16(2s^2-3)x^2 - 8 \tag{183}$$

This will yield the values of both x_o and $d(f^{**}(x_o))/d(x^2)$, and $f'(x_o)$ can then be calculated as follows:

By Eqs. 159 and 160:

$$f^{*}(x_o) = 2(2x_o^2-1)^2 \tag{184}$$

By differentiation of Eq. 161:

$$2x_o \frac{d}{d(x^2)} f^{**}(x_o) = f'(x_o) f^{*}(x_o) \tag{185}$$

and finally by Eqs. 184 and 185:

$$f'(x_o) = \frac{x_o}{(2x_o^2-1)^2} \frac{d}{d(x^2)} f^{**}(x_o) \tag{186}$$

Asymptotic Expression for v(x)

In order to determine the "cut-off" K and the remainder R it is necessary to study the behavior of v(x) for large values of x. According to the definition of v(x) we have:

$$v(x) = \frac{\sqrt{x^2-s^2}}{f(x)}\, bes(x) \tag{187}$$

which is finite and real for $x > x_o \sim 1$. It can be shown by standard methods that:

$$\frac{\sqrt{x^2-s^2}}{f(x)} = \frac{1}{2x(s^2-1)} + o(x^{-3}) \tag{188}$$

where $o(x^{-3})$ stands for a term which decreases as x^{-3} when $x \to \infty$, and a similar expression can be obtained for the function $bes(x) = J_o(ax) \cdot J_1(a_o x)$ if the Bessel functions are replaced by their asymptotic expansions:

$$J_o(ax) = \sqrt{\frac{2}{\pi a x}}\left[\cos\left(ax - \frac{\pi}{4}\right) + \frac{\sin(ax - \pi/4)}{8ax}\right] + o(x^{-2.5}) \tag{189}$$

$$J_1(a_o x) = \sqrt{\frac{2}{\pi a_o x}}\left[\cos\left(a_o x - \frac{3\pi}{4}\right) - \frac{3\sin(a_o x - \frac{3\pi}{4})}{8a_o x}\right] + o(x^{-2.5}) \tag{190}$$

which are valid for large values of ax and $a_o x$.

By multiplication of Eqs. 189 and 190 we find:

$$bes(x) = \frac{2}{\pi x\sqrt{aa_o}}\left[\begin{array}{l} \cos(ax - \pi/4)\cos(a_o x - 3\pi/4) \\ + \dfrac{\sin(ax - \pi/4)\cos(a_o x - 3\pi/4)}{8ax} \\ - \dfrac{3\cos(ax - \pi/4)\sin(a_o x - 3\pi/4)}{8a_o x} \end{array}\right] + o(x^{-3}) \tag{191}$$

which can be reduced to:

$$bes(x) = \frac{1}{\pi x\sqrt{aa_o}}\left[\begin{array}{l} \sin(a_o-a)x - \cos(a_o+a)x \\ + \dfrac{\cos(a_o-a)x - \sin(a_o+a)x}{8ax} \\ - \dfrac{\cos(a_o-a)x + \sin(a_o+a)x}{8a_o x/3} \end{array}\right] + o(x^{-3}) \qquad (192)$$

Substitution of Eqs. 188 and 192 into Eq. 187 gives finally the following asymptotic expression for v(x):

$$\begin{aligned} V(x) \approx\ & \frac{c_1}{x^2}\left[\sin(a_o-a)x - \cos(a_o+a)x\right] \\ & + \frac{c_2}{x^3}\cos(a_o-a)x + \frac{c_3}{x^3}\sin(a_o+a)x \end{aligned} \qquad (193)$$

where

$$c_1 = \frac{1}{2\pi(s^2-1)\sqrt{aa_o}} \qquad (194)$$

$$c_2 = \frac{3a+a_o}{8aa_o}\,c_1 \qquad (195)$$

$$c_3 = \frac{3a-a_o}{8aa_o}\,c_1 \qquad (196)$$

The expansion is not valid for a or a_o=0, and these cases will therefore have to be investigated separately:

For a = 0, but $a_o \neq 0$, the above method can be used to show that the asymptotic expression for v(x) is:

$$V(x) \approx \frac{c_4}{x^{1.5}}\cos\left(a_o x - \frac{3\pi}{4}\right) + \frac{c_5}{x^{2.5}}\sin\left(a_o x - \frac{3\pi}{4}\right) \qquad (197)$$

where

$$c_4 = \frac{1}{(s^2-1)\sqrt{2\pi a_o}} \tag{198}$$

$$c_5 = \frac{-3}{8a_o} c_4 \tag{199}$$

The case $a = a_o = 0$, which corresponds to the case of static loading, will be discussed on page 102.

Determination of K and R

Substitution of the above asymptotic expressions into Eq. 180 gives the following formulas for the remainder R:

For $a \neq 0$, $a_o \neq 0$, $K \gg 1$:

$$R \approx \frac{1}{\pi}\left[\begin{array}{l} c_1\int_K^\infty x^{-2}\sin(a_o-a)x\,dx - c_1\int_K^\infty x^{-2}\cos(a_o+a)x\,dx \\ + c_2\int_K^\infty x^{-3}\cos(a_o-a)x\,dx + c_3\int_K^\infty x^{-3}\sin(a_o+a)x\,dx \end{array}\right] \tag{200}$$

For $a = 0$, $a_o \neq 0$, $K \gg 1$:

$$R \approx \frac{c_4}{\pi}\int_K^\infty x^{-1.5}\cos\left(a_o x - \frac{3\pi}{4}\right)dx + \frac{c_5}{\pi}\int_K^\infty x^{-2.5}\sin\left(a_o x - \frac{3\pi}{4}\right)dx \tag{201}$$

Both these expressions contain integrals of the types:

$$I_1 = \int_K^\infty x^{-m}\cos(\alpha x - \beta\pi)\,dx \tag{202}$$

and

$$I_2 = \int_K^\infty x^{-m} \sin(\alpha x - \beta\pi)\, dx \tag{203}$$

where m is greater than unity. These integrals can be evaluated as follows:

First consider the case $\alpha > 0$. The integral I_1 can then be written as:

$$I_1 = \int_K^{K_1} x^{-m} \cos(\alpha x - \beta\pi)\, dx + \sum_{n=N_1}^{\infty} J_n \tag{204}$$

where

$$J_n = \int_{(n+\beta)\pi/\alpha}^{(n+\beta+1)\pi/\alpha} x^{-m} \cos(\alpha x - \beta\pi)\, dx \tag{205}$$

and K_1 is chosen in such a way that:

$$(N_1 + \beta - 1)\frac{\pi}{\alpha} < K \leq K_1 = (N_1 + \beta)\frac{\pi}{\alpha} \tag{206}$$

where N_1 is a large integer.

The substitution $x = u + (n + \beta)\pi/\alpha$ reduces Eq. 205 to:

$$J_n = (-1)^n \alpha^{m-1} \int_0^\pi \left[u + (n+\beta)\pi\right]^{-m} \cos u\, du \tag{207}$$

since $n + \beta > 0$ this shows that the terms of the series in Eq. 204 are of alternating sign. By a well known theorem it can therefore be concluded that the absolute value of the series is smaller than its first term. This value can be estimated if we rewrite Eq. 207 in the form:

$$J_n = (-1)^n \alpha^{m-1} \int_0^{\pi/2} \left[\left(u + (n+\beta)\pi\right)^{-m} \cos u - \left(u + (n+\beta+\tfrac{1}{2})\pi\right)^{-m} \sin u \right] du \quad (208)$$

from which it can be seen that:

$$\left| J_n \right| < \frac{(n+\beta)^{-m} - (n+\beta+1)^{-m}}{\alpha^{m-1}\pi^m} < \frac{m\,\alpha^{m-1}}{\pi^m (n+\beta)^{m+1}} \quad (209)$$

Hence, by Eq. 206:

$$\left| \sum_{n=N_1}^{\infty} J_n \right| < \left| J_{N_1} \right| < \frac{m\pi}{\alpha^2 K_1^{m+1}} \quad (210)$$

This result can be generalized to cover also <u>the case when $\alpha < 0$</u>, provided Eq. 206 is replaced by:

$$\pi \left(\frac{N_1 - 1}{|\alpha|} + \frac{\beta}{\alpha} \right) < K \leq K_1 = \pi \left(\frac{N_1}{|\alpha|} + \frac{\beta}{\alpha} \right) \quad (211)$$

Equations 204 and 210 show that the error made by assuming

that:

$$I_1 = \int_K^{K_1} x^{-m} \cos(\alpha x - \beta\pi)\, dx \quad , \quad \alpha \neq 0 \tag{212}$$

is numerically smaller than:

$$\Delta_1 = \frac{m\pi}{\alpha^2 K_1^{m+1}} \tag{213}$$

provided K_1 is chosen according to Eq. 211.

Similarly it can be shown that the error made by replacing I_2 with:

$$I_2 = \int_K^{K_2} x^{-m} \sin(\alpha x - \beta\pi)\, dx \quad , \quad \alpha \neq 0 \tag{214}$$

is numerically smaller than:

$$\Delta_2 = \frac{m\pi}{\alpha^2 K_2^{m+1}} \tag{215}$$

provided K_2 is chosen such that:

$$\pi\left(\frac{N_2 - 1}{|\alpha|} + \frac{\beta + 1/2}{\alpha}\right) < K \leq K_2 = \pi\left(\frac{N_2}{|\alpha|} + \frac{\beta + 1/2}{\alpha}\right) \tag{216}$$

where N_2 is a large integer.

Finally, by noting from Eqs. 211 and 216 that:

$$K_1 - K < \frac{\pi}{|\alpha|} \quad , \quad K_2 - K < \frac{\pi}{|\alpha|} \tag{217}$$

we conclude from Eq. 212 that the error made by neglecting I_1 or I_2 entirely is smaller than:

$$\Delta_3 = \frac{\pi}{|\alpha|} K^{-m} \tag{218}$$

Now let K_1 and K_2 be two large numbers, which are chosen in such a way that:

$$K_2 = \pi \left(\frac{N_2}{|a_o - a|} - \frac{1/2}{a_o + a} \right) < K_1 = \frac{\pi N_1}{a_o + a} \tag{219}$$

where N_1 is taken as the smallest integer which satisfies this condition. Then Eq. 200 can be written in the form:

$$R + \frac{c_1}{\pi} \int_{K_2}^{K_1} x^2 \cos(a_o + a)x \, dx = \tag{220}$$

$$\frac{1}{\pi} \left[\begin{array}{l} c_1 \int_{K_2}^{\infty} x^{-2} \sin(a_o - a)x \, dx - c_1 \int_{K_1}^{\infty} x^{-2} \cos(a_o + a)x \, dx \\ + c_2 \int_{K_2}^{\infty} x^{-3} \cos(a_o - a)x \, dx + c_3 \int_{K_2}^{\infty} x^{-3} \sin(a_o + a)x \, dx \end{array} \right]$$

Hence, by Eqs. 213, 215 and 218:

$$\left| R + \frac{c_1}{\pi}\int_{K_2}^{K_1} x^{-2}\cos(a_o+a)x\,dx \right| < \left[\begin{array}{c} \frac{2|c_1|}{(a_o-a)^2K_2^3} + \frac{2|c_1|}{(a_o+a)K_1^3} \\ + \frac{|c_2|}{|a_o-a|K_2^3} + \frac{|c_3|}{(a_o+a)K_2^3} \end{array} \right] \quad (221)$$

which, in connection with the approximation $K_1 \approx K_2$, shows that the error made by putting:

$$R = -\frac{c_1}{\pi}\int_{K_2}^{K_1} x^{-2}\cos(a_o+a)x\,dx \quad (222)$$

is smaller than:

$$\Delta_4 = K_2^{-3}\left[\left| \frac{2c_1}{(a_o-a)^2} \right| + \left| \frac{2c_1}{(a_o+a)^2} \right| + \left| \frac{c_2}{a_o-a} \right| + \left| \frac{c_3}{a_o+a} \right| \right] \quad (223)$$

or by Eqs. 138-140:

$$\Delta_4 = \frac{\frac{2}{(a_o-a)^2} + \frac{2}{(a_o+a)^2} + \left| \frac{3a+a_o}{8aa_o(a_o-a)} \right| + \left| \frac{3a-a_o}{8aa_o(a_o+a)} \right|}{2\pi(1-s^2)\sqrt{aa_o}\,K_2^3} \quad (224)$$

It is a simple matter to verify that Δ_4 is smaller than:

$$\Delta_5 = \frac{0.2}{(1-s^2)(a_1K_2)^3} \quad (225)$$

where a_1 is the smallest of the quantities a, a_o, $|a_o-a|$. And this expression for the error will be used in the following as it is much more convenient to work with than Eq. 224.

It is clear from Eq. 224 that the approximation Eq. 222 cannot be used for the calculation of R when $a = a_o$. A special formula is therefore needed for the case $a = a_o$:

Substitution of $a = a_o$ into Eq. 200 gives:

$$R = -\frac{c_1}{\pi}\int_{K_1}^{\infty} x^{-2}\cos 2ax\,dx + \frac{c_2}{\pi}\int_{K_1}^{\infty} x^{-3}dx + \frac{c_3}{\pi}\int_{K_1}^{\infty} x^{-3}\sin 2ax\,dx \qquad (226)$$

which, after evaluation of the second integral, reduces to:

$$R - \frac{c_2}{2\pi}K_1^{-2} = -\frac{c_1}{\pi}\int_{K_1}^{\infty} x^{-2}\cos 2ax\,dx + \frac{c_3}{\pi}\int_{K_1}^{\infty} x^{-3}\sin 2ax\,dx \qquad (227)$$

Now if K_1 is chosen according to Eq. 219, it can be seen from Eqs. 213 and 218 that the error made by assuming that:

$$R = \frac{c_2}{2\pi}K_1^{-2} \qquad (228)$$

is numerically smaller than:

$$\Delta_6 = K_1^{-3}\left[\frac{|c_1|}{a^2} + \frac{|c_3|}{2a}\right] \qquad (229)$$

or by Eqs. 194 and 196:

$$\Delta_6 = \frac{9}{16\pi(1-s^2)}(aK_1)^{-3} \approx \frac{0.2}{(1-s^2)(aK_1)^3} \qquad (230)$$

which is similar to Eq. 225.

The remainder for the case $a = 0$, $a_o \neq 0$ is given by Eq. 201 which in connection with Eqs. 215 and 218 shows that:

$$\Delta_7 = K_1^{-2.5}\left[\frac{3|c_4|}{2a_o^2} + \frac{|c_5|}{a_o}\right] \qquad (231)$$

or by Eqs. 198 and 199:

$$\Delta_7 = \frac{15}{8\sqrt{2\pi}(1-s^2)}(a_oK_1)^{-2.5} \approx \frac{0.75}{(1-s^2)(a_oK_1)^{2.5}} \qquad (232)$$

provided the "cut-off" K_1 is chosen such that:

$$K_1 = \frac{N_1 + 3/4}{a_o}\pi \qquad (233)$$

where N_1 is a large integer.

Formulas for the Calculation of g_1 and g_2

From the above expressions for the remainder it is now a simple matter to set up procedures from which the function g_1 can be calculated to any given accuracy Δ. Depending on the values of a and a_o we must distinguish between the following three cases:

1) $a \neq 0$, $a_o \neq 0$, $a \neq a_o$:

Choose two large K-values such that:

$$\frac{1}{a_1\sqrt[3]{5(1-s^2)\Delta}} < K_2 = \pi\left[\frac{N_2}{|a_o-a|} - \frac{1/2}{a_o-a}\right] < K_1 = \frac{\pi N_1}{a_o+a} \qquad (234)$$

where a_1 = The smallest of the quantities $a, a_o, |a-a_o|$

N_2 = A large integer

N_1 = The smallest integer which satisfies Eq. 234.

and calculate g_1 from:

$$g_1 = \left[\begin{array}{l} \frac{1}{\pi}\int_s^1 U(x)\,dx + \frac{1}{\pi}\int_1^{x_o} W(x)\,dx + \\ \frac{1}{\pi}\int_{2x_c-1}^{K_2} V(x)\,dx + \int_{K_2}^{K_1} \frac{\cos(a+a_o)x\,dx}{2\pi^2(1-s^2)\sqrt{aa_o}\,x^2} \end{array}\right] \qquad (235)$$

2) $a_o \neq 0$, $a \neq 0$, $a = a_o$:

Choose a large K-value such that:

$$\frac{1}{a\sqrt[3]{5(1-s^2)\Delta}} < K = \frac{\pi N}{2a} \qquad (236)$$

where N is a large integer, and calculate g_1 from:

$$g_1 = \left[\begin{array}{l} \frac{1}{\pi}\int_s^1 U(x)\,dx + \frac{1}{\pi}\int_1^{x_o} W(x)\,dx + \\ \frac{1}{\pi}\int_{2x_c-1}^{K} V(x)\,dx - \frac{1}{8\pi^2(1-s^2)a^2K^2} \end{array}\right] \qquad (237)$$

3) $a = 0$, $a_o \neq 0$:

Choose a large K-value such that:

$$\frac{1.2}{a_o(\Delta(1-s^2))^{0.4}} < K = \frac{N+3/4}{a_o}\pi \qquad (238)$$

where N is a large integer, and calculate g_1 from:

$$g_1 = \frac{1}{\pi}\int_s^1 v(x)dx + \frac{1}{\pi}\int_1^{x_o} w(x)dx + \frac{1}{\pi}\int_{2x_o-1}^{K} v(x)dx \qquad (239)$$

The function g_2 can for all values of a and a_o be calculated directly from Eq. 178, which will be repeated here for convenience:

$$g_2 = \frac{1}{\pi}\int_0^s r(x)dx + \frac{1}{\pi}\int_s^1 t(x)dx - \frac{\sqrt{x_o^2-s^2}}{f'(x_o)}\,bes(x) \qquad (240)$$

All the functions appearing in the above formulas are defined on page 85 and they are well behaved in the intervals of interest. The integrals can therefore be evaluated by numerical integration.

The Static Case

Reissner's displacement function is not defined in the point $a = a_o = 0$, which according to the definition of a and a_o corresponds to the case of static loading.

The vertical displacement of the surface for a uniform static loading of intensity p_o over a circular area is known

to be:

$$\delta = \frac{-p_o r_o}{\pi (1-s^2) G} = \begin{cases} \int_0^{\pi/2} \frac{\cos^2 x \, dx}{\sqrt{(r/r_o)^2 - \sin^2 x}}, & r > r_o \\ \int_0^{\pi/2} \sqrt{1 - \left(\frac{r \sin x}{r_o}\right)^2} \, dx, & r < r_o \end{cases} \tag{241}$$

By comparing these with the following form of Eq. 50:

$$\delta = \pi \frac{p_o r_o}{G} (g_1 + i g_2) e^{i\omega t} \tag{242}$$

it can be seen that if $\omega \to 0$, while the ratio $a/a_o = r/r_o$ is kept constant, the components of $g(a,a_o)$ will approach the limits:

$$\lim_{\omega \to 0} g_1 = \frac{-1}{\pi^2 (1-s^2)} \begin{cases} \int_0^{\pi/2} \frac{\cos^2 x \, dx}{\sqrt{(a/a_o)^2 - \sin^2 x}}, & a > a_o \\ \int_0^{\pi/2} \sqrt{1 - \left(\frac{a \sin x}{a_o}\right)^2} \, dx, & a < a_o \end{cases} \tag{243}$$

$$\lim_{\omega \to 0} g_2 = 0 \tag{244}$$

The elliptical integrals appearing in Eq. 243 cannot be reduced further, but it is known that their values lie in the range 0 to 1 depending on the ratio a/a_o. Hence, the function g_1 can attain any value in the range 0 to $1/\pi^2(s^2-1)$ in the point $a = a_o = 0$, depending on the ratio between a and a_o as they approach zero.

The limits Eq. 243 are useful if it is wanted to tabulate g_1 for small values of a and a_o. Instead of using a

and a_o as entries in the table one can use a and a/a_o if $a < a_o$ or a_o, and a_o/a, if $a > a_o$. By this procedure g_1 is transformed into a well behaved, single valued function and the resulting tables are well suited for interpolation.

Numerical Calculations

A computer program was written for the procedures outlined on page 100 and the functions g_1 and g_2 were evaluated in the range $0 \leq a_o \leq 8$ and $0 \leq a \leq 8$ for Poisson's ratio equal to 1/3, using the formulas Eqs. 178 to 184. A graphical presentation of the results is given in Figs. 36 and 37.

Also a table of the type mentioned in the previous section was prepared on punched cards. These cards made the values of Reissner's function easily available, and they formed part of the input for the computer program for the ring method. See page 32.

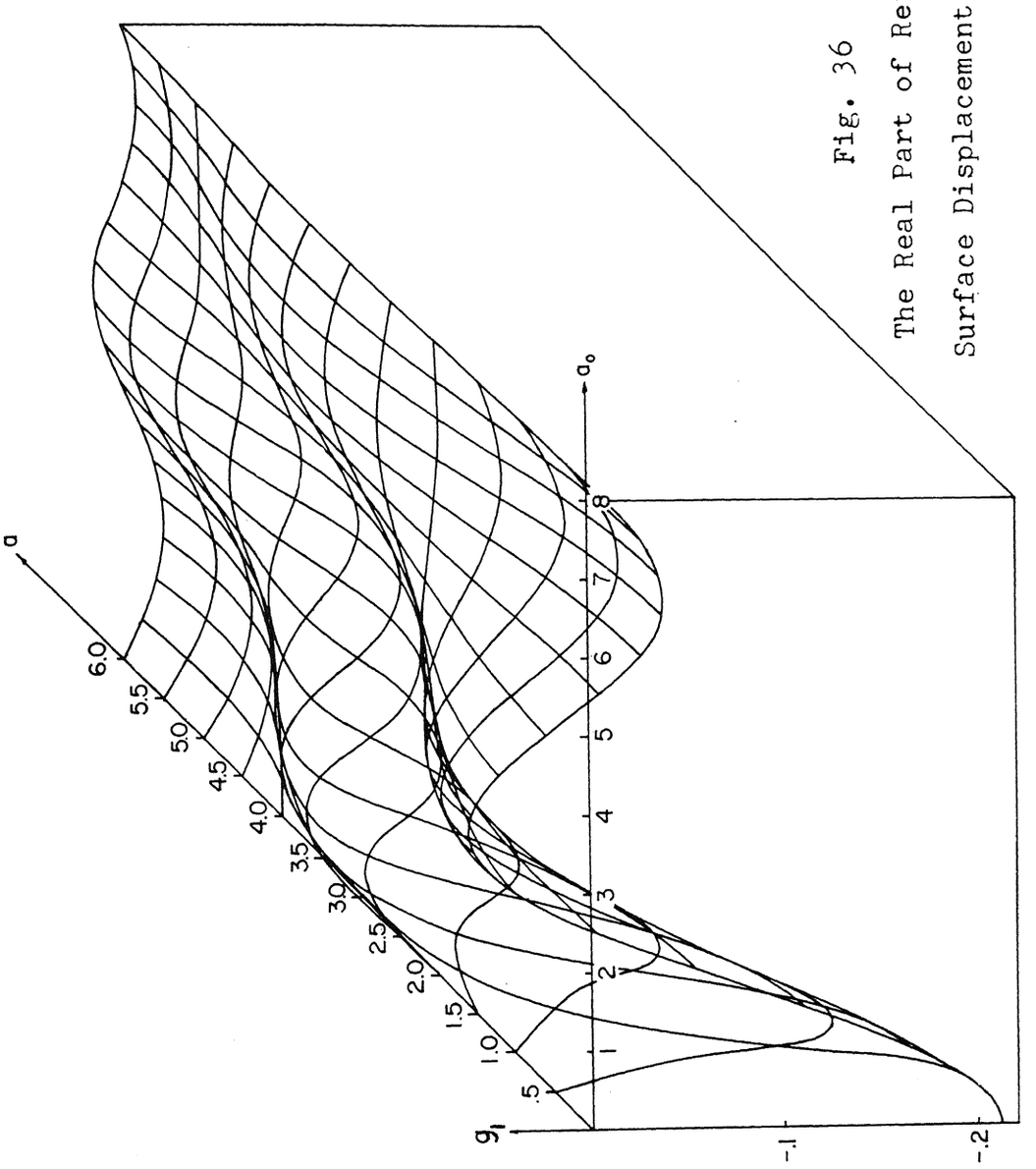

Fig. 36

The Real Part of Reissner's Surface Displacement Function

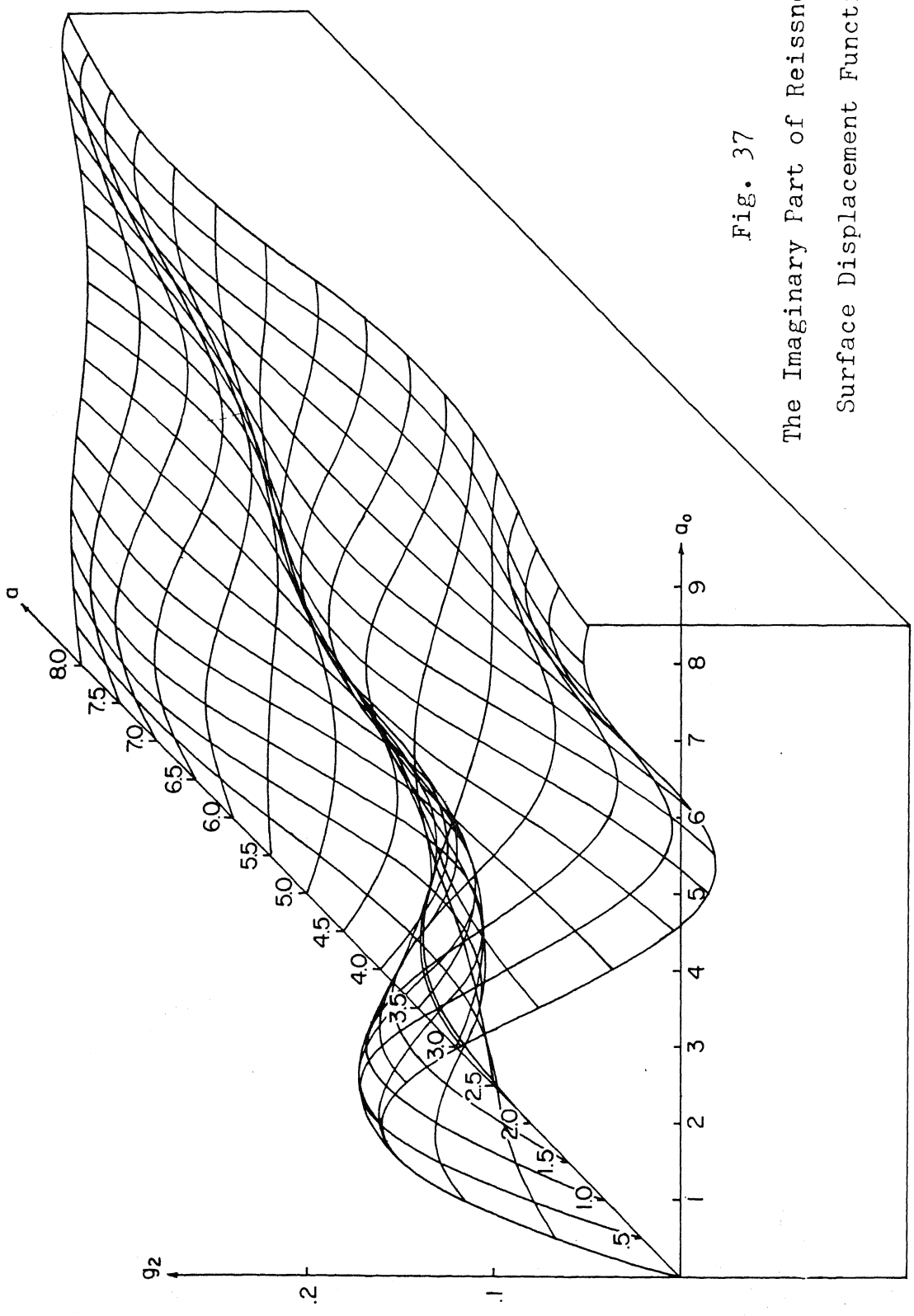

Fig. 37

The Imaginary Part of Reissner's Surface Displacement Function

APPENDIX II

COMPUTER PROGRAM FOR IMPULSIVE LOADING

The computer program shown on the following pages is written in the FORTRAN II language. Only the most basic statements have been used and the program should therefore be able to run on most modern computers with only minor modifications.

The program calculates the dynamic response of the footing-soil system shown in Fig. 10 due to the piecewise linear pulse shown in Fig. 26b. The method used is the Fourier technique described in Chapter III.

The comment cards shown on page 109 explain how the input should be arranged and two sets of output are shown on pages 116 and 123. These outputs correspond to the curves shown in Figs. 28 and 35 respectively.

It should be noted that the program automatically generates an appropriate time interval for the final table showing the actual response. This time interval will always come out as a "nice" number for easy plotting of the response curves. The program also determines the number m of intervals in the pulse by locating the last non-zero ordinate from the data. Hence, the number m is not part of the data as one might expect from the development in Chapter

III.

The controling variables ε_1 and ε_2, EPS1 and EPS2 in the program, are preset to the common value 0.05. They can be chosen smaller, but experience with the program has shown that only a small gain in accuracy is achieved by doing so.

As a special feature the program checks the sign of the soil reaction:

$$R(t) = Q(t) + W(1 - \ddot{\delta}/g) \qquad (245)$$

where g = acceleration at gravity, to establish whether jumping occurs. If R(t) is negative the acceleration in the final table is printed out with an F-conversion instead of the usual E-conversion.

The subroutine shown on page 114 generates the displacement functions F_1 and F_2 for the half-space model. These functions are shown graphically in Fig. 16 and numerically in the table on page 115. The functions were evaluated for Poisson's ratio equal to 1/3. However, as shown on page 34, the same subroutine can be used for all values of Poisson's ratio.

The execution time varies with the number of points necessary to define the pulse, the duration of the pulse and the choice of the preset variables EPS1 and EPS2. The execution times for the two data sets presented below were approximately 30 seconds each.

```
C FORTRAN II PROGRAM TO CALCULATE THE DYNAMIC RESPONSE OF A
C RIGID CIRCULAR FOOTING RESTING ON AN ELASTIC HALF-SPACE
C
C CODED BY JOHN LYSMER, UNIVERSITY OF MICHIGAN, MARCH 1965
C
C THE PROGRAM CONSISTS OF A MAIN PROGRAM PLUS A SUBROUTINE
C WHICH YIELDS THE DISPLACEMENT FUNCTION F = F1 + I*F2
C
C EACH DATA SET CONSISTS OF 11 CARDS AS FOLLOWS
C    CARD 1
C      COLS.  1-10  R      (FT)  RADIUS OF FOOTING
C      COLS. 11-20  W      (LB)  WEIGHT OF FOOTING
C      COLS. 21-30  GAMMA  (PCF) DENSITY OF SOIL
C      COLS. 31-40  G      (PSI) SHEAR MODULUS OF SOIL
C      COLS. 41-50  MU           POISSONS RATIO OF SOIL
C      COLS. 51-60  D      (SEC) DURATION OF PULSE
C      COLS. 61-70  Q      (LB)  FACTOR ON PULSE ORDINATES
C      COLS. 71-80  IDENTIFICATION, MAY BE LEFT BLANK,
C                   ANY CHARACTERS PUNCHED IN THESE COLUMNS
C                   WILL APPEAR AS A HEADING ON THE OUTPUT
C
C    CARD 2
C      COLS.  1-10  Y(1)  FIRST NON-ZERO ORDINATE OF PULSE
C      COLS. 11-20  Y(2)
C      ----------
C      COLS. 71-80  Y(8)
C
C    AND SO ON UP TO
C
C    CARD 11
C      COLS.  1-10  Y(73)
C      COLS. 11-20  Y(74)
C      ---------
C      COLS. 71-80  Y(80)
C
C    THE DATA CAN BE PLACED ANYWHERE IN THE RESPECTIVE
C    FIELDS PROVIDED THE DECIMAL POINT IS PUNCHED.
C    ALL BLANK FIELDS ARE ASSUMED TO MEAN ZERO.
C
C THE OUTPUT CONSISTS OF
C    1. A TABLE OF THE DISPLACEMENT FUNCTION USED
C    2. A PAGE SHOWING THE DATA AND CONSTANTS OF THE SYSTEM
C    3. A TABLE SHOWING THE MAGNITUDE OF THE FOURIER TERMS
C    4. A TABLE OF DISPLACEMENTS, VELOCITIES, ACCELERATIONS
C       AND THE EXCITING FORCE (FROM THE TRUNCATED FOURIER
C       SERIES). WHENEVER THE ACCELERATIONS ARE PRINTED IN
C       THE FORMAT XXXX.X INSTEAD OF THE USUAL X.XXXE+XX IT
C       MEANS THAT THE FOOTING JUMPS FREE OF THE HALF-SPACE
C       AND THE RESULTS MUST BE TAKEN WITH SOME RESERVATION
C
C THE CONSTANTS EPS1 AND EPS2 ARE PRESET TO
      EPS1 = .05
      EPS2 = .05
C THEY CAN BE CHANGED BY CHANGING THE TWO PRECEEDING CARDS
```

```
      DIMENSION Y(85),C( 400),PSI( 400),BN( 400),PHASE( 400)
C
C TABLE OF DISPLACEMENT FUNCTION
      A = 0.
      CALL TABLE(-1.,F1,F2)
    1 CALL TABLE( A ,F1,F2)
      PRINT                100,A,F1,F2
      A = A+.2
      IF(A-8.1) 1,1,2
C
C READ INPUT FROM THE 11 DATA CARDS
    2 READ                 114,R,W,GAMMA,G,POIS,D,Q,A1,A2
      READ                 101,(Y(I), I=3,82)
C
C CALCULATE BASIC CONSTANTS OF THE SYSTEM
      V = SQRTF(G/GAMMA*4632.5)
      SPRING = 576.*G*R/(1.-POIS)
      RV = R/V
      RVD = RV/D
      B = W/32.17/SPRING/RV/RV
      AJ = 2.- LOGF(EPS1)*(.85+2.6*B)*RVD
      J = AJ
      AJ = J
      IF(B) 4,4,3
    3 AN = 1.+AJ/6.28/SQRTF(B*EPS2)/RVD
      N = AN
      AN = N
    4 PJ = 3.14159265/AJ
C
C FIND THE NUMBER OF INTERVALS IN THE PULSE
      DO 6 I = 3,82
      IF(Y(I)) 5,6,5
    5 M = I
    6 CONTINUE
      M1 = M-1
      AM = M1
      DT = D/AM
C
C PRINT DATA AND CONSTANTS
      SPRING = SPRING/12.
      PRINT                113,A1,A2
      PRINT                102,R,W,G,GAMMA,POIS,V,SPRING,B
      Y(1) = 0.
      Y(2) = 0.
      T = 0.
      PRINT                108,D,Q
      M2 = M + 1
      Y(M2) = 0.
      DO 7 I = 2,M2
      LINE = I-2
      FORCE = Y(I)*Q
      PRINT                103,LINE,T,Y(I),FORCE
```

```
      IF(LINE-26)7,36,7
   36 PRINT                  112
    7 T = T+DT
      IF ((LINE-21)*(LINE-25)) 42,42,43
   42 PRINT                  112
   43 PRINT                  111,EPS1,EPS2
C
C CALCULATE FOURIER CONSTANTS FOR THE EXCITING FORCE
      PRINT                  109
      N1 = N+1
      DO 16 K = 1,N1
      AK = K
      H = PJ*(2.*AK-1.)
      ALFA = 0.
      BETA = 0.
      DO 8 I = 1,M
      AI = I
      COEFF = 2.*Y(I+1)-Y(I)-Y(I+2)
      ANGLE = H*(AI-1.)/AM
      ALFA = ALFA+COEFF*COSF(ANGLE)
    8 BETA = BETA+COEFF*SINF(ANGLE)
      C(K) = 2.*Q*AM/AJ/H/H*SQRTF(ALFA*ALFA+BETA*BETA)
      SWITCH = 1.
C
C CALCULATE PHASE ANGLE
    9 IF(ABSF(ALFA)-ABSF(BETA)) 11,11,10
   10 PHI = ATANF(-BETA/ALFA)
      IF(ALFA) 12,13,13
   11 PHI = 1.5707963-ATANF(-ALFA/BETA)
      IF(BETA) 13,13,12
   12 PHI = PHI+3.14159265
   13 IF(SWITCH) 14,15,14
   14 PSI(K) = PHI
C
C CALCULATE FOURIER CONSTANTS FOR DISPLACEMENTS
      A = H*RVD
      CALL TABLE(A,F1,F2)
      FF = F1*F1+F2*F2
      ALFA = F1/FF-B*A*A
      BETA = -F2/FF
      BN(K) = C(K)/SQRTF(ALFA*ALFA+BETA*BETA)/SPRING
      SWITCH = 0.
      GO TO 9
   15 PHASE(K) = PSI(K)+PHI
      IF(K- 49) 16,41,37
   37 IF(K-103) 16,41,38
   38 IF(K-157) 16,41,39
   39 IF(K-211) 16,41,40
   40 IF(K-265) 16,41,16
   41 PRINT                  112
   16 PRINT                  104,K,A,C(K),BN(K)
```

```
C CALCULATION OF TIME INCREMENT
      IF(B-.5) 18,18,17
   17 DT = RV/5.*SQRTF(B)
      GO TO 19
   18 DT = MAX1F(D/AM/2.,D*AJ/100.)
   19 ALOG =  LOGF(DT)*.434294482+18.
      CHR = INTF(ALOG)
      ALOG = ALOG-CHR
      IF(ALOG-.84) 20,20,25
   20 IF(ALOG-.50) 21,21,24
   21 IF(ALOG-.16) 22,22,23
   22 DT = 10.**(CHR-18.)
      GO TO 26
   23 DT = 10.**(CHR-17.69897)
      GO TO 26
   24 DT = 10.**(CHR-17.30103)
      GO TO 26
   25 DT = 10.**(CHR-17.)
C
C PRINT FINAL TABLE OF DISPLACEMENTS ETC.
   26 T = 0.
   27 JUMP = 50
      PRINT                    105
   28 IF(JUMP) 27,27,29
   29 JUMP = JUMP -1
      IF(T-D*AJ) 30,30,35
   30 ACCEL = 0.
      DISPL = 0.
      VLOCT = 0.
      FORCE = 0.
      DO 31 K = 1,N1
      AK = K
      H = PJ* (2.*AK-1.)/D
      BNK = BN(K)
      ANGLE = H*T+PHASE(K)
      DISPL = DISPL + BNK* COSF(ANGLE)
      VLOCT = VLOCT - BNK* SINF(ANGLE)*H
      ACCEL = ACCEL - BNK* COSF(ANGLE)*H*H
   31 FORCE = FORCE + C(K)*COSF(H*T+PSI(K))
      IF(FORCE+W*(1.-ACCEL/386.4))33,32,32
   32 PRINT                    106,T,DISPL,VLOCT,ACCEL,FORCE
      GO TO 34
   33 PRINT                    107,T,DISPL,VLOCT,ACCEL,FORCE
   34 T = T+DT
      GO TO 28
   35 PRINT                    110
      GO TO 2
C
```

```
  100 FORMAT (21X,F3.1,2F15.5)
  101 FORMAT (8F10.0)
  1020FORMAT(1H1/// 14X,13HF O O T I N G/14X,13(1H-)/17X,
     16HRADIUS,19(1H.),3HR =F9.2,4H  FT/17X,6HWEIGHT,19(1H.)
     2,3HW =F9.2,4H  LB//14X,7HS O I L/14X,7(1H-)/
     317X,13HSHEAR MODULUS,12(1H.),3HG =F9.2,5H  PSI/17X,
     428HDENSITY.............GAMMA =F9.2,5H  PCF/17X,
     528HPOISSONS RATIO.........MU = F9.4/17X,
     628HSHEAR WAVE VELOCITY.....V =F9.2,8H  FT/SEC//14X,
     711HS Y S T E M/14X,11(1H-)/17X,
     828HSTATIC SPRING CONSTANT...K = F9.0,9H  LB/INCH/17X,
     910HMASS RATIO,15(1H.),3HB = F9.4/ )
  103 FORMAT (I21,2X,3(1PE12.3))
  104 FORMAT (I18,3(1PE14.3))
  1050FORMAT (1H1/// 11X,32HT I M E  DISPLACEMENT  VELOCITY
     122H  ACCELERATION   FORCE // 13X,3HSEC, 7X,
     241HINCHES     INCH/SEC   INCH/SEC/SEC    LBS /  )
  106 FORMAT (7X,5(1PE12.3))
  107 FORMAT (7X,3(1PE12.3),0PF12.1,1PE12.3)
  1080FORMAT (14X,9HP U L S E / 14X,9(1H-)/
     117X, 28HDURATION.................D =1PE10.3,5H  SEC /
     217X, 28HFACTOR ON ORDINATES......Q =1PE10.3,5H  LBS //
     318X,41HPOINT    T I M E    ORDINATE    F O R C E     /
     428X,5H(SEC),19X,5H(LBS)   /)
  1090FORMAT (1H1///  24X,28HF O U R I E R   S E R I E S /
     124X,28(1H- )/
     215X,47HTERM    FREQUENCY     AMPLITUDE OF FOURIER TERM/
     314X,48HNUMBER     RATIO          FORCE      DISPLACEMENT
     4/17X,1HK8X,4HA(K),10X,4HC(K),10X,5HBN(K)/)
  110 FORMAT (1H1 ////10X,18HLOOK FOR MORE DATA )
  1110FORMAT(1H0,13X,15HA C C U R A C Y  /14X,15(1H-)/
     117X,6HEPS1 =F6.4,33H  GOVERNS DISTANCE BETWEEN PULSES/
     217X,6HEPS2 =F6.4,33H  GOVERNS NUMBER OF FOURIER TERMS)
  112 FORMAT (1H1 // )
  113 FORMAT (1H1/// 34X,2(A5))
  114 FORMAT (7F10.0,2(A5))
C
      END
```

```
      SUBROUTINE TABLE(A,F1,F2)
C
      IF(A) 1,2,3
    1 PRINT                  100
 1000FORMAT(1H16(/)21X,33HT A B L E   O F   F1   A N D   F2
     1/S21,33(1H-)/23X,  31H      HALF-SPACE MODEL          /
     2              23X,  31H    POISSONS RATIO = 1/3        /
     3/22X,1HA,12X,2HF1,13X,2HF2 /)
      RETURN
    2 F1 = 1.
      F2 = 0.
      RETURN
    3 Y = A*A
      IF( A-1.) 4,4,5
    4 F1 = 1.-Y*(.60000-Y*.15000)
      GO TO 6
    5 F1 = (.25000 +(1.10000-.80000/A)/A)/Y
    6 IF(A-1.18) 7,7,8
    7 F2 = -A*(.78378-Y*(.25800-Y*.03030))
      RETURN
    8 F2 = (-.95493+(.7873-(1.618-1.276/A)/A)/A)/A
      RETURN
      END
```

Note:

The above subroutine is a polynomial approximation to the displacement function F determined by the ring method described in Chapter II. It can be used for all values of Poisson's ratio.

T A B L E O F F1 A N D F2

HALF-SPACE MODEL
POISSONS RATIO = 1/3

A_o	F1	F2
.0	1.00000	.00000
.2	.97624	-.15470
.4	.90784	-.29731
.6	.80344	-.41690
.8	.67744	-.50486
1.0	.55000	-.55608
1.2	.42438	-.57003
1.4	.32018	-.53791
1.6	.24414	-.48961
1.8	.18957	-.44341
2.0	.15000	-.40314
2.2	.12081	-.36888
2.4	.09886	-.33979
2.6	.08206	-.31495
2.8	.06898	-.29357
3.0	.05864	-.27501
3.2	.05035	-.25874
3.4	.04363	-.24437
3.6	.03810	-.23159
3.8	.03352	-.22014
4.0	.02969	-.20982
4.2	.02645	-.20047
4.4	.02369	-.19195
4.6	.02133	-.18416
4.8	.01929	-.17700
5.0	.01752	-.17040
5.2	.01597	-.16429
5.4	.01462	-.15861
5.6	.01342	-.15333
5.8	.01236	-.14840
6.0	.01142	-.14379
6.2	.01058	-.13947
6.4	.00982	-.13540
6.6	.00914	-.13157
6.8	.00853	-.12795
7.0	.00798	-.12454
7.2	.00747	-.12130
7.4	.00701	-.11823
7.6	.00659	-.11532
7.8	.00621	-.11255
8.0	.00586	-.10991

TRAPEZOID

F O O T I N G

RADIUS.....R = 5.00 FT
WEIGHT.....W =483000.00 LB

S O I L

SHEAR MODULUS.....G = 2500.00 PSI
DENSITY.....GAMMA = 128.68 PCF
POISSONS RATIO.....MU = .3333
SHEAR WAVE VELOCITY.....V = 300.00 FT/SEC

S Y S T E M

STATIC SPRING CONSTANT...K = 900000 LB/INCH
MASS RATIO.....B = 5.0047

P U L S E

DURATION.....D = 1.000E 00 SEC
FACTOR ON ORDINATES.....Q = 2.500E 05 LBS

POINT	T I M E (SEC)	ORDINATE	F O R C E (LBS)
0	.000E 00	.000E 00	.000E 00
1	5.000E-02	1.000E 00	2.500E 05
2	10.000E-02	1.000E 00	2.500E 05
3	1.500E-01	1.000E 00	2.500E 05
4	2.000E-01	1.000E 00	2.500E 05
5	2.500E-01	1.000E 00	2.500E 05
6	3.000E-01	1.000E 00	2.500E 05
7	3.500E-01	1.000E 00	2.500E 05
8	4.000E-01	1.000E 00	2.500E 05
9	4.500E-01	1.000E 00	2.500E 05
10	5.000E-01	1.000E 00	2.500E 05
11	5.500E-01	1.000E 00	2.500E 05
12	6.000E-01	1.000E 00	2.500E 05
13	6.500E-01	1.000E 00	2.500E 05
14	7.000E-01	1.000E 00	2.500E 05
15	7.500E-01	1.000E 00	2.500E 05
16	8.000E-01	1.000E 00	2.500E 05
17	8.500E-01	1.000E 00	2.500E 05
18	9.000E-01	1.000E 00	2.500E 05
19	9.500E-01	1.000E 00	2.500E 05
20	10.000E-01	.000E 00	.000E 00

A C C U R A C Y

EPS1 = .0500 GOVERNS DISTANCE BETWEEN PULSES
EPS2 = .0500 GOVERNS NUMBER OF FOURIER TERMS

F O U R I E R S E R I E S

TERM NUMBER K	FREQUENCY RATIO A(K)	AMPLITUDE OF FOURIER TERM FORCE C(K)	DISPLACEMENT BN(K)
1	2.618E-02	2.160E 05	2.408E-01
2	7.854E-02	8.313E 04	9.513E-02
3	1.309E-01	3.514E 04	4.245E-02
4	1.833E-01	3.918E 04	5.159E-02
5	2.356E-01	1.450E 04	2.163E-02
6	2.880E-01	2.631E 04	4.664E-02
7	3.403E-01	6.361E 03	1.416E-02
8	3.927E-01	1.963E 04	5.596E-02
9	4.451E-01	2.041E 03	6.204E-03
10	4.974E-01	1.523E 04	3.511E-02
11	5.498E-01	5.299E 02	8.406E-04
12	6.021E-01	1.195E 04	1.357E-02
13	6.545E-01	2.104E 03	1.801E-03
14	7.069E-01	9.337E 03	6.279E-03
15	7.592E-01	3.030E 03	1.651E-03
16	8.116E-01	7.186E 03	3.249E-03
17	8.639E-01	3.500E 03	1.339E-03
18	9.163E-01	5.396E 03	1.772E-03
19	9.687E-01	3.640E 03	1.040E-03
20	1.021E 00	3.910E 03	9.824E-04
21	1.073E 00	3.538E 03	7.885E-04
22	1.126E 00	2.695E 03	5.369E-04
23	1.178E 00	3.264E 03	5.852E-04
24	1.230E 00	1.726E 03	2.802E-04
25	1.283E 00	2.876E 03	4.255E-04
26	1.335E 00	9.795E 02	1.327E-04
27	1.388E 00	2.423E 03	3.018E-04
28	1.440E 00	4.347E 02	4.997E-05
29	1.492E 00	1.946E 03	2.071E-04
30	1.545E 00	6.713E 01	6.640E-06
31	1.597E 00	1.478E 03	1.361E-04
32	1.649E 00	1.486E 02	1.279E-05
33	1.702E 00	1.045E 03	8.422E-05
34	1.754E 00	2.395E 02	1.810E-05
35	1.806E 00	6.687E 02	4.753E-05
36	1.859E 00	2.330E 02	1.560E-05
37	1.911E 00	3.602E 02	2.276E-05
38	1.963E 00	1.562E 02	9.328E-06
39	2.016E 00	1.262E 02	7.135E-06
40	2.068E 00	3.461E 01	1.856E-06

T I M E	DISPLACEMENT	VELOCITY	ACCELERATION	FORCE
SEC	INCHES	INCH/SEC	INCH/SEC/SEC	LB
.000E 00	4.276E-05	8.345E-02	1.036E 01	1.215E 04
1.000E-02	1.729E-03	2.924E-01	3.348E 01	4.497E 04
2.000E-02	6.839E-03	7.831E-01	6.537E 01	9.585E 04
3.000E-02	1.847E-02	1.592E 00	9.497E 01	1.541E 05
4.000E-02	3.947E-02	2.632E 00	1.095E 02	2.050E 05
5.000E-02	7.123E-02	3.707E 00	1.018E 02	2.379E 05
6.000E-02	1.130E-01	4.599E 00	7.371E 01	2.514E 05
7.000E-02	1.620E-01	5.144E 00	3.428E 01	2.525E 05
8.000E-02	2.145E-01	5.281E 00	-6.330E 00	2.499E 05
9.000E-02	2.664E-01	5.036E 00	-4.158E 01	2.488E 05
1.000E-01	3.142E-01	4.474E 00	-6.942E 01	2.496E 05
1.100E-01	3.551E-01	3.671E 00	-9.002E 01	2.505E 05
1.200E-01	3.870E-01	2.698E 00	-1.034E 02	2.505E 05
1.300E-01	4.087E-01	1.629E 00	-1.089E 02	2.499E 05
1.400E-01	4.196E-01	5.463E-01	-1.063E 02	2.496E 05
1.500E-01	4.198E-01	-4.729E-01	-9.641E 01	2.499E 05
1.600E-01	4.105E-01	-1.363E 00	-8.091E 01	2.502E 05
1.700E-01	3.932E-01	-2.079E 00	-6.168E 01	2.502E 05
1.800E-01	3.696E-01	-2.590E 00	-4.023E 01	2.499E 05
1.900E-01	3.421E-01	-2.880E 00	-1.793E 01	2.498E 05
2.000E-01	3.128E-01	-2.950E 00	3.698E 00	2.500E 05
2.100E-01	2.838E-01	-2.814E 00	2.308E 01	2.501E 05
2.200E-01	2.571E-01	-2.500E 00	3.898E 01	2.501E 05
2.300E-01	2.342E-01	-2.048E 00	5.072E 01	2.500E 05
2.400E-01	2.164E-01	-1.501E 00	5.804E 01	2.499E 05
2.500E-01	2.044E-01	-9.024E-01	6.087E 01	2.500E 05
2.600E-01	1.984E-01	-2.979E-01	5.934E 01	2.501E 05
2.700E-01	1.983E-01	2.712E-01	5.387E 01	2.501E 05
2.800E-01	2.036E-01	7.690E-01	4.524E 01	2.500E 05
2.900E-01	2.134E-01	1.169E 00	3.439E 01	2.499E 05
3.000E-01	2.266E-01	1.453E 00	2.230E 01	2.500E 05
3.100E-01	2.420E-01	1.613E 00	9.819E 00	2.500E 05
3.200E-01	2.584E-01	1.651E 00	-2.219E 00	2.500E 05
3.300E-01	2.746E-01	1.573E 00	-1.302E 01	2.500E 05
3.400E-01	2.896E-01	1.396E 00	-2.193E 01	2.500E 05
3.500E-01	3.023E-01	1.142E 00	-2.849E 01	2.500E 05
3.600E-01	3.122E-01	8.350E-01	-3.254E 01	2.500E 05
3.700E-01	3.189E-01	5.000E-01	-3.405E 01	2.500E 05
3.800E-01	3.222E-01	1.621E-01	-3.315E 01	2.500E 05
3.900E-01	3.222E-01	-1.558E-01	-3.009E 01	2.500E 05
4.000E-01	3.192E-01	-4.338E-01	-2.526E 01	2.500E 05
4.100E-01	3.137E-01	-6.567E-01	-1.917E 01	2.500E 05
4.200E-01	3.063E-01	-8.148E-01	-1.238E 01	2.500E 05
4.300E-01	2.977E-01	-9.036E-01	-5.385E 00	2.500E 05
4.400E-01	2.885E-01	-9.235E-01	1.333E 00	2.500E 05
4.500E-01	2.794E-01	-8.793E-01	7.353E 00	2.500E 05
4.600E-01	2.711E-01	-7.799E-01	1.232E 01	2.500E 05
4.700E-01	2.640E-01	-6.372E-01	1.599E 01	2.500E 05
4.800E-01	2.584E-01	-4.648E-01	1.825E 01	2.500E 05
4.900E-01	2.547E-01	-2.770E-01	1.907E 01	2.500E 05

T I M E	DISPLACEMENT	VELOCITY	ACCELERATION	FORCE
SEC	INCHES	INCH/SEC	INCH/SEC/SEC	LB
5.000E-01	2.529E-01	-8.798E-02	1.853E 01	2.500E 05
5.100E-01	2.529E-01	8.952E-02	1.679E 01	2.500E 05
5.200E-01	2.546E-01	2.446E-01	1.409E 01	2.500E 05
5.300E-01	2.577E-01	3.689E-01	1.069E 01	2.500E 05
5.400E-01	2.619E-01	4.570E-01	6.880E 00	2.500E 05
5.500E-01	2.667E-01	5.062E-01	2.954E 00	2.500E 05
5.600E-01	2.719E-01	5.166E-01	-8.089E-01	2.500E 05
5.700E-01	2.769E-01	4.914E-01	-4.159E 00	2.500E 05
5.800E-01	2.816E-01	4.355E-01	-6.913E 00	2.500E 05
5.900E-01	2.856E-01	3.555E-01	-8.959E 00	2.500E 05
6.000E-01	2.886E-01	2.589E-01	-1.023E 01	2.500E 05
6.100E-01	2.907E-01	1.536E-01	-1.070E 01	2.500E 05
6.200E-01	2.917E-01	4.760E-02	-1.037E 01	2.500E 05
6.300E-01	2.917E-01	-5.159E-02	-9.364E 00	2.500E 05
6.400E-01	2.907E-01	-1.379E-01	-7.837E 00	2.500E 05
6.500E-01	2.890E-01	-2.071E-01	-5.955E 00	2.500E 05
6.600E-01	2.866E-01	-2.563E-01	-3.844E 00	2.500E 05
6.700E-01	2.839E-01	-2.837E-01	-1.633E 00	2.500E 05
6.800E-01	2.810E-01	-2.892E-01	5.075E-01	2.500E 05
6.900E-01	2.782E-01	-2.744E-01	2.384E 00	2.500E 05
7.000E-01	2.756E-01	-2.428E-01	3.877E 00	2.500E 05
7.100E-01	2.734E-01	-1.982E-01	4.977E 00	2.499E 05
7.200E-01	2.717E-01	-1.445E-01	5.704E 00	2.500E 05
7.300E-01	2.705E-01	-8.547E-02	6.021E 00	2.501E 05
7.400E-01	2.700E-01	-2.569E-02	5.853E 00	2.501E 05
7.500E-01	2.700E-01	3.003E-02	5.226E 00	2.500E 05
7.600E-01	2.705E-01	7.785E-02	4.309E 00	2.499E 05
7.700E-01	2.715E-01	1.159E-01	3.287E 00	2.500E 05
7.800E-01	2.728E-01	1.434E-01	2.202E 00	2.501E 05
7.900E-01	2.744E-01	1.595E-01	9.837E-01	2.501E 05
8.000E-01	2.760E-01	1.627E-01	-3.258E-01	2.500E 05
8.100E-01	2.776E-01	1.534E-01	-1.482E 00	2.498E 05
8.200E-01	2.790E-01	1.344E-01	-2.249E 00	2.499E 05
8.300E-01	2.802E-01	1.096E-01	-2.678E 00	2.502E 05
8.400E-01	2.812E-01	8.105E-02	-3.045E 00	2.502E 05
8.500E-01	2.818E-01	4.859E-02	-3.434E 00	2.499E 05
8.600E-01	2.822E-01	1.337E-02	-3.520E 00	2.496E 05
8.700E-01	2.821E-01	-1.955E-02	-2.952E 00	2.499E 05
8.800E-01	2.818E-01	-4.426E-02	-1.982E 00	2.505E 05
8.900E-01	2.813E-01	-6.054E-02	-1.400E 00	2.505E 05
9.000E-01	2.806E-01	-7.490E-02	-1.560E 00	2.496E 05
9.100E-01	2.798E-01	-9.131E-02	-1.568E 00	2.488E 05
9.200E-01	2.788E-01	-1.011E-01	-1.056E-01	2.499E 05
9.300E-01	2.778E-01	-9.012E-02	2.216E 00	2.525E 05
9.400E-01	2.770E-01	-6.759E-02	1.226E 00	2.514E 05
9.500E-01	2.763E-01	-9.735E-02	-9.196E 00	2.379E 05
9.600E-01	2.745E-01	-2.949E-01	-3.237E 01	2.050E 05
9.700E-01	2.694E-01	-7.750E-01	-6.438E 01	1.541E 05
9.800E-01	2.579E-01	-1.575E 00	-9.416E 01	9.586E 04
9.900E-01	2.371E-01	-2.608E 00	-1.089E 02	4.497E 04

T I M E	DISPLACEMENT	VELOCITY	ACCELERATION	FORCE
SEC	INCHES	INCH/SEC	INCH/SEC/SEC	LB
10.000E-01	2.057E-01	-3.679E 00	-1.014E 02	1.215E 04
1.010E 00	1.642E-01	-4.568E 00	-7.359E 01	-1.409E 03
1.020E 00	1.155E-01	-5.112E 00	-3.439E 01	-2.507E 03
1.030E 00	6.330E-02	-5.252E 00	6.028E 00	8.907E 01
1.040E 00	1.170E-02	-5.010E 00	4.112E 01	1.184E 03
1.050E 00	-3.585E-02	-4.454E 00	6.884E 01	3.678E 02
1.060E 00	-7.658E-02	-3.657E 00	8.938E 01	-5.401E 02
1.070E 00	-1.084E-01	-2.690E 00	1.028E 02	-4.577E 02
1.080E 00	-1.301E-01	-1.628E 00	1.083E 02	1.466E 02
1.090E 00	-1.409E-01	-5.509E-01	1.058E 02	3.801E 02
1.100E 00	-1.413E-01	4.633E-01	9.596E 01	8.059E 01
1.110E 00	-1.321E-01	1.350E 00	8.057E 01	-2.357E 02
1.120E 00	-1.149E-01	2.062E 00	6.148E 01	-1.793E 02
1.130E 00	-9.153E-02	2.572E 00	4.017E 01	8.644E 01
1.140E 00	-6.417E-02	2.863E 00	1.799E 01	1.838E 02
1.150E 00	-3.501E-02	2.934E 00	-3.529E 00	2.934E 01
1.160E 00	-6.175E-03	2.800E 00	-2.283E 01	-1.309E 02
1.170E 00	2.040E-02	2.489E 00	-3.866E 01	-9.448E 01
1.180E 00	4.315E-02	2.040E 00	-5.036E 01	5.553E 01
1.190E 00	6.089E-02	1.497E 00	-5.767E 01	1.086E 02
1.200E 00	7.291E-02	9.019E-01	-6.053E 01	1.363E 01
1.210E 00	7.891E-02	3.005E-01	-5.904E 01	-8.395E 01
1.220E 00	7.903E-02	-2.658E-01	-5.363E 01	-5.858E 01
1.230E 00	7.383E-02	-7.614E-01	-4.505E 01	3.897E 01
1.240E 00	6.413E-02	-1.159E 00	-3.428E 01	7.257E 01
1.250E 00	5.102E-02	-1.443E 00	-2.227E 01	7.261E 00
1.260E 00	3.569E-02	-1.603E 00	-9.866E 00	-5.943E 01
1.270E 00	1.936E-02	-1.642E 00	2.117E 00	-4.044E 01
1.280E 00	3.237E-03	-1.565E 00	1.289E 01	2.947E 01
1.290E 00	-1.161E-02	-1.390E 00	2.176E 01	5.304E 01
1.300E 00	-2.431E-02	-1.138E 00	2.829E 01	4.174E 00
1.310E 00	-3.419E-02	-8.327E-01	3.232E 01	-4.549E 01
1.320E 00	-4.087E-02	-4.998E-01	3.385E 01	-3.029E 01
1.330E 00	-4.418E-02	-1.636E-01	3.299E 01	2.381E 01
1.340E 00	-4.421E-02	1.528E-01	2.996E 01	4.169E 01
1.350E 00	-4.126E-02	4.296E-01	2.515E 01	2.457E 00
1.360E 00	-3.580E-02	6.516E-01	1.909E 01	-3.724E 01
1.370E 00	-2.844E-02	8.092E-01	1.235E 01	-2.428E 01
1.380E 00	-1.985E-02	8.980E-01	5.419E 00	2.050E 01
1.390E 00	-1.071E-02	9.184E-01	-1.260E 00	3.501E 01
1.400E 00	-1.691E-03	8.750E-01	-7.273E 00	1.386E 00
1.410E 00	6.608E-03	7.764E-01	-1.224E 01	-3.251E 01
1.420E 00	1.369E-02	6.346E-01	-1.589E 01	-2.078E 01
1.430E 00	1.920E-02	4.634E-01	-1.811E 01	1.873E 01
1.440E 00	2.291E-02	2.770E-01	-1.894E 01	3.129E 01
1.450E 00	2.474E-02	8.907E-02	-1.844E 01	6.108E-01
1.460E 00	2.473E-02	-8.777E-02	-1.674E 01	-3.017E 01
1.470E 00	2.306E-02	-2.424E-01	-1.405E 01	-1.890E 01
1.480E 00	1.998E-02	-3.663E-01	-1.063E 01	1.822E 01
1.490E 00	1.585E-02	-4.539E-01	-6.841E 00	2.974E 01

T I M E	DISPLACEMENT	VELOCITY	ACCELERATION	FORCE
SEC	INCHES	INCH/SEC	INCH/SEC/SEC	LB
1.500E 00	1.103E-02	-5.029E-01	-2.968E C0	-2.011E-02
1.510E 00	5.921E-03	-5.138E-01	7.474E-C1	-2.981E 01
1.520E 00	8.784E-04	-4.891E-01	4.101E 00	-1.829E 01
1.530E 00	-3.759E-03	-4.336E-01	6.886E C0	1.884E 01
1.540E 00	-7.713E-03	-3.539E-01	8.930E C0	3.012E 01
1.550E 00	-1.078E-02	-2.578E-01	1.015E 01	-6.524E-01
1.560E 00	-1.284E-02	-1.535E-01	1.058E 01	-3.132E 01
1.570E 00	-1.385E-02	-4.852E-02	1.029E 01	-1.879E 01
1.580E 00	-1.383E-02	5.024E-02	9.357E C0	2.073E 01
1.590E 00	-1.289E-02	1.367E-01	7.856E C0	3.245E 01
1.600E 00	-1.116E-02	2.059E-01	5.931E C0	-1.432E 00
1.610E 00	-8.835E-03	2.546E-01	3.785E C0	-3.504E 01
1.620E 00	-6.136E-03	2.816E-01	1.618E C0	-2.055E 01
1.630E 00	-3.274E-03	2.874E-01	-4.370E-01	2.424E 01
1.640E C0	-4.542E-04	2.735E-01	-2.299E 00	3.721E 01
1.650E 00	2.138E-03	2.423E-01	-3.872E C0	-2.521E 00
1.660E 00	4.347E-03	1.974E-01	-5.037E C0	-4.175E 01
1.670E 00	6.056E-03	1.433E-01	-5.710E 00	-2.388E 01
1.680E 00	7.197E-03	8.479E-02	-5.911E C0	3.023E 01
1.690E 00	7.752E-03	2.633E-02	-5.725E 00	4.544E 01
1.700E 00	7.736E-03	-2.864E-02	-5.219E C0	-4.209E 00
1.710E 00	7.201E-03	-7.703E-02	-4.408E C0	-5.307E 01
1.720E 00	6.227E-03	-1.159E-01	-3.321E 00	-2.953E 01
1.730E 00	4.923E-03	-1.429E-01	-2.080E C0	4.038E 01
1.740E 00	3.410E-03	-1.575E-01	-8.533E-01	5.940E 01
1.750E 00	1.811E-03	-1.604E-01	2.548E-01	-7.298E 00
1.760E 00	2.372E-04	-1.528E-01	1.249E 00	-7.261E 01
1.770E 00	-1.213E-03	-1.357E-01	2.144E C0	-3.903E 01
1.780E 00	-2.450E-03	-1.105E-01	2.859E 00	5.851E 01
1.790E 00	-3.404E-03	-7.963E-02	3.258E C0	8.387E 01
1.800E 00	-4.036E-03	-4.654E-02	3.310E 00	-1.370E 01
1.810E 00	-4.338E-03	-1.419E-02	3.138E C0	-1.086E 02
1.820E 00	-4.327E-03	1.596E-02	2.881E C0	-5.560E 01
1.830E 00	-4.028E-03	4.312E-02	2.523E C0	9.440E 01
1.840E 00	-3.480E-03	6.564E-02	1.938E C0	1.309E 02
1.850E 00	-2.739E-03	8.110E-02	1.131E C0	-2.934E 01
1.860E 00	-1.836E-03	8.829E-02	3.333E-C1	-1.838E 02
1.870E 00	-9.965E-04	8.861E-02	-2.235E-01	-8.652E 01
1.880E 00	-1.280E-04	8.447E-02	-5.944E-01	1.792E 02
1.890E 00	6.802E-04	7.640E-02	-1.052E C0	2.356E 02
1.900E 00	1.382E-03	6.286E-02	-1.664E C0	-8.059E 01
1.910E 00	1.918E-03	4.380E-02	-2.071E 00	-3.802E 02
1.920E 00	2.253E-03	2.348E-02	-1.888E 00	-1.467E 02
1.930E 00	2.403E-03	7.342E-03	-1.336E 00	4.576E 02
1.940E 00	2.415E-03	-4.609E-03	-1.180E 00	5.402E 02
1.950E 00	2.303E-03	-1.881E-02	-1.744E 00	-3.677E 02
1.960E 00	2.017E-03	-3.888E-02	-2.106E C0	-1.184E 03
1.970E 00	1.535E-03	-5.557E-02	-9.260E-01	-8.943E 01
1.980E 00	9.700E-04	-5.381E-02	1.196E 00	2.506E 03
1.990E 00	4.986E-04	-4.213E-02	9.231E-02	1.409E 03

T I M E	DISPLACEMENT	VELOCITY	ACCELERATION	FORCE
SEC	INCHES	INCH/SEC	INCH/SEC/SEC	LB
2.000E 00	-4.272E-05	-8.344E-02	-1.036E 01	-1.214E 04

LOOK FOR MORE DATA

TEST T-3

F O O T I N G

RADIUS.....R = .50 FT
WEIGHT.....W = 239.90 LB

S O I L

SHEAR MODULUS.....G = 4200.00 PSI
DENSITY.....GAMMA = 109.00 PCF
POISSONS RATIO.....MU = .2500
SHEAR WAVE VELOCITY.....V = 422.49 FT/SEC

S Y S T E M

STATIC SPRING CONSTANT...K = 134400 LB/INCH
MASS RATIO.....B = 3.3014

P U L S E

DURATION.....D = 2.050E-02 SEC
FACTOR ON ORDINATES.....Q = 4.970E 00 LBS

POINT	T I M E (SEC)	ORDINATE	F O R C E (LBS)
0	.000E 00	.000E 00	.000E 00
1	5.000E-04	4.500E 01	2.236E 02
2	10.000E-04	6.100E 01	3.032E 02
3	1.500E-03	5.200E 01	2.584E 02
4	2.000E-03	4.800E 01	2.386E 02
5	2.500E-03	5.200E 01	2.584E 02
6	3.000E-03	6.800E 01	3.380E 02
7	3.500E-03	7.400E 01	3.678E 02
8	4.000E-03	7.000E 01	3.479E 02
9	4.500E-03	5.200E 01	2.584E 02
10	5.000E-03	2.900E 01	1.441E 02
11	5.500E-03	1.300E 01	6.461E 01
12	6.000E-03	1.000E 00	4.970E 00
13	6.500E-03	1.000E 00	4.970E 00
14	7.000E-03	1.700E 01	8.449E 01
15	7.500E-03	2.000E 01	9.940E 01
16	8.000E-03	1.300E 01	6.461E 01
17	8.500E-03	5.000E 00	2.485E 01
18	9.000E-03	-3.000E 00	-1.491E 01
19	9.500E-03	-6.000E 00	-2.982E 01
20	10.000E-03	-2.000E 00	-9.940E 00
21	1.050E-02	5.000E 00	2.485E 01
22	1.100E-02	2.000E 00	9.940E 00
23	1.150E-02	-3.000E 00	-1.491E 01
24	1.200E-02	-6.000E 00	-2.982E 01
25	1.250E-02	-7.000E 00	-3.479E 01
26	1.300E-02	-3.000E 00	-1.491E 01

27	1.350E-02	3.000E 00	1.491E 01
28	1.400E-02	3.000E 00	1.491E 01
29	1.450E-02	-.000E 00	-.000E 00
30	1.500E-02	-6.000E 00	-2.982E 01
31	1.550E-02	-7.000E 00	-3.479E 01
32	1.600E-02	-2.000E 00	-9.940E 00
33	1.650E-02	5.000E 00	2.485E 01
34	1.700E-02	4.000E 00	1.988E 01
35	1.750E-02	-3.000E 00	-1.491E 01
36	1.800E-02	-4.000E 00	-1.988E 01
37	1.850E-02	-2.000E 00	-9.940E 00
38	1.900E-02	2.000E 00	9.940E 00
39	1.950E-02	4.000E 00	1.988E 01
40	2.000E-02	2.000E 00	9.940E 00
41	2.050E-02	.000E 00	.000E 00

A C C U R A C Y

EPS1 = .0500 GOVERNS DISTANCE BETWEEN PULSES
EPS2 = .0500 GOVERNS NUMBER OF FOURIER TERMS

F O U R I E R S E R I E S

TERM NUMBER K	FREQUENCY RATIO A(K)	AMPLITUDE OF FOURIER TERM FORCE C(K)	DISPLACEMENT BN(K)
1	6.045E-02	4.815E 01	3.623E-04
2	1.814E-01	4.749E 01	3.916E-04
3	3.023E-01	4.581E 01	4.624E-04
4	4.232E-01	4.170E 01	5.844E-04
5	5.441E-01	3.494E 01	5.700E-04
6	6.650E-01	2.827E 01	2.799E-04
7	7.859E-01	2.397E 01	1.383E-04
8	9.068E-01	2.041E 01	7.716E-05
9	1.028E 00	1.659E 01	4.473E-05
10	1.149E 00	1.392E 01	2.830E-05
11	1.270E 00	1.178E 01	1.883E-05
12	1.390E 00	8.572E 00	1.113E-05
13	1.511E 00	5.174E 00	5.584E-06
14	1.632E 00	3.387E 00	3.090E-06
15	1.753E 00	4.455E 00	3.485E-06
16	1.874E 00	6.705E 00	4.549E-06
17	1.995E 00	8.231E 00	4.892E-06
18	2.116E 00	1.027E 01	5.392E-06
19	2.237E 00	1.336E 01	6.247E-06
20	2.358E 00	1.433E 01	6.002E-06
21	2.479E 00	1.087E 01	4.105E-06
22	2.600E 00	4.373E 00	1.497E-06

T I M E	DISPLACEMENT	VELOCITY	ACCELERATION	FORCE
SEC	INCHES	INCH/SEC	INCH/SEC/SEC	LB
.000E 00	-2.649E-06	2.246E-02	1.382E 02	8.378E 01
5.000E-04	3.112E-05	1.226E-01	2.570E 02	1.779E 02
1.000E-03	1.278E-04	2.687E-01	3.128E 02	2.483E 02
1.500E-03	3.007E-04	4.203E-01	2.806E 02	2.741E 02
2.000E-03	5.427E-04	5.406E-01	1.977E 02	2.715E 02
2.500E-03	8.344E-04	6.203E-01	1.276E 02	2.768E 02
3.000E-03	1.159E-03	6.755E-01	9.875E 01	3.090E 02
3.500E-03	1.508E-03	7.201E-01	7.471E 01	3.473E 02
4.000E-03	1.875E-03	7.394E-01	-1.261E 01	3.459E 02
4.500E-03	2.237E-03	6.915E-01	-1.930E 02	2.759E 02
5.000E-03	2.549E-03	5.391E-01	-4.154E 02	1.568E 02
5.500E-03	2.759E-03	2.865E-01	-5.759E 02	4.729E 01
6.000E-03	2.827E-03	-1.274E-02	-5.952E 02	8.385E-01
6.500E-03	2.750E-03	-2.858E-01	-4.803E 02	2.441E 01
7.000E-03	2.554E-03	-4.849E-01	-3.168E 02	7.532E 01
7.500E-03	2.276E-03	-6.106E-01	-1.988E 02	9.862E 01
8.000E-03	1.950E-03	-6.971E-01	-1.581E 02	7.153E 01
8.500E-03	1.582E-03	-7.745E-01	-1.514E 02	1.704E 01
9.000E-03	1.177E-03	-8.426E-01	-1.115E 02	-2.216E 01
9.500E-03	7.455E-04	-8.756E-01	-1.175E 01	-2.289E 01
1.000E-02	3.114E-04	-8.498E-01	1.144E 02	1.432E 00
1.050E-02	-9.468E-05	-7.667E-01	2.089E 02	1.837E 01
1.100E-02	-4.499E-04	-6.513E-01	2.431E 02	8.628E 00
1.150E-02	-7.452E-04	-5.303E-01	2.379E 02	-1.794E 01
1.200E-02	-9.808E-04	-4.126E-01	2.367E 02	-3.535E 01
1.250E-02	-1.157E-03	-2.891E-01	2.612E 02	-2.801E 01
1.300E-02	-1.267E-03	-1.501E-01	2.929E 02	-4.680E 00
1.350E-02	-1.305E-03	-1.194E-03	2.952E 02	1.195E 01
1.400E-02	-1.270E-03	1.372E-01	2.510E 02	7.743E 00
1.450E-02	-1.173E-03	2.450E-01	1.786E 02	-1.066E 01
1.500E-02	-1.031E-03	3.170E-01	1.130E 02	-2.423E 01
1.550E-02	-8.605E-04	3.628E-01	7.460E 01	-2.052E 01
1.600E-02	-6.707E-04	3.947E-01	5.403E 01	-4.350E 00
1.650E-02	-4.676E-04	4.156E-01	2.698E 01	8.729E 00
1.700E-02	-2.581E-04	4.182E-01	-1.966E 01	8.100E 00
1.750E-02	-5.379E-05	3.944E-01	-7.546E 01	-2.786E 00
1.800E-02	1.320E-04	3.451E-01	-1.177E 02	-1.142E 01
1.850E-02	2.889E-04	2.813E-01	-1.329E 02	-8.890E 00
1.900E-02	4.130E-04	2.158E-01	-1.273E 02	2.454E 00
1.950E-02	5.054E-04	1.546E-01	-1.184E 02	1.264E 01
2.000E-02	5.680E-04	9.589E-02	-1.180E 02	1.396E 01
2.050E-02	6.010E-04	3.551E-02	-1.236E 02	7.186E 00
2.100E-02	6.032E-04	-2.676E-02	-1.236E 02	-7.420E-01
2.150E-02	5.748E-04	-8.573E-02	-1.099E 02	-3.880E 00
2.200E-02	5.192E-04	-1.346E-01	-8.448E 01	-1.908E 00
2.250E-02	4.425E-04	-1.697E-01	-5.594E 01	1.260E 00
2.300E-02	3.517E-04	-1.912E-01	-3.105E 01	2.154E 00
2.350E-02	2.531E-04	-2.015E-01	-1.060E 01	6.534E-01
2.400E-02	1.518E-04	-2.021E-01	8.236E 00	-1.028E 00
2.450E-02	5.261E-05	-1.932E-01	2.715E 01	-1.201E 00

T I M E	DISPLACEMENT	VELOCITY	ACCELERATION	FORCE
SEC	INCHES	INCH/SEC	INCH/SEC/SEC	LB
2.500E-02	-3.986E-05	-1.752E-01	4.459E 01	-1.673E-01
2.550E-02	-1.213E-04	-1.494E-01	5.776E 01	6.987E-01
2.600E-02	-1.884E-04	-1.184E-01	6.532E 01	6.313E-01
2.650E-02	-2.392E-04	-8.485E-02	6.810E 01	1.822E-02
2.700E-02	-2.731E-04	-5.082E-02	6.757E 01	-3.800E-01
2.750E-02	-2.902E-04	-1.771E-02	6.444E 01	-3.069E-01
2.800E-02	-2.912E-04	1.318E-02	5.866E 01	-4.558E-02
2.850E-02	-2.776E-04	4.052E-02	5.035E 01	1.132E-01
2.900E-02	-2.515E-04	6.322E-02	4.018E 01	1.585E-01
2.950E-02	-2.153E-04	8.053E-02	2.895E 01	1.656E-01
3.000E-02	-1.719E-04	9.209E-02	1.725E 01	8.186E-02
3.050E-02	-1.242E-04	9.780E-02	5.650E 00	-1.414E-01
3.100E-02	-7.505E-05	9.790E-02	-5.011E 00	-3.257E-01
3.150E-02	-2.712E-05	9.309E-02	-1.389E 01	-1.951E-01
3.200E-02	1.738E-05	8.434E-02	-2.079E 01	2.220E-01
3.250E-02	5.671E-05	7.254E-02	-2.623E 01	4.889E-01
3.300E-02	8.951E-05	5.827E-02	-3.064E 01	2.232E-01
3.350E-02	1.147E-04	4.215E-02	-3.354E 01	-3.718E-01
3.400E-02	1.315E-04	2.516E-02	-3.394E 01	-6.273E-01
3.450E-02	1.399E-04	8.682E-03	-3.154E 01	-1.667E-01
3.500E-02	1.405E-04	-6.101E-03	-2.746E 01	5.650E-01
3.550E-02	1.342E-04	-1.877E-02	-2.331E 01	7.195E-01
3.600E-02	1.220E-04	-2.950E-02	-1.965E 01	3.084E-02
3.650E-02	1.050E-04	-3.834E-02	-1.548E 01	-7.775E-01
3.700E-02	8.410E-05	-4.470E-02	-9.651E 00	-7.485E-01
3.750E-02	6.083E-05	-4.778E-02	-2.603E 00	1.767E-01
3.800E-02	3.690E-05	-4.744E-02	3.634E 00	9.863E-01
3.850E-02	1.382E-05	-4.457E-02	7.410E 00	7.017E-01
3.900E-02	-7.455E-06	-4.037E-02	9.214E 00	-4.444E-01
3.950E-02	-2.642E-05	-3.533E-02	1.109E 01	-1.168E 00
4.000E-02	-4.258E-05	-2.905E-02	1.422E 01	-5.696E-01
4.050E-02	-5.519E-05	-2.111E-02	1.733E 01	7.586E-01
4.100E-02	-6.351E-05	-1.214E-02	1.800E 01	1.302E 00
4.150E-02	-6.741E-05	-3.667E-03	1.546E 01	3.463E-01
4.200E-02	-6.747E-05	3.124E-03	1.177E 01	-1.102E 00
4.250E-02	-6.455E-05	8.393E-03	9.719E 00	-1.365E 00
4.300E-02	-5.915E-05	1.321E-02	9.743E 00	-2.856E-02
4.350E-02	-5.132E-05	1.807E-02	9.382E 00	1.456E 00
4.400E-02	-4.121E-05	2.209E-02	6.127E 00	1.336E 00
4.450E-02	-2.963E-05	2.380E-02	5.762E-01	-3.834E-01
4.500E-02	-1.787E-05	2.286E-02	-3.850E 00	-1.796E 00
4.550E-02	-6.992E-06	2.059E-02	-4.583E 00	-1.193E 00
4.600E-02	2.791E-06	1.869E-02	-2.920E 00	8.870E-01
4.650E-02	1.181E-05	1.741E-02	-2.737E 00	2.097E 00
4.700E-02	2.007E-05	1.534E-02	-6.042E 00	9.131E-01
4.750E-02	2.679E-05	1.118E-02	-1.038E 01	-1.476E 00
4.800E-02	3.100E-05	5.550E-03	-1.132E 01	-2.327E 00
4.850E-02	3.247E-05	6.766E-04	-7.582E 00	-4.695E-01
4.900E-02	3.208E-05	-1.867E-03	-2.903E 00	2.143E 00
4.950E-02	3.087E-05	-2.907E-03	-2.135E 00	2.448E 00

T I M E	DISPLACEMENT	VELOCITY	ACCELERATION	FORCE
SEC	INCHES	INCH/SEC	INCH/SEC/SEC	LB
5.000E-02	2.903E-05	-4.745E-03	-5.619E 00	-1.682E-01
5.050E-02	2.580E-05	-8.403E-03	-8.370E 00	-2.874E 00
5.100E-02	2.060E-05	-1.215E-02	-5.564E 00	-2.408E 00
5.150E-02	1.411E-05	-1.321E-02	1.552E 00	1.042E 00
5.200E-02	7.959E-06	-1.099E-02	6.360E 00	3.653E 00
5.250E-02	3.239E-06	-8.077E-03	4.128E 00	2.137E 00
5.300E-02	-5.383E-07	-7.560E-03	-2.069E 00	-2.210E 00
5.350E-02	-4.740E-06	-9.421E-03	-4.074E 00	-4.456E 00
5.400E-02	-9.778E-06	-1.021E-02	2.105E 00	-1.523E 00
5.450E-02	-1.423E-05	-6.872E-03	1.078E 01	3.774E 00
5.500E-02	-1.616E-05	-7.131E-04	1.202E 01	5.242E 00
5.550E-02	-1.530E-05	3.380E-03	3.132E 00	3.692E-01
5.600E-02	-1.369E-05	2.240E-03	-6.705E 00	-5.913E 00
5.650E-02	-1.351E-05	-1.433E-03	-5.625E 00	-5.926E 00
5.700E-02	-1.448E-05	-1.420E-03	6.678E 00	1.731E 00
5.750E-02	-1.385E-05	4.754E-03	1.601E 01	9.014E 00
5.800E-02	-9.592E-06	1.161E-02	8.142E 00	6.283E 00
5.850E-02	-3.599E-06	1.057E-02	-1.298E 01	-5.834E 00
5.900E-02	-6.507E-07	2.241E-04	-2.467E 01	-1.408E 01
5.950E-02	-3.250E-06	-9.246E-03	-8.342E 00	-5.362E 00
6.000E-02	-7.553E-06	-5.165E-03	2.454E 01	1.599E 01
6.050E-02	-6.247E-06	1.110E-02	3.235E 01	2.476E 01
6.100E-02	1.772E-06	1.632E-02	-2.341E 01	-6.944E 00

LOOK FOR MORE DATA

ALL INPUT DATA HAVE BEEN PROCESSED

REFERENCES

1. REISSNER, E. : Stationäre, axialsymmetrische durch eine schüttelnde Masse erregte Schwingungen eines homogenen elastischen Halbraumes. Ingenieur-Archiv, vol. 7, pp. 381 - 396, Dec. 1936.

2. SUNG, T. Y.: Vibrations in Semi-infinite Solids Due to periodic Loading. Symp. Dyn. Testing Soils, ASTM Spec. Tech. Publ. No. 156, pp. 35-68, 1953.

3. BYCROFT, G. N.: Forced Vibrations of a Rigid Circular Plate on a Semi-Infinite Elastic Space or an Elastic Stratum. Phil. Trans. Roy., Ser. A, vol. 248, pp. 327-368, 1956.

4. HSIEH, T. K.: Foundation Vibrations. Proc. Inst. Civil Engrs., vol. 22, pp. 211-226, 1962.

5. RICHART, F. E., JR.: Foundation Vibrations. Jour. Soil Mech. Found. Div. ASCE, Proc. ASCE, vol. 86, pp. 1-34, Aug., 1960.

6. FRY, Z. B.: Development and Evaluation of Soil Bearing Capacity, Foundations of Structures. U. S. Army Engineer Waterways Experiment Station, Corps of Engineers, Vicksburg, Miss., Technical Report No. 3-632, Report 1, July, 1963.

7. CHAE, Y. S.: Dynamic Pressure Distribution at the Base of a Rigid Footing Subjected to Vibratory Loads. U. S. Army Engineer Waterways Experiment Station, Corps of Engineers, Vicksburg, Miss., Contract Report No. 3-88, May, 1964.

8. DRNEVICH, V. P., HALL, J. R., JR., RICHART, F.E., JR.: Report on Impact Tests to be prepared at the University of Michigan under contract No. DA-22-079-ENG-340 with the U. S. Army Engineer Waterways Experiment Station, Vicksburg, Miss. Expected completion date June 1965.

9. RAYLEIGH, LORD: On Waves Propagated along the surface of an Elastic Solid, Proc. London Math. Soc., vol. 17, pp. 3-11, London 1885.

10. EWING, W. M., JARDETZKY, W. S. and PRESS, F.: Elastic Waves in Layered Media. McGraw-Hill, 1957.

11. WHITMAN, R. V.: Analysis of Foundation Vibrations. Massachusetts Institute of Technology, Dept. Civil Engr. Professional Paper P65-02, Soils Publication No. 169. To be presented at: Symp. Man-made Vibrations in Civil Engineering. Brit. Nat. Sect. Int. Assoc. Earthquake Engineering, London, April 1965.

12. SHANNON, W. L., YAMANE, G., and DIETRICH, R. J.: Dynamic Triaxial Tests on Sands. Proc. 1st Panamerican Conf. on Soil Mech. and Found. Engng., vol. 1, pp. 473-489, 1959.

13. HARDIN, B. O. and RICHART, F. E., JR.: Elastic Wave Velocities in Granular Soils. Jour. Soil Mech. & Found. Div. ASCE, vol. 89, pp. 33-65, Feb. 1965.

14. HALL, J. R., JR.: Effect of Amplitude on Damping and Wave Propagation in Granular Materials, Ph. D. Dissertation, University of Florida, August, 1962.

15. JONES, R.: In-Situ Measurement of the Dynamic Properties of Soil by Vibration Methods. Geotechnique, Vol. 8, pp. 1-21, March, 1958.

16. BALLARD, R. F., JR.: Determination of Soil Shear Moduli at Depth by In-Situ Vibratory Techniques. U. S. Army Engineer Waterways Experiment Station, Vicksburg, Miss., Misc. Paper No. 4-691, Dec. 1965.

17. FRY, Z. B.: A Procedure for Determining Elastic Moduli of Soils by Field Vibratory Techniques. U. S. Army Engineer Waterways Experiment Station, Vicksburg, Miss., Misc. Paper No. 4-577, June 1963.

18. HERTWIG, A., FRÜH, G. and LORENZ, H.: Die Ermittlung der für das Bauwesen wichtigsten Eigenschaften des Bodens durch erzwungene Schwingungen. DEGEBO No. 1, Springer Verlag, Berlin 1933.